Post-transcriptional regulation of *Hox* genes during *Drosophila* neural development: mechanisms and biological roles

João Guilherme Patrício Picão de Almeida Osório

Submitted in partial fulfilment of the requirements for the degree of Doctor of Philosophy at theUniversity of Sussex

January 2014

I hereby declare that this thesis has not been and will not be, submitted in whole or in part to another University for the award of any other degree.

Signed:……..

João Picão Osório

UNIVERSITY OF SUSSEX

João Guilherme Patrício Picão de Almeida Osório, DPhil Biology

Post-transcriptional regulation of *Hox* genes during *Drosophila* neural development: mechanisms and biological roles

Summary

During the formation of the insect and mammalian nervous system the embryo activates specific programs of cellular differentiation along the main body axis so that the specification and organization of neural cells is set in coordination with axial level. At the genetic level such cellular specification programs rely on the regulated expression of a family of transcription factors encoded by the *Hox* genes. However, the precise molecular mechanisms controlling *Hox* expression in the nervous system are not well understood. In this thesis we investigate the molecular mechanisms underlying *Hox* gene expression within the *Drosophila* central nervous system (CNS) with a focus on post-transcriptional control via RNA binding proteins (RBP) and microRNAs (miRNAs). Much of the work is centred on the analysis of the *Hox* gene *Ultrabithorax* (*Ubx*) as this is the *Hox* gene for which post-transcriptional regulation is currently best understood. Through the combination of genetic, molecular and imaging methods we first show that the pan-neural RBP ELAV regulates *Ubx* RNA processing and protein expression during the embryonic development of the CNS. Secondly, using a suite of genetic and behavioural methods we report that *Ubx* repression by miRNAs encoded within the *iab-4/iab-8* locus (*miR-iab4/iab8*) is required for the coordination of a specific larval behaviour: self-righting behaviour. Third, we explore the cellular basis of larval self-righting behaviour in the context of miRNA-dependent *Ubx* regulation and find that: (i) removal of *miR-iab4/iab8* does not lead to major anatomical defects in the CNS or muscles; (ii) artificial increase in UBX protein expression in cholinergic interneurons disrupts self-righting behaviour; and (iii) UBX protein expression in cholinergic interneurons is regulated by *miR-iab4/iab8*. These observations imply that UBX regulation by *miR-iab4/iab8* in cholinergic interneurons controls self-righting behaviour. Altogether our work adds to the current understanding of the molecular mechanisms underlying *Hox* gene expression during CNS formation and gives new insights on the role of RBP and miRNA regulation on the control of gene expression and behaviour.

Acknowledgements

First, I want to thank my supervisor, Claudio, for his persistent encouragement and guidance, for challenging me everyday, and most of all for transforming my innocent enthusiasm in science into the more mature understanding of Biology of a junior scientist.

I also thank all members of the Alonso Lab past and present – Stefan, Rich, Patraquim, Elvira, Casandra, Ali, Ana, Ipek, Wan, Raúl and Sofia – for providing a fun and intellectual stimulating environment. Special thanks go to Patraquim for his great camaraderie, constant discussion and special support on the finals days of this thesis.

To all the members of the Couso lab. In special to the smoking gang: Unum, Ali, John, Inyaki and Emile. Thanks to Dan and Roger for their technical support.

I would like to extend my acknowledgements to Mathias and Jimena for hosting me in their Lab several times, for all the thought-provoking conversations, analysis of data, introducing me to larval behaviour and enthusiasm.

To Gerd and Ana at the Technau Lab, thanks for hosting me more than once in your lab, for your kindness and for teaching me the basic set of embryonic CNS analysis techniques.

I'd also like to thank all the friends I made during my years in Brighton, especially Bruce, Mafalda, Lambros, Dani, Juan, Maro, Giulio, Sandra, Renanzinho, Cae, Marta, as well as all the friends back home: "Brigada dos Velhos", Élio, Emília, Alex, Aninhas, Marialva, Lima, Zuka, Sara, Cocas and all my friends whose names are not here.

I'd like to thank the FCT for providing me the funding to pursue my PhD project.

To all my family, especially my mum, my dad, my siblings and my uncle: thank you.

Finally, I'd like to thank a lot my Malaki Eva for her love, friendship, companion and silliness!!!!!!!!!!!!!!!

To Eva

Table of contents

List of Figures

List of Tables

Abbreviations

ΔmiR-iab4/iab8	*miR-iab4/iab8* mutant
A-P axis	Anterior-posterior axis
abd-A	*abdominal-A*
Abd-B	*Abdominal-B*
Ach	Acetylcholine
ANT-C	*Antennapedia*-complex
Antp	*Antennapedia*
APA	Alternative Polyadenylation
AS	Alternative splicing
BX-C	*Bithorax*-complex
Cha	*Choline acetyltransferase*
CLIP	Crosslinking immunoprecipitation
CNS	Central Nervous System
CPG	Central pattern generators
ddaC	dorsal dendritic arborisation C
DNA	Deoxyribonucleic acid
elav	*embryonic lethal abnormal vision*
En	*Engrailed*
FISH	Fluorescence *in situ* hybridization
GMC	Ganglion mother cell
ISN	Intersegmental nerve
min	Minute
miRNA	microRNA
ms	Milliseconds
NB	Neuroblast
PAS	Polyadenylation signal
PBS	Phosphate buffered saline

PBTx	Phosphate buffered saline with TritonX detergent
Pc-G	Polycomb *group*
PNS	Peripheral nervous system
ppk	*pickpocket*
RBP	RNA Binding Protein
repo	*reversed polarity*
PCR	Polymerase chain reaction
RNA	Ribonucleic acid
RT	Reverse transcriptase
RT-PCR	Reverse transcription polymerase chain reaction
sec	Seconds
SN	Segmental nerve
TN	Transverse nerve
trx-G	*trithorax group*
Ubx	*Ultrabithorax*
VNC	Ventral nerve cord

"The game was that of continually inventing a possible world, or a piece of a possible world, and then of comparing it with the real world… What mattered more than the answers were the questions and how they were formulated"

François Jacob

in The Statue Within

Chapter 1

General Introduction

1.1 Preface

One of the most intriguing questions in modern biology is how the central nervous system (CNS) of animals dictates behaviour. The development of the CNS, a corollary of the previous question, largely relies on the differential cell-specification along the anteroposterior axis (Krumlauf et al. 1993). Bilateral animals, ranging from *Homo sapiens* to *Mus musculus* and the fly *Drosophila melanogaster*, deploy *Hox* genes during the formation of the nervous tissue to provide differential identity and thus polarity to the CNS. However, the complete picture of how their correct patterns of expression are promoted remains blurry. The study of *Hox* genes in disparate tissues such as the mesenchymal stem-cells of humans, the developing mouse forelimb and the thoracic dorsal appendages of flies has functioned as a test tube for the larger question of how multiple levels of gene regulation act cooperatively to achieve a coordinated output. Additionally, the CNS has been shown to exhibit a noticeable enrichment in tissue-specific RNA processing events in both flies and humans (Castle et al. 2008; Clark et al. 2007; Hilgers et al. 2011; Thomsen et al. 2010) and in *cis*-regulatory motifs due to CNS-specific 3'UTR (3' untranslated region) elongation in humans, zebrafish and flies (Hilgers et al. 2011, Thomsen et al. 2010, Ulitsky et al. 2012, Zhang et al. 2005), implying that the nervous tissue heavily relies on RNA-based regulation to achieve its correct pattern and function. These observations thus beg the following question: how is *Hox* expression regulated in the developing CNS?

The following work addresses the role of the *Hox* gene *Ultrabithorax* (*Ubx*) in the establishment of CNS anatomy and function in *Drosophila,*

presents a case for the importance of multiple RNA-based regulatory mechanisms on *Hox* CNS expresssion and links the post-transcriptional regulation of *Hox* expression in the developing CNS of embryos to the behaviour of free-living larvae.

In this chapter, we will, first introduce the *Hox genes* as important evolutionary and developmental actors in *Bilateria*, second, discuss the regulation of the expression of *Hox* gene *Ubx*, third, describe how the CNS is formed in *Drosophila* embryos and finally explore the roles of *Hox* genes in the *Drosophila* CNS.

1.2 The *Hox* genes

At the end of the 19th century William Bateson coined the term “homeotic” to describe phenotypic variation in which “something has been changed into the likeness of something else” (Bateson 1894). Two decades later, in 1915 Calvin B. Bridges and Thomas H. Morgan discovered the first homeotic mutation in the fruit fly *Drosophila melanogaster* (in Bridges & Morgan 1923), demonstrating that homeotic phenotypes could be induced through gene mutation. They found a surprising new character, a partial duplication of a thoracic segment. *Drosophila* has three thoracic segments (T1, T2 and T3), each one bearing specific appendages: a ventral pair of legs on each segment, a pair of wings in T2 and a pair of halteres (flight balancing organs) in T3. In Bridges and Morgan’s mutant, the halteres of T3 had been transformed into a

structure that resembled the wings in T2. They named this mutant *bithorax* (*bx*)(Bridges & Morgan 1923).

In the following decades hundreds of homeotic mutants were isolated and it was discovered that some of them are mapped into two separate clusters of the 3rd chromosome. These clusters contain eight individual homeotic genes, termed the *Hox* genes (Kaufman et al. 1980; R. A. Lewis et al. 1980; Sánchez-Herrero et al. 1985). In *D. melanogaster Hox* genes are organised in two separate gene clusters: the Antennapedia complex (ANT-C, (Kaufman et al. 1980; R. A. Lewis et al. 1980) and the Bithorax complex (BX-C, (E. B. Lewis 1978) (see Figure 1.1A).

The groundbreaking work of Ed Lewis on the BX-C showed that the "gene" arrangement along the chromosome (inferred from genetic maps) was directly related to the body segments they affected along the anterior-posterior (A-P) axis (E. B. Lewis 1978). His work suggested that *Hox* genes would provide a genetic coordination system to assign segmental identity in the fly. This correlation between genomic location and body axis is known as spatial collinearity. The cloning of the BX-C (Bender et al. 1983; Karch et al. 1985) gave the molecular basis to clarify the genetic data collected over decades. Additionally, expression analysis of *Hox* genes confirmed the observations of Ed Lewis: *Hox* expression was segmentally regulated along the A-P axis (Akam 1983; Akam & Martinez-Arias 1985; Beachy et al. 1985; Harding et al. 1985; Karch et al. 1990; R. A. H. White & Wilcox 1984). Around the same time, sequence comparison of different *homeotic* genes revealed a common DNA region, the homeobox (McGinnis, Levine, et al. 1984c; Scott & Weiner 1984). The homeobox encodes a DNA binding domain called homeodomain (Desplan

et al. 1985; Desplan et al. 1988). Thus, *homeotic* genes encode a homeodomain transcription factor that regulate gene expression of target genes by binding DNA *cis*-regulatory regions (Gould et al. 1990; Gehring et al. 1994).

At the same time that the molecular characterisation of *Drosophila Hox* genes was being revealed, *Hox* genes were also found in the genomes of other invertebrates and even conserved in vertebrate genomes all the way to humans (McGinnis, Garber, et al. 1984a; McGinnis, Hart, et al. 1984b) (see Figure 1.1B). Subsequently, it was shown that homeboxes are evolutionary conserved in a widespread range of animal phyla (Holland & Hogan 1986). Shortly after, it was discovered by two independent laboratories that the basic genomic organisation and expression of the murine *Hox* gene family resembles that of *Drosophila Hox* genes (Graham et al. 1989; Duboule & Dollé 1989). However, mammals have 39 *Hox* genes arranged in four gene clusters, while *Drosophila* have 8 *Hox* arranged in one gene cluster split into two complexes. The four *Hox* gene clusters are a result of two rounds of genome duplication that occurred in the vertebrate lineage (McGinnis & Krumlauf 1992; Garcia-Fernandez & Holland 1994) (Figure 1.1). These observations raised the provocative possibility that *Hox* genes could be shaping the form of all metazoans (Akam 1989; McGinnis & Krumlauf 1992).

Hox genes have been demonstrated to be involved in the evolution of animal body plan (Carroll 1995; Hughes & Kaufman 2002). In arthropods, expression domains of different *Hox* genes correlate with the diversification of insect and crustacean body plans (Averof & Akam 1995; Averof & Patel 1997). These observations were later corroborated with the establishment of conditional misexpression tools in crustacean (Pavlopoulos et al. 2009). Also,

the regulation of *Hox* expression was involved in the evolution of appendage morphology in insects (Khila et al. 2009; Stern 1998). In vertebrates, it was shown that *Hox* expression shaped the diversification of axial morphology (Burke et al. 1995). Alongside with the evolution of animal body plan and axial morphology, *Hox* genes are expressed in the CNS of most *Bilateria*, and as such, are hypothesized to have been important for the evolutionary diversification of animal CNSs (Kourakis et al. 1997; Krumlauf et al. 1993).

Hox genes play major roles in the specification of the vertebrate CNS along the A-P axis (Keynes and Krumlauf 1994; Krumlauf et al. 1993). During segmentation of the neural tube, *Hox* genes are expressed in nested domains along the A-P axis (see Figure 1.1B) and control segmental identity (reviewed in Alexander et al. 2009; Dasen & Jessell 2009; Tümpel et al. 2009). A good example of this is the segmental differentiation of the hindbrain. The hindbrain is divided in seven segmental compartments – the rhombomeres – that give rise to the neuronal organization of the cranial nerves [e.g. the trigeminal motorneurons arising from rhombomere 2 innervate the muscles responsible for mastication whereas the facial motorneurons stemming from rhombomere 4 innervate the muscles that control facial expression (see Guthrie 2007)]. The patterns of *Hox* expression of paralogous groups 1-4 are differentially expressed in the rhombomeres and control their segment specification (Maconochie et al. 1996; Murphyet al. 1989; Wilkinson et al. 1989). While *Hoxa2* is required for the segmental identity of rhombomere 2 (Gavalas et al. 1997), *Hoxb1* establishes the properties of rhombomere 4 (Studer et al. 1996)

Another key example of the role of *Hox* genes in the development of the vertebrate CNS is the differential motorneuron innervation along the thoracic

and lumbar regions (Dasen et al., 2003, 2005; Dasen & Jessell 2009; Jung et al., 2010).

As in vertebrates, *Hox* genes are also involved in the segment-specific differentiation of the CNS in invertebrates (see Section 1.11)

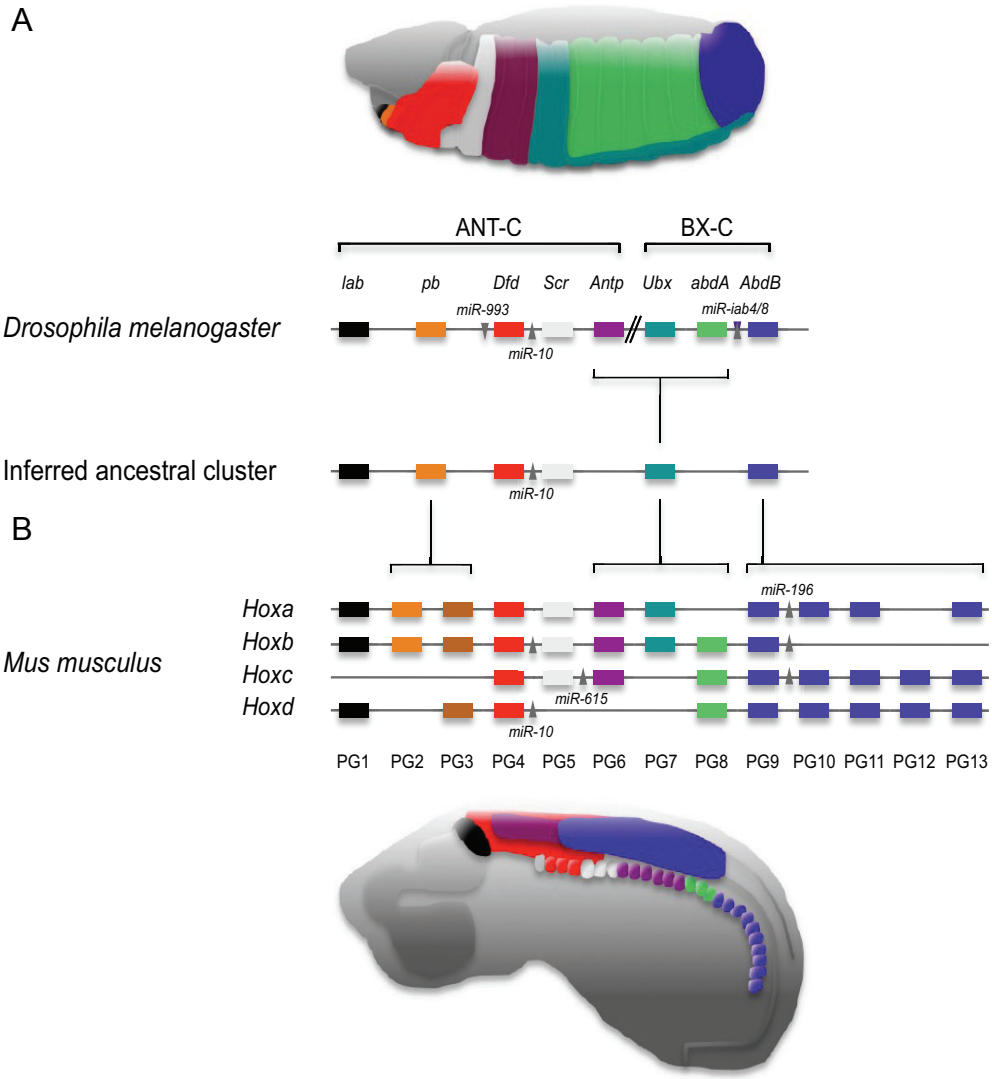

Figure 1.1 *Hox* gene clusters are conserved across Bilateria and provide position information across the A-P axis during development

(Legend on the following page)

Figure 1.1 *Hox* gene clusters are conserved across *Bilateria* and provide position information across the A-P axis during development

(A-B) Diagram depicting the embryonic expression, genome organization and evolutionary relationship among the *Hox* genes of Bilateria (taken from Mallo and Alonso 2013). *miRNA loci* are represented, as some *Hox* cluster *miRNA*s have the ability to regulate *Hox* genes. (A) Diagram of a *Drosophila melanogaster* embryo (top panel) showing the anterior domains of expression of the eight *Drosophila Hox* genes along the A-P axis. Axial *Hox* expression patterns lay out the positional information for further axial development. *Hox* genes are found in two clusters (*Antennapedia* and *Bithorax* complexes) within the *Drosophila melanogaster* genome, in an order that is colinear to their respective embryonic expression. Animal comparative genomics enables us to reconstruct, through individual patterns of *Hox* gene loss and gain and phylogenetics, the inferred ancestral *Hox* cluster, which seems to have consisted of 10 *Hox* genes. (B) Diagram of a *Mus musculus* embryo (bottom panel) displaying the A-P axis expression patterns of the 39 mammalian *Hox* genes. Mammalian *Hox* genes are found in four clusters, each in a distinct chromosome. These clusters are paralogous, and descend from a single ancestral *Hox* cluster [(see (A)], as the tetrapod lineage underwent two private rounds of whole genome duplications. As such, individual mammalian *Hox* genes have a paralogous genes in other clusters. This evolutionary relationship leads to the grouping of related genes in 13 paralogous groups. Mammalian *Hox* genes also display colinearity between genomic position and embryonic A-P axis expression. Anterior is left.

1.3 Regulation of *Hox* genes

The spectrum of molecular process that regulate *Hox* expression and function are highly diverse and complex (Alonso & Wilkins 2005; Maeda & Karch 2009; Mallo & Alonso 2013). They involve molecular processes such as: nuclear dynamics, chromatin remodelling, transcription regulation, RNA processing, microRNA (miRNA) regulation and translation regulation (see review (Mallo & Alonso 2013)) (see Figure 1.2). Furthermore, *Hox* genes cross-regulate themselves by a process termed “posterior prevalence”: posterior *Hox* genes repress the expression of more anterior *Hox* (Duboule & Morata 1994; Hafen et al. 1984; Struhl & R. A. White 1985). Changes in these regulatory processes can lead to severe developmental problems and disease (e.g (Boncinelli 1997; Del Bene & Wittbrodt 2005; Raman et al. 2000; Sun et al. 2013)). Thus, investigating the molecular mechanisms that regulate *Hox* expression and function during development can provide more insights into this problem.

Here we use the *Drosophila Hox* gene *Ubx* to investigate (i) the molecular mechanisms of RNA processing and its relevance for *Hox* expression and function during the formation of the CNS, and (ii) the biological role of *Hox* post-transcriptional regulation by miRNAs during the development of the central nervous system. The *Drosophila Ubx* gene instructs developmental programs that pattern the posterior thoracic and anterior abdominal segments, influencing the differentiation of distinct cell-lineages that will give rise to tissues such as the epidermis, mesoderm and central nervous system (Morata & Kerridge 1981). *Ubx* mutations in transcriptional control regions can also lead to a homeotic transformation of halteres to wings (see Figures 1.3A and 1.3B).

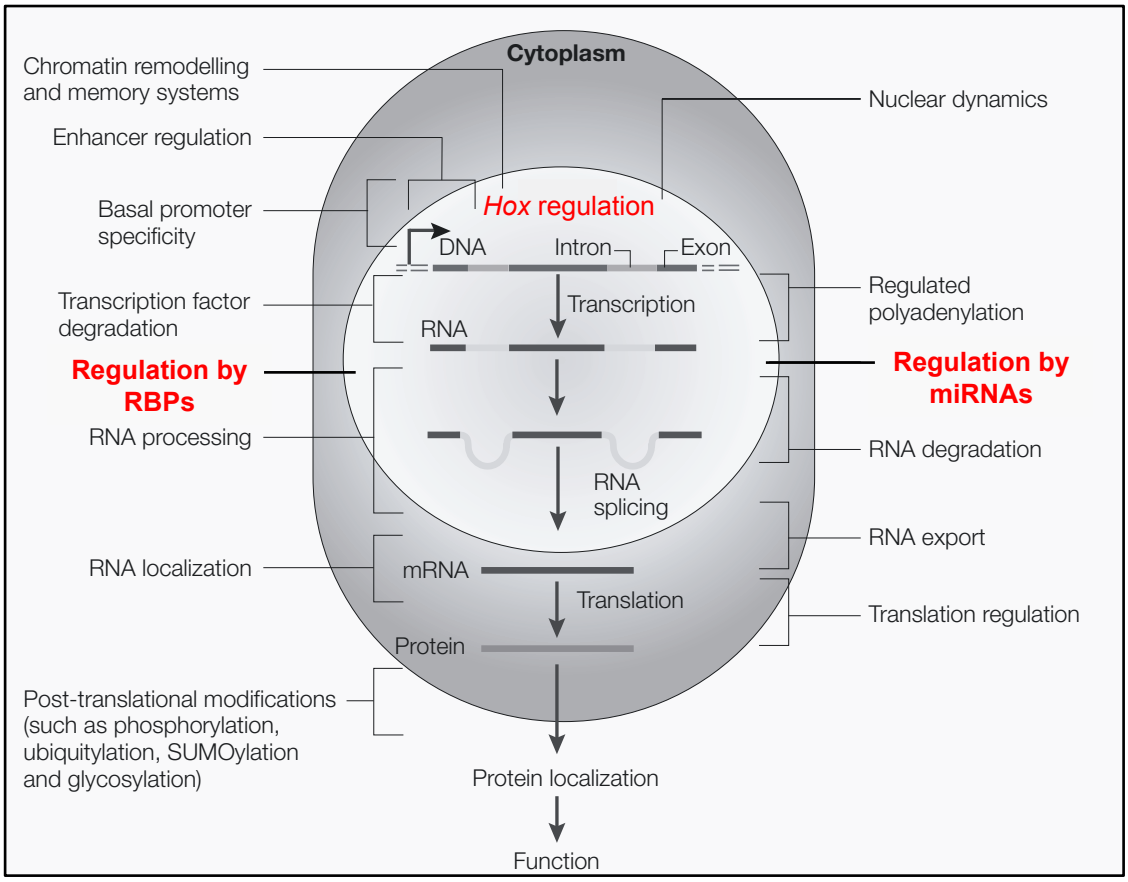

Figure 1.2 Hox gene expression is regulated at multiple levels

Diagram depicting different levels of *Hox* gene regulation. *Hox* gene expression has been shown to be regulated at the chromatin level, through the chromosome nuclear dynamics and modulation of epigenetic marks that control the accessibility of DNA strands to transcriptional regulators, as well as through the direct regulation of transcriptional initiation by transcriptional enhancers. Additionally, *Hox* genes can be the target of regulatory processes acting at the RNA level. Among these are the production of alternative mature RNAs from a single nascent *Hox* transcript (alternative RNA processing involving alternative polyadenylation and alternative splicing) and the repression of translation and/or mRNA degradation by miRNAs. Both processes are mediated by RNA-binding proteins (RBPs), which target specific sequences in *Hox* RNAs. Figure adapted from (Alonso & Wilkins 2005).

1.4 Expression patterns of UBX protein during embryogenesis

The embryonic expression of *Ubx* has been well documented (Akam & Martinez-Arias 1985; Irvine et al. 1991; R. A. White & Wilcox 1985a) (see Figure 1.3C-H). UBX protein is first detected in the epidermis of parasegment (PS) 6 shortly after gastrulation (about 3h45 after egg laying, stage 9) (Figure 1.3C). During germ band extension (stage 11/12), UBX is expressed in the epidermis (PS5-12), CNS (PS6-12), somatic mesoderm (PS6-12) and visceral mesoderm (PS7) as these tissues start to develop (Figure 1.3D and 1.3E). At this point differences in expression become noticeable in PS patterns in the epidermis and somatic mesoderm. In the epidermis, UBX is expressed at low levels in the anterior part of the PS5 and almost absent in the posterior part. In PS6, UBX is highly expressed throughout the parasegment. In PS7-12 gradients of UBX expression are apparent: high levels at the posterior and low at the anterior part of each parasegment, but constant expression on the posterior part along the A-P axis. In contrast to this clear expression modulation, in the somatic mesoderm UBX continues to be expressed from PS6 to PS12 (Akam & Martinez-Arias 1985; Müller & Bienz 1991). By the end of germ band retraction (around 9h30 after egg laying, stage 13) UBX is expressed in PS5-12 of the central nervous system, with low levels in PS5, high levels in PS6, and declining levels from PS7 to PS13 (Figure 1.3F). As development proceeds, the relative abundance of UBX towards the posterior declines further (Figure 1.3H) (Akam & Martinez-Arias 1985; R. A. White & Wilcox 1985a). Furthermore, detailed analysis of UBX protein expression in the CNS reveals that the levels of expression are not uniform within each PS (Figure 1.3I). In fact, levels of UBX

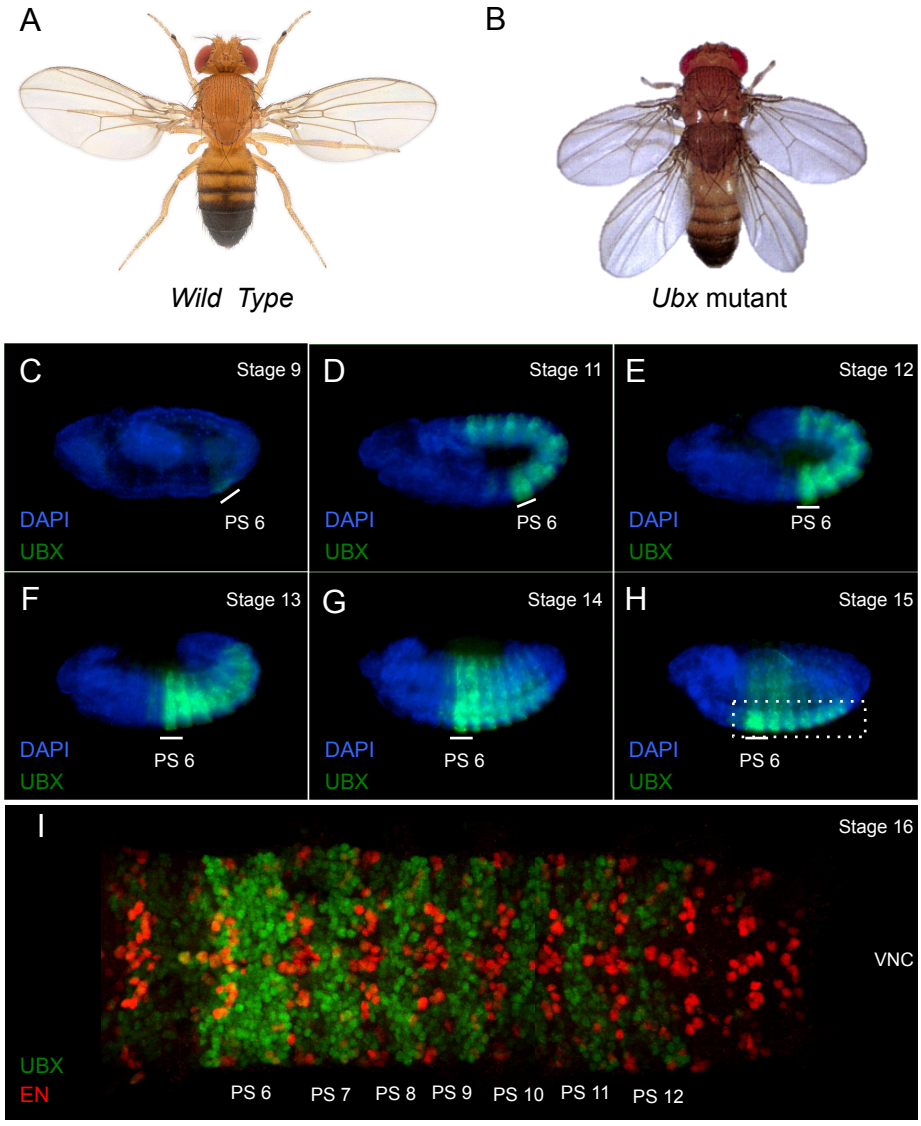

Figure 1.3 The *Drosophila Hox* gene *Ubx* provides identity in the T3 segment and is expressed in the embryonic CNS.

(Legend on the following page)

Figure 1.3 The *Drosophila* Hox gene *Ubx* provides identity in the T3 segment and is expressed in the embryonic CNS.

(A-B) Dorsal view of adult *Drosophila melanogaster wild type* (A) and *Ubx* mutant (B) flies. (B) (Photo taken by E. B. Lewis). Two co-ocurring homozygous mutations in the *Ubx* transcriptional control regions *bx* (*bithorax*) and *pbx* (postbithorax) lead to the loss of UBX protein in the developing T3 segment, leading to a homeotic transformation of halteres to wings. This consists of the transformation of one segment into the likeness of another (T3 -> T2 in this case). **(C-H)** Embryonic expression of UBX protein (green) at mid and late developmental stages. Blue denotes nuclear DNA (DAPI). (H) UBX protein expression becomes progressively restricted to the CNS, which consists of the brain and the ventral nerve cord (VNC, dashed white line); lateral view; anterior is left. **(I)** Dissected VNC at stage 16. Engrailed (En, red) was used as a segmental marker. UBX protein expression (green) is stronger in parasegment 6 and progressively decreases towards more posterior segments. Dorsal view. anterior is left.

vary greatly from cell-to-cell within each PS. Thus, the different tissue types show different expression patterns of UBX and within a particular tissue such as the CNS, the pattern and levels of UBX are seen to change over time as development proceeds.

How are these patterns and levels of UBX regulated during development? This question is discussed in the next subsections. We will describe how *Ubx* expression is regulated from transcription initiation and maintenance to RNA processing and miRNA regulation.

1.5 *Ubx* transcription regulation and epigenetics

The description of UBX expression in classic BX-C “alleles” (*abx*, *bx*, *pbx* and *bxd*) showed that they represent *cis*-regulatory regions involved in the control of *Ubx* transcription (Beachy et al. 1985; Cabrera et al. 1985; R. A. White & Akam 1985; R. A. White & Wilcox 1985b). The regions of *abx*/*bx* and *pbx*/*bxd* regulate *Ubx* expression in PS5 and PS6-13, respectively. In addition, when these elements were linked with a *lacZ* reporter gene, they reproduced to some extent the endogenous UBX expression pattern (Bender & Hudson 2000; Irvine et al. 1991; Simon et al. 1990). The regulation of these *cis*-elements is divided into two phases: initiation and maintenance.

The initial expression domains of *Ubx* are set by a combinatorial activity of gap, pair-rule and segment-polarity genes (Akam 1987; Irish et al. 1989). For example, genetic studies showed that the gap genes *hunchback* (*hb*) and *tailless* (*tll*) set the limits of *Ubx* expression outside PS5-13 by repressing its transcription (Reinitz & Levine 1990; R. A. White & Lehmann 1986), while the

pair-rule gene *fushi-tarazu* (*ftz*) activates *Ubx* transcription (Ingham & Martinez-Arias 1986). Furthermore, these transcription factors bind to *cis*-regulatory elements of *Ubx* regulating its transcription (Müller & Bienz 1992; Zhang & Bienz 1992).

Since many of these factors are transiently expressed in early embryo development, a maintenance mechanism is necessary to ensure *Ubx* transcription throughout development. This maintenance mechanism is based on the epigenetic regulators *Polycomb group* (*Pc-G*) and *trithorax group* (*trx-G*). While *Pc-G* products maintain an inactive state of the transcriptional *cis*-regulatory elements acting as a negative regulator, the *trx-G* products sustain an active state of the transcriptional elements, acting as positive regulators (Chan et al. 1994; Pirrotta 1997; Simon et al. 1993). Both groups function as "memory systems" of chromatin structure by modifying histones (Y. B. Schwartz & Pirrotta 2008). This mechanism of regulation ensures that the initial transcription profiles of *Hox* are maintained all the way through development.

1.6 *Ubx* alternative splicing

The process of alternative splicing (AS) generates different mRNA isoforms from a single gene, increasing protein isoform diversity (Kornblihtt et al. 2013; Matlin et al. 2005; Smith & Valcárcel 2000). According to the central dogma of molecular biology, the production of a functional protein relies on the formation of a mature messenger RNA that conveys the genetic information encoded in the DNA to the ribosome. Splicing, a key step in the maturation of

eukaryotic mRNA transcripts, consists in the removal of intronic sequences and consequent re-positioning the protein-coding exons in tandem, resulting in a translatable message. This process is regulated by the spliceossome which consists of a number of core RNA-binding proteins (RBPs) and small regulatory RNAs that identify splice-sites both upstream and downstream of exons (3' splice-site and 5' splice-site, respectively; reviewed in Witten and Ule 2011 & Licatalosi and Darnell 2010). These RBPs further ensure that intronic excision is precise and does not affect the reading frame of the protein-coding sequence. RBPs also mediate the choice between exclusion and inclusion in the event of optional exon occurrence, thus regulating the production of alternative RNA isoforms from a single locus by AS (Figure 1.4) (reviewed in Witten and Ule 2011 & Licatalosi and Darnell 2010). The *Drosophila* sex-determination cascade is a stark example of this process. The protein product of the Drosophila *transformer* (*tra*) gene is a key regulator of sex-related genes involved in female differentiation. Both developing males and females exhibit transcription of the *tra* locus, resulting in a pre-mRNA containing two constitutive exons in 5' and 3', and a middle optional exon containing an early STOP codon (reviewed in Black 2003). When present, this optional exon leads to the truncation of the *tra* mRNA protein product during translation. In order to produce full Tra proteins in females, the RBP Sex-lethal (*Sxl*) is deployed, binding the 3' splice-site upstream of the optional *tra* exon, thus promoting its exclusion during splicing of the *tra* mRNA. As such, only females produce full Tra proteins due to the RBP-based regulation of *tra* AS (Reviewed in Black 2003). RBP-mediated alternative splicing can also occur in a tissue-specific manner. As an example, the *Drosophila* gene *embryonic lethal abnormal vision*

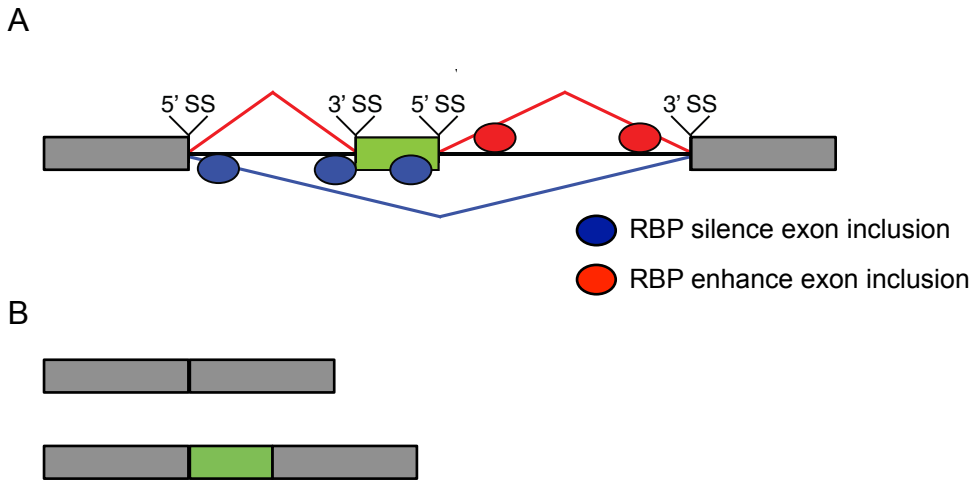

Figure 1.4 Exon inclusion/exclusion is regulated by RNA-binding proteins to produce alternatively spliced mRNAs

(A) Diagram of a pre-mRNA with constitutive exons (grey boxes) and optional exons (green box). Alternative splicing results in either the inclusion or the exclusion of the optional exon. This process is mediated by intronic sequences in *cis*, adjacent to the optional exon [5'Splice Site (SS) and 3'SS]. These sequences are either bound by RBPs that silence exon inclusion (blue circles) or by RBPs that enhance exon inclusion (red circles). **(B)** This process can result in two alternatively spliced mRNA isoforms, one that doesn't include the optional exon (top) and one that includes the optional exon (green box, bottom). The specific isoform produced will depend on the relative strength of 5'SS, 3'SS and RBP binding, as well as the competition between antagonistic RBPs. (Adapted from Witten and Ule 2011)

(*elav*) gene encodes for a neuronal-specific RBP (ELAV) that promotes the production of neuronal-specific splicing isoforms of the otherwise broadly expressed *neuroglian* (*nrg*) gene (Koushika et al. 1996, Lisbin et al. 2001). This is achieved through direct binding of ELAV to *nrg* pre-mRNAs, which promotes alternative inclusion of a 3'-terminal exon (Lisbin et al. 2001).

Many *Hox* genes in *Drosophila* have multiple protein isoforms generated via AS (see (Mallo & Alonso 2013). A good example of this phenomenon is the production of six *Ubx* mRNA isoforms during development (Kornfeld et al. 1989; O'Connor et al. 1988). The *Ubx* locus is composed by a 5' exon, two microexons (M1 and M2) and a 3' exon (homeobox). *Ubx* splicing isoforms differ from one another by the absence or presence of the two microexons that separate the 5' exon from the 3' exon. The resulting isoforms are named according to which exons are included in the transcript: all exons (I); 5' exon, M2 and 3' exon (II); and just the 5' exon and 3' exon (IV). Additionally, each isoform is named as "a" or "b" depending on the exclusion (a) or inclusion (b) of a b element located between the two donor splicing sites of the first exon (5'exon). *Ubx* AS isoforms are formed by a process of resplicing, where the splicing of the first intron generates a transcript substrate with a consensus 5' splice site (between 5' exon and M1) that is used for sequential splicing events (Hatton et al. 1998). This process is affected by the rate of RNA polymerase II elongation in *Ubx* transcripts (la Mata et al. 2003).

Interestingly, the expression pattern of the different *Ubx* isoforms varies in space and time during embryonic development (Artero et al. 1992; Lopez & Hogness 1991). In early development, UBX Ia is the predominant isoform being expressed in the epidermis and mesoderm. As development proceeds (after germ band retraction), UBX Ia continues to be expressed in the epidermis and mesoderm but is not detected in the CNS. In contrast, isoforms that lack microexon 1 are expressed primarily (UBX IIa) or exclusively (UBX IVa) in the CNS at late stages of embryogenesis. Remarkably, the spectrum and expression pattern of UBX isoforms is conserved in *Drosophila* species that diverged at least 60 million years ago (Bomze & Lopez 1994). These observations strongly suggest (i) a functional role for the different isoforms during embryogenesis and (ii) that the molecular mechanisms that regulate *Ubx* alternative splicing are conserved over long evolutionary distances. In fact, work in our laboratory and elsewhere demonstrated that different UBX isoforms perform distinct functions in embryonic and adult development (Mann & Hogness 1990; de Navas et al. 2011; Reed et al. 2010). Nonetheless, the molecular mechanisms that regulate *Ubx* alternative splicing during embryonic development remain largely unknown.

1.7 *Ubx* alternative polyadenylation

The original molecular work describing the *Ubx* gene products indicated the existence of two *Ubx* transcripts with different 3' Untranslated Region (UTR) lengths (short and long *Ubx* 3'UTRs) generated through alternative

polyadenylation (APA) (Kornfeld et al. 1989; O'Connor et al. 1988). *Ubx* has two polyadenylation (pA) sites in the 3'UTR, a proximal site located approximately 1kilobase (Kb) after the last exon and a more distal site located ~2.1kb from the last exon. Since then, 3'UTRs were shown to contain information that dictates mRNA stability, localisation and transport, translation efficiency through interactions with trans-acting regulators like RBPs and miRNAs (Alonso 2012; Bartel & Chen 2004; Bartel 2009; Kedde et al. 2010; Lutz 2008; Moore 2005). Thus, the two *Ubx* 3'UTRs could contain different regulatory information, so that the expression of alternative *Ubx* transcripts can be differentially regulated during embryonic development.

Interestingly, recent work in our laboratory described that the two *Ubx* 3'UTR isoforms display distinct temporal and spatial patterns of expression during embryogenesis (see Figure 1.5) (Thomsen et al. 2010). Notably, longer *Ubx* 3'UTRs are exclusively expressed in the CNS (Figures 1.5D and 1.5E) after germ band retraction until the end of embryogenesis, while shorter *Ubx* 3'UTRs are expressed in all tissues throughout development (Figures 1.5B and 1.5C). These expression patterns of *Ubx* APA isoforms resemble the expression patterns observed in *Ubx* AS isoforms (see above). Indeed, there is an association between *Ubx* splicing isoforms and 3'UTR isoforms: *Ubx* Ia has a shorter 3'UTR, and *Ubx* IIa and *Ubx* Iva have predominately a long 3'UTR (Kornfeld et al. 1989; Thomsen et al. 2010). This raises the possibility that the two RNA processing events could be coupled and/or regulated by common factors.

Moreover, other *Hox* genes from the BX-C (*abd-A* and *Abd-B*) and ANT-C (*Antp*) show similar and synchronous APA events during embryogenesis to

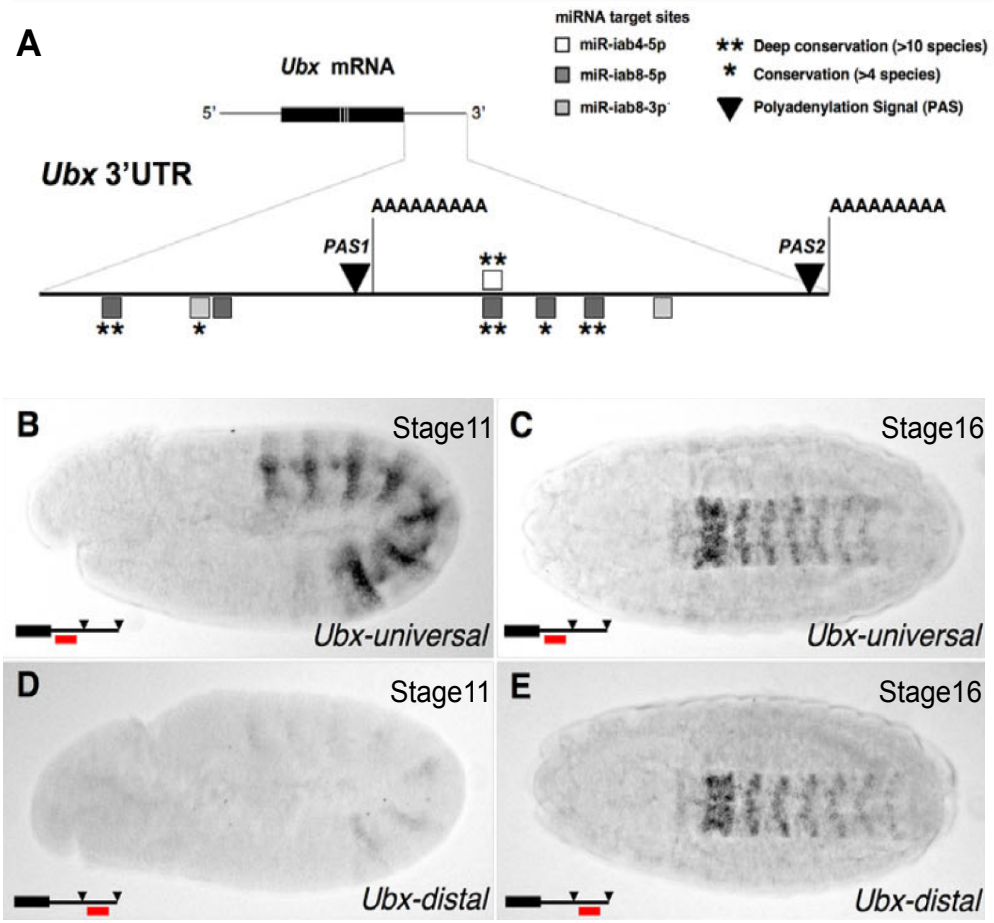

Figure 1.5 *Ubx* shows alternative 3'UTR formation that mediates differential visibility to miRNAs in a developmentally regulated manner

(Legend on the following page)

Figure 1.5 *Ubx* shows alternative 3'UTR formation that mediates differential visibility to miRNAs in a developmentally regulated manner

(A) *Ubx* pre-mRNAs can be processed alternatively so that the resulting mRNAs display alternative 3'UTRs of different lengths (Short *Ubx* 3'UTR: 951 b.p.; long *Ubx* 3'UTR: 2396 b.p.). The production of these distinct 3'UTR tracts is dependent on signals in *cis* (polyadenylation signal sites or PASs). The alternative *Ubx* 3'UTRs also possess conserved miRNA target-sites for different miRNAs of the *iab4/iab8* locus. The number and type of these miRNA sites is also distinct between the two versions of the *Ubx* 3'UTR (*e.g. miRNA-iab4-5p* target-sites only occur in the distal *Ubx* 3'UTR). **(B-E)** Expression analysis of alternative *Ubx* 3'UTRs at different stages of embryonic development by RNA *in-situ* hybridization. Anterior is left. (B) At stage 11, the signal intensity is very strong for the universal probe (*Ubx* Short 3'UTR). (C) The strength of the universal probe signal is maintained at later stages (stage 16, CNS). (D) While the signal intensity for the distal probe (*Ubx* Long 3'UTR) is almost non-existent in early stages, (E) stage 16 embryos exhibit strong expression in the CNS. These results led Thomsen et al. 2011 to conclude that Early stages display mostly *Ubx* Short 3'UTR expression, whereas in late stages, *Ubx* mRNAs mostly carry the Long version of the Ubx 3'UTR. Figure taken from Thomsen et al. 2010.

the ones observed in *Ubx* (Thomsen et al. 2010). A recent computational study observed that *Hox* APA is conserved across different *Drosophila* species that diverged more than 60 million years ago (Patraquim et al. 2011). These observations suggest that *Hox* APA is an ancestral attribute of the *Drosophila* group.

Regarding the functional implications of *Ubx* APA, computational analysis revealed that the short and long *Ubx* 3'UTRs contain very different target sites for miRNA regulation (Figure 1.5A) (Thomsen et al. 2010). Indeed, when the short and long *Ubx* 3'UTRs were linked with a fluorescent reporter (Figure 1.6A) they showed differential regulatory capacity in the CNS: short isoforms had a constant expression along the A-P axis (Figure 1.6B), while the expression of the long isoforms decayed towards the posterior abdomen (Figure 1.6C). Remarkably, the declining expression towards posterior of the long isoform resembles endogenous expression of UBX protein in the CNS (R. A. White & Wilcox 1985a) .

1.8 *Ubx* regulation by miRNAs

miRNAs are an endogenous class of small RNAs ~22 nucleotide long, pervasive in multicellular eukaryotes that negatively regulate gene expression (reviewed in Bartel 2009; Winter et al. 2009). miRNAs are loaded into the RNA Induced Silencing Complex (RISC) and guide the RISC complex to target specific mRNAs. The specificity of target detection is based on miRNA-mRNA complementarity: miRNA bind complementary sites in the 3'UTR of target

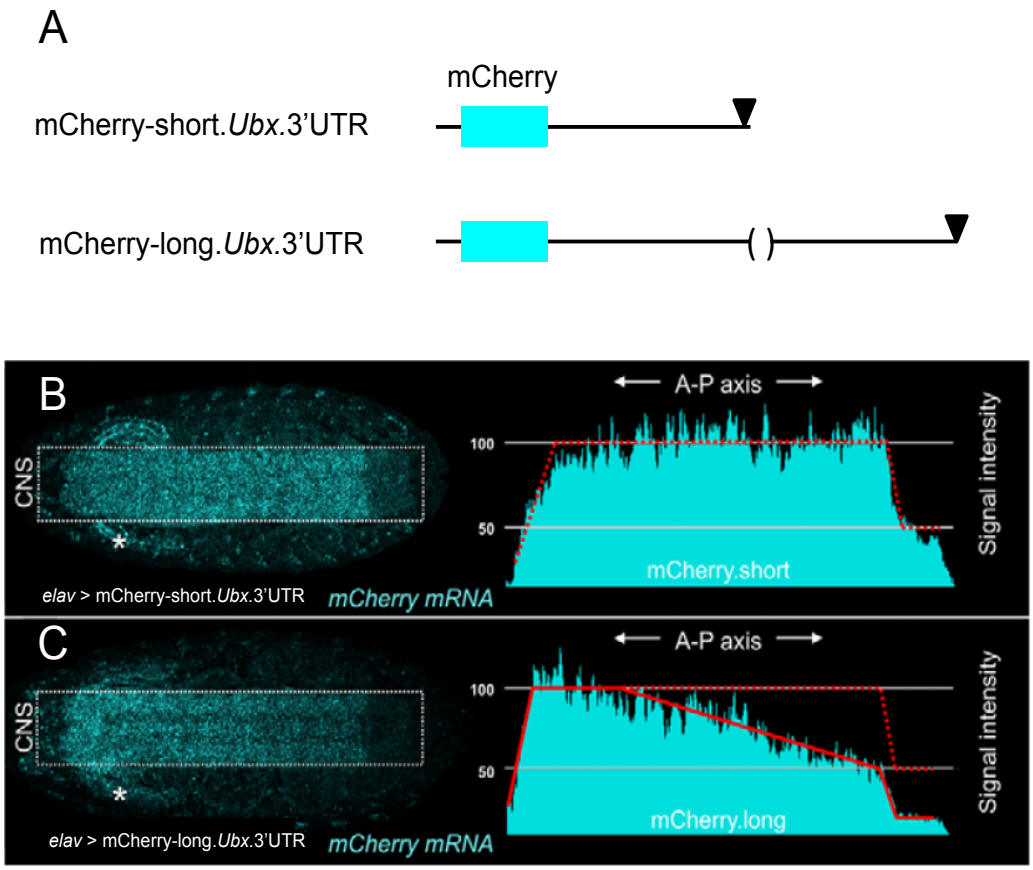

Figure 1.6 The long version of the *Ubx* 3'UTR recapitulates the CNS expression of UBX protein in late embryonic stages

(Legend on the following page)

Figure 1.6 The long version of the *Ubx* 3'UTR recapitulates the CNS expression of UBX protein in late embryonic stages

(A) Structure of *Ubx* 3'UTR expression reporter constructs. Two constructs carrying an mCherry coding-sequence were attached to each of the alternative 3'UTR sequences of *Ubx* (*Ubx* Short and *Ubx* Long) of the *Ubx* gene. The first PAS of the mCherry-Long construct (parenthesis) was mutated so that no secondary production of Short *Ubx* 3'UTRs was possible. Inverted black triangles define the position of existing PASs. Both constructs were produced by Thomsen et al. 2011. **(B-C)** Expression of the *mCherry-Ubx 3'UTR* constructs in the CNS of stage 16 embryos, using a *elav-Gal4* driver. mCherry expression was detected by RNA *In-situ* hybridizations using probes antiparallel to the mCherry RNA sequence. (B) The expression pattern of the mCherry construct expanded posteriorly in the CNS, when attached to a Short version of the *Ubx* 3'UTR. (C) Expression of the reporter construct seemed to decrease progressively in the posterior portion of the CNS when attached to a Long *Ubx* 3'UTR. This expression pattern recapitulates the UBX protein expression previously observed, leading Thomsen et al. 2011 to conclude that the *Ubx* Long 3'UTR contains sufficient regulatory information in *cis* to correctly define the general patterns of *Ubx* expression in the CNS of late embryos. Anterior is left. Figure taken from Thomsen et al. 2010.

mRNAs and induce RNA degradation and/or translation repression (Figure 1.7).

Within the BX-C two genes encoding miRNAs are present between *abd-A* and *Abd-B*: *miR-iab-4* and *miR-iab-8* (Aravin et al. 2003; Stark et al. 2008; Tyler et al. 2008). *miR-iab-4* and *miR-iab-8* are located on the same genomic region but are transcribed from opposite DNA strands in two long non-coding RNAs: *iab4* and *iab8* (*iab* stands for *infraabdominal*). In spite of this, they are functionally different in their targeting and expression domains (Tyler et al. 2008; Stark et al. 2008). In germ band extended embryos they are both expressed in the ectoderm and mesoderm but in different segments: *miR-iab4* is expressed from A5 to A7 (PS10-PS12) and *miR-iab8* in A8-A9 (PS13-14). As development advances, they became exclusively expressed in the CNS and the expression of *miR-iab4* expands to A2 until A7 (PS7-12).

Ectopic overexpression and cell culture experiments showed that *miR-iab-4* and *miR-iab-8* are sufficient to regulate UBX and ABD-A protein expression by targeting the 3'UTRs of their corresponding mRNAs (Ronshaugen et al. 2005; Stark et al. 2008; Tyler et al. 2008). In contrast, genetic removal of *miR-iab4/iab8* (*ΔmiR-iab4/iab8*) through gene conversion only affected UBX protein expression with no apparent changes in the expression pattern of ABD-A (Bender 2008). In absence of *miR-iab4/iab8*, expression of UBX protein increased drastically in abdominal segments of the CNS (PS7-13) of the late stage embryos (after germ band retraction), but not in early embryos (germ band extension) (Bender 2008; Thomsen et al. 2010). These results are compatible with the hypothesis that long *Ubx* 3'UTRs are regulated by miRNAs in the CNS due to a suite of unique miRNA target sites, as the CNS expression of long *Ubx* 3'UTRs attached to an mCherry reporter

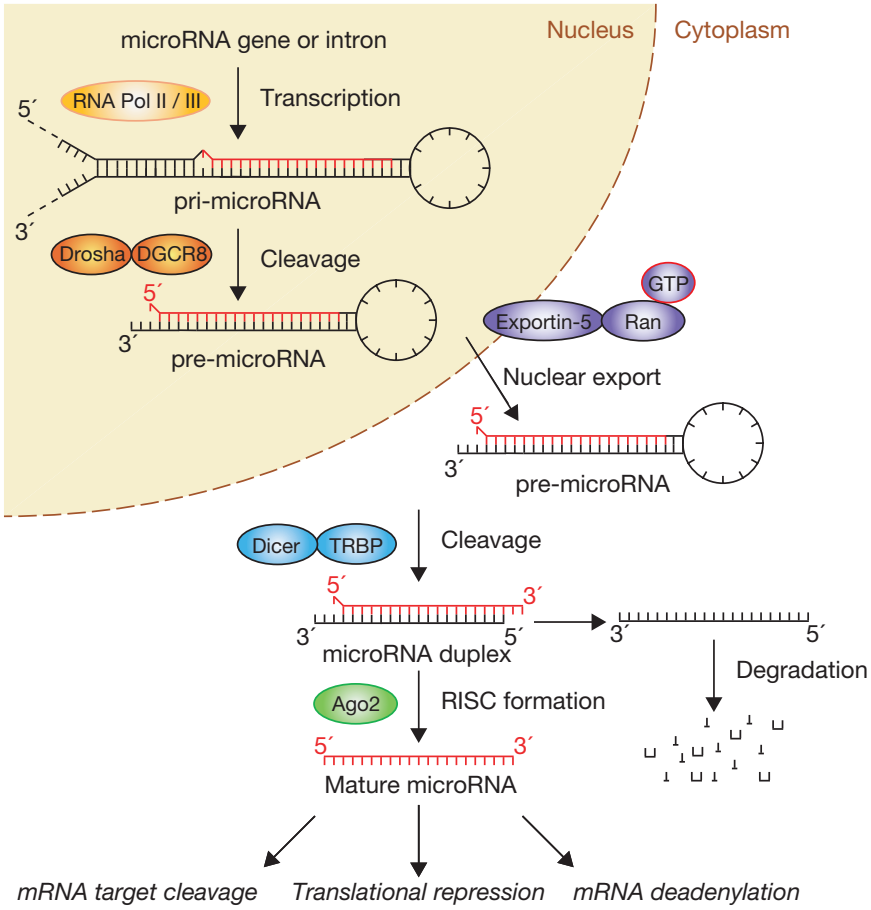

Figure 1.7 miRNAs are a regulatory class of non-coding genes that act with the RISC complex to post-transcriptionally regulate target mRNAs

(Legend on the following page)

Figure 1.7 miRNAs are a regulatory class of non-coding genes that act with the RISC complex to post-transcriptionally regulate target mRNAs

(A) Schematic diagram of miRNA biogenesis (taken from Winter et al. 2009). miRNA biogenesis starts with the transcription of the miRNA locus in the nucleus, effected by RNA Polymerases II (mainly) and III. The resulting nascent RNA transcript of about 70-100 ribonucleotides in length (pri-microRNA), which folds in a stereotypical stem loop structure, is then recognized by the microprocessor complex [(consisting of proteins Drosha and DGCR8 (Pasha)]. Drosha proteins recognize and cleave an overhang in the terminal portion of the pri-miRNA stem, generating a 65-70 ribonucleotide-long pre-miRNA. The pre-miRNA is exported to the cytoplasm by Exportin 5, a nuclear membrane protein. This process is energy-dependent and thus relies on the Ran-GTP cofactor. In the cytoplasm, pre-miRNAs are recognized and their characteristic loop is cleaved by Dicer, a protein of the RNA-induced silencing complex (RISC), generating a double-stranded RNA molecule carrying the mature miRNA strand (usually the most thermodynamically unstable) and its complementary (passenger) strand. The latter usually undergoes degradation but can also be used as a mature RNA (miRNA*). The mature miRNA is then bound by another member of the RISC, Argonaute (Ago). Together, miRNA and Argonaute bind miRNA target-sites in complementary 3'UTRs and direct the cleavage, repression or deadenylation of the target mRNA. Figure taken from Winter et al. 2009.

shows a decay in reporter signal in the same abdominal segments of the CNS (PS7-13) (Thomsen et al. 2010). Furthermore, it is at this point in embryonic development when *Hox* input modulates the differentiation/specification of post-mitotic neurons (Karlsson et al. 2010; Miguel-Aliaga & Thor 2004; Miguel-Aliaga et al. 2008; Suska et al. 2011; Rogulja-Ortmann et al. 2008; Rogulja-Ortmann & Technau 2008).

These findings raise the intriguing hypothesis that miRNA-regulation of *Ubx* might be dictating the fine-grain intra-segmental expression of UBX during *Drosophila* CNS development which ultimately controls specific patterns of neuronal differentiation.

1.9 Development of the embryonic CNS of *Drosophila*

The CNS typically displays high cellular diversity and complexity in structure. In order to orchestrate CNS development, large numbers of genes and cell interactions are tightly regulated in time and space (for reviews see (Skeath & Thor 2003; Technau et al. 2006). The CNS of insects is composed of the ventral nerve cord (VNC) and the brain (Figure 1.8A). We will focus on the development of the *Drosophila* VNC, since *Ubx* is expressed in this region. The VNC consists of a sequence of segmental units (neuromeres) that develop from a monolayer of ventral neuroectodermal cells (ventral neurogenic region) (Hartenstein & Campos-Ortega 1984). After gastrulation, cells in the neuroectoderm go in one of two alternative developmental pathways: neurogenesis or epidermogenesis. This differentiation occurs in two steps and

is controlled by two groups of genes: proneural genes (*Achaete Scute Complex*) and neurogenic genes (Notch/Delta signalling pathway). In a first step, expression of proneural genes confers neuronal competence to groups of neuroectodermal cells, proneural clusters (Jiménez & Campos-Ortega 1990). Initially, within each proneural cluster the expression of proneural genes is uniform and all cells have the same developmental potential (neural equivalence group). However, only one cell per cluster adopts a neuronal fate, while all others will assume an epidermogenic fate. This decision is based on cell-to-cell interactions mediated by Notch/Delta signalling (lateral inhibition) (Campos-Ortega 1995). In an equivalence group, the cell that has higher levels of Delta (or lower levels of Notch) will activate Notch signalling in the neighbouring cells and consequentially repress the expression of proneural genes. Therefore, this cell will have the highest expression of proneural genes and will become a neuronal progenitor/stem cell, neuroblast (NB) (Campos-Ortega 1995). Subsequently, the NBs enlarge and delaminate from the ventral neurogenic region to the interior of the embryo (Figure 1.8).

During germ band extension (stages 8-11), five sequential waves of NB delamination result in the formation of a stereotypic pattern of approximately thirty NBs per hemisegment (bilateral half of a segment/neuromere) (Figure 1.8C) (Doe 1992; Hartenstein & Campos-Ortega 1984). Each NB is characterised by the time of delamination, position and expression of molecular markers (Broadus et al. 1995; Doe 1992). Upon delamination, each NB divides asymmetrically in a stem cell manner, renewing itself in each division and generating a chain of smaller secondary precursor cells called ganglion mother cells (GMCs) into the interior of the embryo. Each GMC is divided once to

produce two postmitotic cells, neurons and/or glia. By the end of embryogenesis each hemisegment of the VNC will have about 350 postmitotic cells (approximately 290 interneurons, 35 motorneurons and 25 glia) (Figure 1.8E) (Beckervordersandforth et al. 2008; Landgraf et al. 1997; Landgraf & Thor 2006).

Each NB produces a nearly invariant and exclusive cell lineage with specific numbers and types of neuronal and/or glial cells (Bossing et al. 1996; Schmid et al. 1999; Schmidt et al. 1997). This unique identity is specified already in ectodermal proneural clusters prior to NB delamination and is determined by their position on each hemisegment. Positional information on each hemisegment is given by a Cartesian grid-like coordination system established by two sets of genes: anterior-posterior and mediolateral patterning genes. The anterior-posterior genes are the segment polarity genes involved in embryonic segmentation (e.g. *wingless*, *engrailed*, *gooseberry* and *patched*). The mediolateral axis is subdivided in three adjacent longitudinal columns through the activity of at least four genes: *ventral nervous system defective* (medial column), *intermediate neuroblast defective* (intermediate column), *Epidermal growth factor receptor* (medial and intermediate) and *muscle segment homeobox* (lateral column) (see in (Technau et al. 2006) (Figure 1.8B).

The Cartesian grid model discussed above explains how the identity of each NB lineage is acquired, but it cannot explain how the cellular diversity is generated within each lineage. This is controlled by a temporal cascade of transcription factors that are expressed in the NB, and transmitted to the GMC and the postmitotic cells: *huncback* (*hb*) → *Kruppel* (*Kr*) → *Pdm* → *castor* (*cas*) →

grainyhead (*grh*) (see Figure 1.8D) (Baumgardt et al. 2009; Brody & Odenwald 2000; Isshiki et al. 2001; Novotny et al. 2002). The temporal cascade occurs during the series of NB asymmetric divisions. NBs express *hb* as they delaminate and start the first rounds of division. The progeny of the *hb*-expressing NB (GMCs and postmitotic cells) retains *hb* expression and differentiates under its control. Then, in the next temporal window, *hb* is downregulated in the NB and expresses *Kr*, starting a new cycle of differentiation. This process continues until the NB enters into apoptosis or into a quiescent state. It was shown that this temporal cascade is controlled by cross-regulatory interaction between the genes in the network. For example, *hb* activates *Kr* expression but repress *Pdm* expression, ensuring *Kr* expression but not *Pdm* in the next temporal window. Although this temporal cascade of transcription factors explains how a given lineage progresses, several questions remain largely unanswered: how do the temporal genes regulate cellular differentiation; what are the downstream targets of these genes; and how, within each expression window, is there generation of different cellular type (reviewed in Skeath and Thor 2003).

The number of NBs and the characteristics of each NB are identical along the A-P axis in the VNC with two exceptions: thoracic NBs delaminate slightly earlier than their abdominal homologs in a single embryo and the two terminal segments (first subesophageal and ninth abdominal) have less NBs (Doe 1992). Also, the Cartesian grid-like is the same on each hemisegment along the A-P axis. Thus, every NB has a “homolog” in the different segments forming a serial of homolog hemisegments along the VNC (see above and Figure 1.8B). Even though the “ground state” of NB specification is the same in

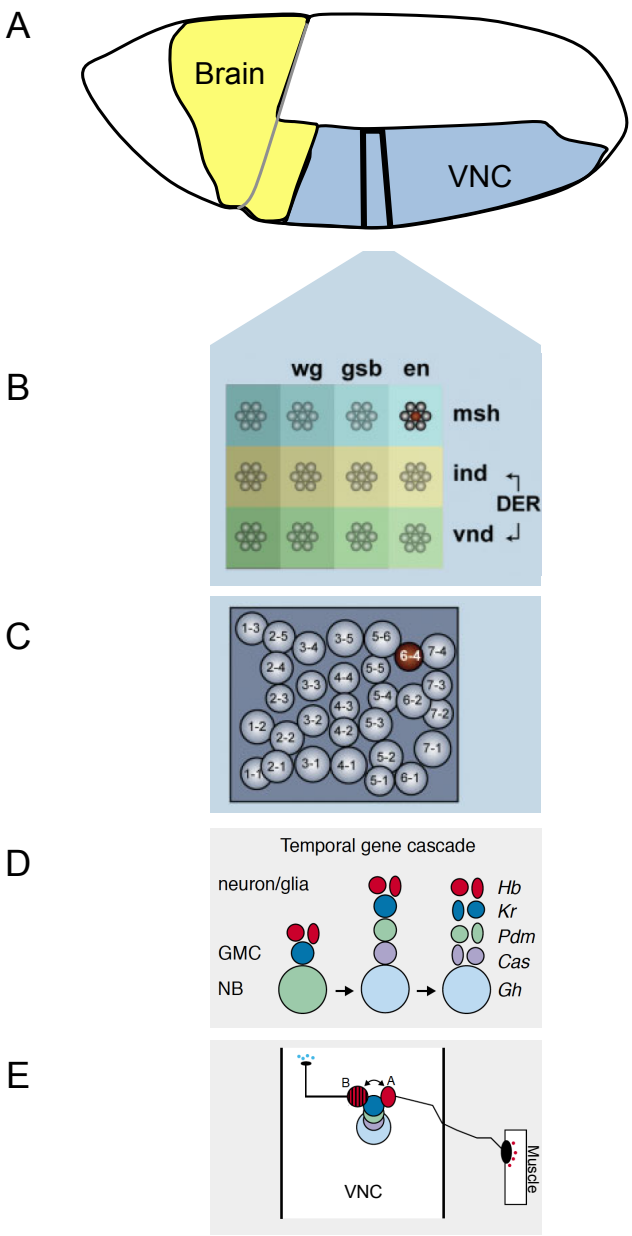

Figure 1.8 Development of the embryonic VNC of *Drosophila*

(Legend on the following page)

Figure 1.8 Development of the embryonic VNC of *Drosophila*

(A-C) Neurogenesis fate map of an embryo at the early gastrula stage (adapted from Technau et al. 2006). (A) The brain develops from the procephalic region apparent at this stage (depicted in yellow). The VNC arises from the ventral neurogenic region (blue). (B) The cartesian grid-like coordination of neuroblast determination is established by two sets of genes: anterior-posterior and mediolateral patterning genes. The anterior-posterior genes are the segment-polarity genes *wingless* (*wg*), *gooseberry* (*gsb*) and *engrailed (en*). The mediolateral axis is subdivided in three adjacent longitudinal columns through the activity of at least four genes: *ventral nervous system defective* (*vnd)*, *intermediate neuroblast defective* (*ind*), *Drosophila* EGF receptor (*DER*) and *muscle segment homeobox* (*msh*). The combinatorial effect of these genes will determine the neuroblast fate according to each position in the Cartesian grid. (C) Diagrammatic representation of all neuroblasts in an hemisegment after determination. Each neuroblast will assume a stereotypical position (numbered) within a given hemisegment. As an example, in NB 6-4, “6” refers to a posterior position within the segment (1-7) and “4” refers to an intermediate position along the mediolateral axis (1-6). **(D-E)** Neuroblast differentiation is regulated by a temporal gene cascade and asymmetric ganglion mother cell (GMC) division (adapted from Skeath and Thor 2003). (D) The differentiation of a neuroblast lineage is controlled by the following sequential expression of the following transcription-factor cascade: *Hb* (red), *Kr* (blue), *Pdm* (green), *Cas* (purple), *Gh* (light-blue). This results in distinct GMC identities. **(E)** Each distinct GMC divides asymmetrically (daughter cells A and B) leading to the specification of glial cell and neuronal with differential identities. **(continued in the next page)**

(continued from the preceding page) This process leads to the formation of approximately 350 postmitotic cells in each hemisegment (approximately 290 interneurons, 35 glial cells and 35 motoneurons which will innervate the muscles).

the different segments, 7 out of 30 serially homologous lineages were shown to differ between thoracic and abdominal segments (Bossing et al. 1996; Schmid et al. 1999; Schmidt et al. 1997; Udolph et al. 1993). For example, the lineage of NB6-4 in the thorax is formed of 4-6 interneurons and 3 glial cells, while in the abdomen only produces 2 glia. This segmental diversity of lineages along the VNC is under *Hox* gene control (see below).

The embryonic development of the CNS leads to the setting of cellular identities and interactions, whose anatomy and function will underlie the behaviour of free-roaming larvae just a few hours later. As such, we expect this process to influence the coordination of larval behaviour.

1.10 Larvae Locomotory Behaviour

Larval motor coordination is established during the last three hours of embryogenesis (Crisp et al. 2008). Muscle contractions controlled by neural activity start at embryonic stage 17 (17 hours after egg laying) and one hour later (still at stage 17) coordinated crawling sequences begin. The maturation of more complex behaviours such as reflex to touch response and the ability for individuals to self-right when turned upside down only occurs 20 hours and 20.5 hours after egg laying, respectively (Crisp et al. 2008). It was shown that the maturation of coordinated crawling movement is dependent on the endogenous patterns of neuronal activity (Crisp et al. 2011), but which types of neurons are necessary remains totally unknown.

Twenty-one hours after egg laying (at 25ºC) larvae hatch from the eggshell and start to explore the environment. This exploratory behaviour of larvae is based on forward crawls interspersed with turns (Berni et al. 2012; Lahiri et al. 2011). A forward crawl consists on a forward peristaltic wave of muscle contraction that is initiated in the most posterior abdominal segments (A8/9) and propagates to the anterior abdominal segments (from A7 to A1). During the propagation of the wave each abdominal segment is transiently lifted from the substrate, pulled forward and lowered. Then, abdominal segments anchor to the substrate through ventral cuticular denticles and move the body forward (Dixit et al. 2008). The forward extension of the thorax and the head and sequential anchoring of the mouth hooks complete the movement. Turns are initiated in the end of a forward wave and consist of an asymmetrical contraction of the abdominal segments. This unilateral contraction starts in A1 and proceeds as far as A4 and consequently bends the anterior part of the animal (Berni et al. 2013). At this point, if a forward wave is initiated the animal will crawl in a different trajectory from where it was before the turn. Thus, the locomotory behaviour of larvae consist of repetitive movements that are dependent on the coordination of central pattern generators (CPG) (Suster & Bate 2002). CPGs are circuits that produce organised and repetitive motor patterns (Marder et al. 2005). Recent work showed that the CPG for substrate exploration is localised in the thoracic and abdominal regions of the nervous system, while the brain simply modulates this exploratory behaviour in response to environmental cues (Berni et al. 2012). However, many questions still remain unresolved. Are the CPGs of these alternative behaviours (crawls and turns)

located in different segments? What is the neuronal network that underlies these CPGs? How do the circuits work?

Past studies tried to tackle some of these questions by silencing neural activity in broad groups of neurons (Suster et al. 2003) or in random interneurons (Iyengar et al. 2011). No matter how promising these studies were, they did not manage to identify specific groups (or networks) of neurons affecting specific behaviours. This may have been due to the complexity of the system (e.g. same neurons involved in different behaviour programs) or the technical limitation of available tools, as they target large groups of neurons. The recent development of thousands of specific neuronal *Gal4* drivers by laboratories in Janelia Farms (Jenett et al. 2012; Pfeiffer et al. 2008; Manning et al. 2012) and high-throughput tools to analyse larvae behaviour (Branson et al. 2009; Gomez-Marin et al. 2012) will shed some light in these questions.

1.11 *Hox* genes in the development of the *Drosophila* CNS

There is accumulating evidence that *Hox* genes are involved at different steps of the embryonic CNS development in *Drosophila* to generate segment-specific lineages (Rogulja-Ortmann & Technau 2008). Studies from the Technau lab at the University of Mainz in Germany showed a role of *Hox* genes in the early differentiation of segment-specific NB lineages (NB1-1 and NB6-4) (Berger, Pallavi, Prasad, Shashidhara & Technau 2005a; Prokop & Technau 1994). It was shown that the thoracic NB1-1 represents the “groundstate” of the lineage (*i.e.* does not require *homeotic* input) where it generates 2 motoneurons and 10 interneurons (Prokop & Technau 1994; Udolph et al. 1993). The activity

of UBX and ABD-A in the abdomen is required and sufficient for the lineage NB1-1 to have an abdominal fate and generate 1 motoneurons, 6 interneurons and 3 glial cells (Prokop & Technau 1994). Nonetheless, the molecular and cellular mechanisms of how *Hox* activity in NB1-1 transforms the lineage according to A-P position are unknown. In a more recent study, the cellular mechanisms of *Hox* action in segment-specific lineage differentiation were explored (Berger, Pallavi, Prasad, Shashidhara & Technau 2005a; Berger, Pallavi, Prasad, Shashidhara & Technau 2005b). Berger and colleagues observed that in the thorax NB6-4 has series of asymmetric divisions producing a lineage of 4-6 interneurons and 3 glia, while in the abdomen NB6-4 divides once symmetrically and produces 2 glia. The transition from asymmetric to symmetric NB division is controlled by the activity of ABD-A (A1-A6) and ABD-B (A7, A8) in the direct repression of the cell cycle gene *Cyclin E* (Kannan et al. 2010).

Hox genes also regulate neuroblast differentiation along the A-P axis during the temporal cascade of transcription factors (Karlsson et al. 2010). In the abdomen, BX-C genes induce the cell cycle exit of NB5-4 blocking the progression of *Pdm* to *cas* expression in the NB. On the other hand, in the thorax, NB5-4 continues to divide and generates *apterous*-expressing neurons under ANTP control. These are a subset of neurons that expresses neuropeptides under the control of Apterous, a transcription factor (TF). Additional studies showed that ABD-A controls neuronal proliferation in the abdomen via NB apoptosis in larvae stages (Bello et al. 2003; Cenci & Gould 2005).

At the level of postmitotic cells, *Hox* genes are involved in multiple

process of neural specification along the A-P axis: neuronal apoptosis (Rogulja-Ortmann et al. 2008), neuronal survival (Miguel-Aliaga & Thor 2004) and neuronal peptide specification (Miguel-Aliaga et al. 2008; Suska et al. 2011). For example, in the NB7-3 lineage levels of *Ubx* control the apoptosis of the GW neuron (Rogulja-Ortmann et al. 2008)

Finally, it was shown that *Hox* genes control the peristaltic crawling of larvae (Dixit et al. 2008). A combination of loss and gain of function experiments showed that *Ubx* and *abd-A* are necessary and sufficient to control the formation of a neuromuscular network that coordinate the movements of peristaltic locomotion.

Altogether, these studies suggest that many steps of the neuronal differentiation process are under *Hox* control. However, few address the control of *Hox* expression itself in the developing CNS.

1.12 Aims and outcomes of the thesis

As argued above, the regulation of *Hox* genes in the *Drosophila melanogaster* central nervous system attains considerable complexity, involving chromatin remodelling, multiple transcriptional inputs, various RNA processing mechanism (alternative splicing and alternative polyadenylation) and post-transcriptional *trans*-regulators. However, not much is known about how different regulatory levels achieve a coordinated *Hox* output. We also know little about which factors affect *Hox* expression beyond transcription. Importantly, the way in which *Hox* expression patterns are impacted by each of the different

levels of *Hox* regulation remains largely unknown. Finally, we are at present unaware of the biological consequences of *Hox* post-transcriptional regulation in the CNS.

This dissertation aims at addressing the aforementioned questions. We start by interrogating the role of RBPs in the correct processing of *Hox* RNAs in Chapter 3. We first characterise the role of the pan-neural RNA-binding protein ELAV on the generation of alternative *Ubx* RNAs. We then show that the ELAV-mediated RNA processing of *Ubx* RNAs is likely direct and that it significantly affects the expression levels of UBX protein, thus highlighting that the correct establishment of *Ubx* RNA processing patterns is key to guarantee normal protein levels. Further, we investigate this regulatory interaction in other *Hox* genes and show that the tight link between ELAV, *Hox* RNA processing patterns and protein levels is a recurring theme in the regulation of *Hox* genes of the *Bithorax*-complex in the developing CNS.

In Chapter 4, we ask whether post-transcriptional regulation of *Ubx* is biologically relevant for neural development. We first ask whether miRNA regulation significantly impacts on the correct establishment of both *Ubx* expression and function in the CNS. We use a series of behavioural assays to show that the disruption of miRNA-based regulation leads to both mispatterning of *Ubx* expression in the CNS and a defect in a specific larval behaviour, self-righting. We then show that these are not independent events as artificially mimicking the effects of miRNA removal on *Ubx* expression leads to the same specific larval behaviour defect. Thus, we show that the *Ubx* repression by miRNAs is required for the coordination of a specific larval behaviour.

With this in mind, in Chapter 5 we explore the cellular basis of larval behaviour in the context of miRNA-dependent *Ubx* regulation. We establish that the removal of miRNAs and consequent mispatterning of *Ubx* expression in the CNS does not lead to major anatomical defects in either the CNS or muscles. Nevertheless, we observe that overexpression of *Ubx* in cholinergic interneurons during neuronal specification leads to defects in self-righting behaviour. Furthermore, we show that UBX protein expression is regulated by miRNAs in the same cholinergic interneurons. This leads us to propose that the post-transcriptional layer of *Hox* regulation is not involved in the establishment of the CNS morphology as such, but rather ensures the correct functional identity of the neuronal networks underlying self-righting behaviour.

Altogether, this work shows that the fine-grained molecular regulation of *Hox* RNAs impacts on CNS development, as correct RNA processing is necessary to ensure HOX protein levels and thus function. Additionally, it shows that post-transcriptional regulation of *Hox* genes in the CNS may have long-range effects on animal behaviour and links this regulatory layer to the establishment of neuronal function.

Chapter 2

Materials and Methods

2.1 - Fly Strains

Drosophila melanogaster (fruit flies) were cultured following standard procedures at 25°C on a 12h light/dark cycle. Oregon Red was used as a wild type strain. Table 2.1 depicts the list of fly strains used in this thesis.

Table 2.1 Fly stocks

ID	Genotype	Details	Origin
Oregon R	*Oregon Red*	Inbred wild type line	Host Laboratory
Outbred	*Outbred*	Outbred wild type line	Élio Sucena Lab (Martins et al. 2013)
w^{1118}	*w^{1118}*	Mutation in the *white* gene	Host Laboratory
elav^{5}	*w, elav[e5]/FM7c-Kr-GFP*	Null mutation in the *elav* gene	Matthias Soller Lab (Robinow and White 1991)
act>Gal4	*y w; act5c>GAL4/CyO*	Ubiquitous expression of Gal4	Rob Ray Laboratory
UAS-ELAV	*w; UAS-ELAV (2e2); UAS-elav (3e1)*	UAS controlled ELAV expression	Matthias Soller Lab (Koushika et al. 2000)
act>ELAV	*w; act>Gal4/ UAS-ELAV; UAS-ELAV/+*	Ubiquitous ELAV expression	This study
Ubx-35UZ	*w; Ubx-35UZ*	*Ubx* transcriptional reporter	Irvine et al. 1991
elav5; Ubx-35UZ	*elav5; Ubx-35UZ/ +*	*Ubx* transcriptional reporter in elav null background	This study
repo>Gal4	*w; +; repo>Gal4/TM3, Sb1*	Glial cell expression of Gal4	Bloomington Stock Center (#7415)
repo>ELAV	*w; UAS-ELAV/+; repo>Gal4/UAS-ELAV*	Glial cell expression of ELAV	This study
∆miR-iab4/iab8	*w+; ∆miR-iab4/iab8 / TM3, Dfd-YFP, Sb1*	Mutation of the *iab4/iab8* miRNA locus	Bender 2008
Ubx.M1>Gal 4	*w; +; Ubx.M1>Gal4/ TM3, Dfd-YFP, Sb1*	*Ubx* domain expression of Gal4	de Navas et al. 2006
Ubx.M3>Gal 4	*w; +; Ubx.M3>Gal4/ TM3, Dfd-YFP, Sb1*	*Ubx* domain expression of Gal4	de Navas et al. 2006
UAS-Ubx Ia	*w; UAS-Ubx Ia*	UAS controlled UBX Ia expression	Reed et al 2010
Ubx.M1>Ubx	*w; UAS-Ubx Ia/+; Ubx.M1>Gal4/+*	UBX overexpression	This study
Ubx.M3>Ubx	*w; UAS-Ubx Ia/+; Ubx.M3>Gal4/+*	UBX overexpression	This study
ppk>GAL4	*w; pickpocket1.9>Gal4*	*pickpocket* domain expression of Gal4	Ainsley et al. 2003
UAS-GFP	*w; UAS-eGFP*	UAS controlled enhanced GFP (eGFP) expression	Bllomington Stock Center (#6659)
ppk>GFP	*w; ppk1.9>Gal4; UAS-eGFP*	*pickpocket* domain expression of eGFP	This study
ppk>Ubx	*w; ppk1.9>Gal4; UAS-Ubx Ia*	*pickpocket* domain expression of UBX Ia	This study
PO163>Gal4	*w; +; PO163>Gal4*	All sensory neurons expression of Gal4	Hummel et al. 2000
PO163>GFP	*w; UAS-eGFP; PO163>Gal4*	All sensory neurons expression of eGFP	This study
PO163>Ubx	*w; UAS-Ubx Ia; PO163>Gal4*	All sensory neurons expression of UBX Ia	This study
Cha>GFP	*w; Cha7.4>Gal4, UAS>eGFP*	Cholinergic neurons expression of eGFP	Salvaterra and Kitamoto 2001
Cha>Ubx	*w; Cha7.4>Gal4, UAS>Ubx Ia*	Cholinergic neurons expression of UBX Ia	This study

2.2 – Embryo/Larva fixation and dissection

Flies were kept in small collection cages with apple juice agar plates supplemented with yeast paste. Embryos were collected from these plates. Overnight collections of embryos were dechorionated in 50% bleach for about 3 minutes. Embryos were fixed in 500µl of 5.18% formaldehyde in 1xPBS (259µl of 10% ultrapure formaldehyde and 241µl of 1xPBS RNase free) with 500µl of heptane on moderate shaking for 22 minutes. The fixative was removed and embryos were devitellinized in methanol with vigorous shaking. Embryos were rinsed three times in 100% methanol and three times in 100% ethanol to remove any traces of formaldehyde and were stored in ethanol at -20ºC (Beckervordersandforth et al. 2008; Rogulja-Ortmann et al. 2007). Embryos were staged according to (Campos-Ortega & Hartenstein 1985).

In the case of muscle and motorneuron axonal projection stainings, late stage 16 embryos were dissected in 1xPBS prior to fixation, as described by Landgraf et al. (1997). Dechorionated embryos were transferred to poly-l-lysine coated coverslips, removed from the vitelline membrane with a glass needle, cut open dorsally and attached to the coverslip. Fat body and gut were removed by gentle suction. The embryos were flattened by blowing a stream of saline solution over them. Flattened embryos were fixed in 4% formaldehyde in 1xPBS in a humidified chamber for 20 minutes.

First instar larvae ventral nerve cords (VNC) were dissected in 1xPBS with forceps - mouth hooks were pulled gently, exposing the VNC but leaving the rest of the specimen still attached to the VNC – and fixed in 4% formaldehyde in 1xPBS with gentle shaking for 20 minutes.

2.3 – Antibody staining

Antibody stainings were performed using standard protocols. Briefly, fixed specimens were rehydrated in increasing proportions of PBTx (1xPBS, 0.3% Triton X-100) and washed several times in PBTx. Primary antibodies incubated overnight at 4ºC and were washed in PBTx. Secondary antibodies incubated for 2 hours at RT, were washed in PBTx and mounted in Vectashield (Vector Laboratories). After the staining, embryonic VNCs were dissected in Vectashield with tungsten needles.

Larval VNCs were mounted between two aluminium-foil spacers to avoid nerve cord distortions (Berni et al. 2012). When comparing protein expression in different genotypes, all the steps of the protocol were conducted in parallel (including fixation).

Primary antibodies used were: monoclonal mouse anti-UBX (FP3.38, 1:20, a gift from Robert White, University of Cambridge, UK; 1:20); mouse anti-ANTP (4C3, 1:20), mouse anti-ABD-B (1A2E9, 1:20), rat anti-ELAV (7E8410, 1:100), mouse anti-ELAV (9F8A9, 1:100), mouse anti-EN (4D9, 1:20), mouse anti-BP102 (1:100) and mouse anti-FasII (1D4, 1:20) (all from the Developmental Studies Hybridoma Bank); goat anti-ABD-A (dH-17, 1:20), rabbit anti-EN (d-300, 1:100) (both from Santa Cruz Biotechnology), rabbit anti-*β*-Gal (1:300, Molecular Probes), rabbit anti-GFP (1:300, Molecular Probes); rat anti-TROPOMYOSIN1 (ab50567, 1:100, from abcam); goat anti-HRP-Cy5 (1:500, Jackson Immuno Research) rabbit anti-Repo (1:500) (a gift from Gerd Technau, University of Mainz). Secondary antibodies used were: anti-mouse-Alexa488 and anti-mouse-Alexa568 (1:500, Molecular probes), anti-rabbit-Rhodamine

and anti-rat-Rhodomine (1:500, Jackson Immunoreserach Laboratories). A Leica DM600 fluorescent microscope, Leica TCS SPII confocal microscope and Zeiss Axiophot confocal microscope were used for fluorescent imaging, and the images were processed and analysed using Image J and Adobe Photoshop. Expression Analysis of immuno-staining expression along the A-P axis was done using the Plot profile Tool of ImageJ (http://rsbweb.nih.gov/ij/). Results were extracted to Microsoft Excel for further analysis.

2.4 - RNA *in situ* hybridization

In situ hybridizations were performed in a modified way from that described by Beckervordersandforth et al. (2008). Fixed specimens were rehydrated in PBTw (1xPBS, 0.1% Tween-20), pre-treated with H_2O_2 (3% in MeOH) for 20min to quench endogenous HRPs and with sodium borohydride (0.001% in PBTw) for 10 min to reduce auto-fluorescence. Then, specimens were pre-hybridised in hybridization solution (50% formamide, 5x SSC, 100 µg/ml Salmon Sperm DNA, 0.1% Tween-20) for at least 1 hour at 55ºC. 200-600ng of probe in hybridization solution were denatured at 83ºC for 3 minutes. Probes were incubated at 55ºC overnight. In the case of *Ubx* nascent transcript *in situs*, three intronic probes were used. In all the other *cases* only one probe was used. Until this point, all the solutions were DEPC treated.

Chromogenic *in situs* were detected with anti-DIG-AP (1:2000; Roche) and developed with NBT/BCIP substrate (4.5µl of NBT and 3.5µl of BCIP in 1ml of AP Buffer – 100mM NaCl, 50mM $MgCl_2$, 100mM Tris-HCl pH 7.5, 0.01%

Tween-20; Roche). For comparison of different genotypes, signal was developed in parallel and stopped at the same time to ensure comparability of results.

Fluorescent *in situs* were detected with anti-DIG-POD (1:300; Roche) followed by Fitc or Cy3 TSA plus amplification Kit (1:50; Perkin Elmer) for 10 minutes.

Signal quantification of *Ubx* nascent RNAs was done from stacks of confocal images using a segmentation pipeline from Fiji software (Schindelin et al. 2012). In brief, confocal stacks were imported to Fiji, Gaussian smoothed (Smooth 3D plug-in), and voxel intensity for each blob/*foci* was quantified (Find Connected Regions plug-in). We measured the *foci* intensity of each embryo (Figure 3.7D) by calculating the integral of number of *foci* per signal intensity (Figure 3.7C).

2.5 - RNA Probes

Templates of RNA probes for RNA *in situ* hybridization were obtained from PCR-amplified genomic fragments (see Table 2.2) cloned into pGEM-T-easy (Promega) according to manufacturer's instructions. Plasmids were linearized with a unique restriction site, Phenol/Chloroform extracted, ethanol precipitated and resuspended in RNase-free water. Concentration was determined in Nanodrop. Antisense RNA probes were synthesized using digoxigenin (DIG) RNA Labeling Kit (Roche) according to the manufacturer's instructions with either T7 or SP6 RNA polymerase (Roche), depending on the

orientation. DNA template was removed with DNase I (New England Biolabs). RNA probes were precipitated in lithium chloride and ethanol at -80ºC overnight, eluted in 50µl of hybridization solution and stored at -20ºC. All steps were done in RNase-free conditions.

Table 2.2 Primer sequences and RNA probe lengths

Probe Primers	Primer sequence (5' to 3')	Probe Length	Source
Ubx distal	FWD CGTGTGTGTGTCCCGATAAT	819	Thomsen et al. 2010
	REV TCCACATTCTCACTGGTTGC		
pri-iab4	FWD ACGTTGGAAAGCAAACAACC	888	Thomsen et al. 2010
	REV GTCCCTCAAAGTCACCGAAA		
Ubx intron 3A	FWD AAGGGTACGACCACTGCAAC	843	This study
	REV GCGGTACCTCGGACAATTTA		
Ubx intron 3B	FWD AGCCGGCATCCAGACTACTA	826	This study
	REV GCATACCAGAGACCCAGCAT		
Ubx intron 3C	FWD ATTGGCTACCCATCTGCAAC	844	This study
	REV TGCTACCCCTCTTCCTACCA		

2.6 - RNA extraction

RNA was extracted from staged embryos using TRI Reagent (Sigma) following the manufacturer's protocol. Briefly, 50-100 staged embryos were homogenized in 50µl of TRI reagent using a sterile RNase free pestle in a 1.5ml Eppendorf. After homogenization, 450µl of TRI reagent were added and tubes incubated for five minutes at room temperature to dissociate nucleoprotein complexes. RNA was separated from DNA and proteins by adding 100µl of RNase free Chloroform, mixing and incubating for fifteen minutes at room temperature. The different phases – aqueous phase (RNA), interphase and organic phase (DNA and proteins) – were separated by 15 minutes of

centrifugation at 4ºC and the aqueous phase (colourless top layer) was transferred to a new tube. RNA was precipitated with 250µl of Isopropanol at -80ºC for 1 hour to overnight, followed by centrifugation at maximum speed for half an hour at 4ºC. Precipitated RNA was washed in RNase free 75% ethanol, resuspended in nuclease-free water and stored at -80ºC. Possible traces of DNA were removed with DNase I (New England Biolabs), and RNA was Phenol/Chloroform extracted, precipitated in ethanol, resuspended in nuclease-free water and stored at -80ºC. RNA concentration was measured in Nanodrop. All steps were done in RNase-free conditions.

2.7 - Reverse Transcription (RT)

Total RNA (1-2 µg) was used for cDNA synthesis using random Hexamer primers (Invitrogen; in the case of CLIP(2.9)) or oligo(dT) primers (Invitrogen) and MuLV Reverse Transcriptase (Invitrogen, Cat. No. N8080018). The same amount of RNA was used when comparing different genotypes or conditions.

Total RNA was mixed with 2µl of primers (either random Hexamers or oligo(dT)) and water (to a final volume of 12 µl), denatured at 75ºC for 3 minutes and placed on ice. Then, the remaining RT components were added - 2µl of 10x RT Buffer (Invitrogen), 4µl of 2.5 mM dNTP mix (Invitrogen), 1µl of RNase inhibitor (Invitrogen) and 1µl of MuLV Reverse Transcriptase (Invitrogen) – and incubated at 44ºC for one hour for cDNA synthesis. An additional incubation at 92ºC for 10 minutes inactivated Reverse Transcriptase. cDNA was stored at -20ºC.

2.8 - Semi-quantitative RT-PCR

PCR reactions were prepared on ice to a final volume of 25µl as follows: 2.5µl of 10x PCR Buffer (New England Biolabs), 0.5µl of 10 mM dNTP mix (New England Biolabs), 1µl of each forward/reverse primer (10mM each, see Table 2.3), 0.25µl of standard *Taq* DNA polymerase (New England Biolabs), 0.9µl of cDNA and 18.85µl of nuclease-free water. PCR was performed using a *BioRad* PCR machine with the following conditions:

1 cycle:	extended DNA denaturation at 94ºC for 5 minutes
29 cycles*:	denaturation at 94ºC for 30 seconds
	primer annealing at 58ºC for 30 seconds
	extension at 72ºC for 30 seconds
hold:	4ºC

Hilary Reed optimised the PCR conditions previously to ensure that the reaction was on the exponential phase of amplification.

Expression values were normalised using reference gene *Rp49*. At least three independent biological replicates were done.

Two negative controls were always done: (i) genomic contamination control in the RNA sample – PCR done with RNA – and (ii) a no template control.

Table 2.3 Semi-quantitative RT-PCR primers

RT-PCR Primers	Primer sequence (5' to 3')	Source
Ubx universal	FWD GAAATGACGCGGAGACAGAT	Thomsen et al. 2010
	REV AATCTGCGCTCCTTCCACTA	
Ubx distal	FWD GAACGAAGGCAGATGCAAAT	Thomsen et al. 2010
	REV GGTAAGTGGTCGGATGCAGT	
abd-A universal	FWD CGGGTTTTATTGCTGTGGAT	Thomsen et al. 2010
	REV CGTTGGCCCAGAGACTCTAC	
abd-A distal	FWD CCTTTTCGATGAGGTCCAAA	Thomsen et al. 2010
	REV CGGTTTCGGTCGGTCTAATA	
Abd-B universal	FWD GCTAGTCCAGCGATTGGAAG	Thomsen et al. 2010
	REV GTCGGTTGGTCACACATCAG	
Abd-B distal	FWD TCCGTACAACACCATTTTCG	Thomsen et al. 2010
	REV AGTGGCGATTACGAGCTGAT	
Antp universal	FWD ATCCAATCCGTTGAACTTCG	Thomsen et al. 2010
	REV TCTTATTTCGCTTTCCCCACT	
Antp distal	FWD GAGGACGGAATGGCAAACTA	Thomsen et al. 2010
	REV GTCTTTTCACCTGGGATTGG	
RpL32 (Rp49)	FWD CCAGTCGGATCGATATGCTAA	Thomsen et al. 2010
	REV TCTGCATGAGCAGGACCTC	

2.9 - Agarose gel electrophoresis

RNA and PCR products were visualized in an agarose gel electrophoresis. Agarose gels were made of 0.9-2% (w/v) depending on fragment size by dissolving agarose in 1x of SB buffer. The mixture was heated in a microwave until it was completely homogenised. After cooling down, 0.4µg/ml ethidium bromide was added to the liquid agarose before pouring into the gel cast. Samples were prepared in 1x loading buffer (New England Biolabs), loaded into the wells of the gel alongside a 100bp and 1Kb DNA ladder (New England Biolabs) and subjected to electrophoresis in 1x SB Buffer.

Gel pictures were taken using an Uvidoc gel documentation system (Uvitec Cambridge) and UviPhotoMW image analysis software. Quantification of the gels was done with imageJ.

2.10 - Cross-linking and imunoprecipitation (CLIP)

Immunoprecipitation on nuclear extracts from overnight wild type embryos was performed essentially following the RNA immunoprecipitation protocol of Hilgers et al., (2012) and Oktaba et al. (2008). Briefly, 1-1.5g of dechorionated embryos were cross-linked for 15 minutes at RT by vigorous shaking in 10ml cross-linking/fixing solution (1.4% ultrapure formaldehyde, 50mM Hepes pH 8.0, 1mM EDTA, 0.5mM EGTA, 100mM NaCl) plus 30ml of n-heptane. Cross-linking was stopped by removing the fixing solution and washing the embryos for 1 minute in 1xPBS/ 0.01% Triton X-100/ 125mM glycine. Embryos were washed for 10 minutes in 15ml of wash A (10mM Hepes pH 7.6, 10mM EDTA, 0.5mM EGTA, 0.25% Triton X-100) and for 10 minutes in 15ml of wash B (10mM Hepes pH 7.6, 200mM NaCl, 1mM EDTA, 0.5mM EGTA, 0.01% Triton X-100) and then flash-frozen in liquid nitrogen and stored at -80ºC. Frozen embryos were broken-up with a loose-fitting pestle in a dounce homogenizer in 4ml ice-cold 1xPBS/ 0.01% Triton X-100 supplemented with Protease inhibitor cocktail (Roche) and 40U/ml of RNase inhibitor. Cells were disrupted with a tight-fitting pestle in a dounce homogenizer in 15ml ice-cold cell lysis buffer (5mM Hepes pH 7.6, 85mM KCl, 0.5% NP-40, Protease inhibitor and 40U/ml of RNase inhibitor). Nuclei were pelleted with centrifugation and

incubated for 50 minutes at RT in 2ml nuclear lysis buffer (50mM Hepes pH7.6, 10mM EDTA, 0.5%N-Lauroylsarcosine, Protease inhibitor and 40U/ml of RNase inhibitor). Nuclear extracts were sonicated in a Bioruptor water bath sonicator (Diagenode) for 10 cycles of 30 seconds on/ 30 seconds off, kept on ice for 30 minutes, sonicated for five additional cycles, aliquoted, flash-frozen in liquid nitrogen and stored at -80ºC.

Sonicated nuclear extracts were pre-cleared with equilibrated beads (Protein G Sepharose; GE Healtcare Life Sciences) for one hour at 4ºC, and beads were removed by centrifugation. Then, nuclear extracts were incubated overnight at 4ºC with 2µg of mouse anti-ELAV-9F8A9 or mouse anti-Tub-E7 (Developmental Studies Hybridoma Bank). In parallel, beads were blocked in 1mg/ml of BSA in RIPA buffer (140mM NaCl, 10mMTris-HCl pH 8.0, 1mM EDTA, 1% Triton X-100, 0.1%SDS, 0.1% Na-deoxycholate, Protease inhibitor and 40U/ml of RNase inhibitor) at 4ºC overnight. Antibody-immunocomplexes were recovered by incubating with blocked beads for 4 hours at 4ºC. Afterwards, beads-antibody-protein (ELAV-RNA) complexes were washed at 4ºC for 10 minutes, five times in RIPA buffer, one time in LiCl buffer (250mM LiCl, 10mM Tris-HCl pH 8.0, 1mM EDTA, 0.5% NP-40, 0.5% Na-deoxycholate, Protease inhibitor and 40U/ml of RNase inhibitor) and two times in TE buffer (10mM Tris-HCl pH8.0, 1mM EDTA). Cross-linking was reverted by incubating the samples at 68ºC for 1hour. RNA was extracted as in Section 2.5, and 0.5µg of RNA was used for the RT using random hexamers. PCRs were done using the sets of primers in Table 2.4.

Table 2.4 Semi-quantitative RT-PCR primers

RT-PCR RNA-CLIP Primers	Primer sequence (5' to 3')	Source
ewg	FWD TGAAATGCTAAATAAAGCCAACAA	This study
	REV CAATATAAAATGAGGACAAGCAAAAA	
Ubx site 3	FWD ATGGTCCAAACACCATCCAT	This study
	REV GCAAAGCGGAGAGAAGAAAA	
Ubx site 8	FWD GTTTTACCCTCTCCGGCATT	This study
	REV AGGGGGCCTAATAAATCAGC	

2.11 - Larval Behaviour

2.11.1 - Exploratory Behaviour

Embryos were collected as described in Section **2.2** and were aged until stage 17. At this point, embryos were selected according to their genotype and transferred to a fresh plate. Freshly hatched first instar larvae (<30 minutes post-hatching) were placed on 0.9% agarose plates and were allowed to acclimatize for 1 minute. Freely moving larvae were recorded for 2 minutes at a rate of 15 frames per second with a Leica DFC 420c camera mounted on a Leica MZ 75 microscope. Larvae were recorded from the ventral side (plates were inverted) for the ventral denticle belts to be seen. Movies were analysed with the open source software VCode 1.2.1 (http://social.cs.uiuc.edu/projects/vcode.html) and the number of full-body peristaltic contractions (forward and backward), number of turns and hits counted. For each genotype, 15–30 larvae were examined.

All larval behaviour experiments were conducted at 25ºC.

2.11.2 – Touch response

Larvae were manipulated and recorded as described above (2.11.1). We tested larval touch response by stroking their head with an eyelash and scored their response according to Kernan et al. (1994): no response=0, hesitation=1, withdraws anterior=2, turns=2, single backward wave=3, multiple backward waves =4; for a maximum score of 12

2.11.3 – Self-Righting Behaviour

Larvae were manipulated and recorded as described above (2.11.1) with the exception that plates were not inverted. Freshly hatched larvae (<30 minutes) were rolled over with forceps to an inverted position (ventral denticle belts up) and the time taken by the larvae to self-right itself – dorsal longitudinal trachea up - was measured (Crisp et al. 2008; Bodily et al. 2001). The sequence of movements during self-righting was analysed with VCode.

2.12 – Statistical Analysis

All statistical analyses were performed with non-parametrical tests (Wilcoxon matched-pairs signed rank test and Mann-Whitney *U* test) because the data did not have a normal distribution. The statistical significance of the molecular data on Chapter 3 was accessed with a Wilcoxon matched-pairs signed rank test and the behaviour data of Chapters 4 and 5 with a Mann-Whitney *U* test. Significance level was binned according to *p*-values' probability: non-significant (n.s.) $p > 0.05$, * $p < 0.05$, ** $p < 0.01$, *** $p < 0.001$. Statistical analyses were executed in Prism GraphPad 6.0 software package.

Chapter 3

The *Drosophila* pan-neural RBP ELAV regulates *Hox* gene RNA processing and expression in the developing nervous system

N.B. This chapter has been submitted for publication in *Development*: Ana Rogulja-Ortmann[1#], Joao Picao-Osorio[2#], Casandra Villava[2#], Pedro Patraquim[2], Elvira Lafuente[2], Julie Aspden[2], Stefan Thomsen[2], Gerhard M. Technau[1] and Claudio R. Alonso[2*] (2013) The RNA binding protein ELAV/Hu regulates *Hox* RNA processing, expression and function within the *Drosophila* nervous system

[1] *Institute of Genetics, University of Mainz, D-55099 Mainz, Germany.*
[2] *John Maynard Smith Building, School of Life Sciences, University of Sussex, Brighton BN1 9QG, United Kingdom.*
[(#)] *These authors contributed equally to this work.*
[(*)] *Corresponding author*

N.B. Collaborators conducted some experiments discussed in this chapter, namely: Casandra Villava (*Ubx* RT-PCRs and *in vitro* RNA binding experiments), Pedro Patraquim (Bioinformatic analysis) and Ana Rogulja-Ortmann (apoptosis of GW neuron). I conducted all the other experiments.

3.1 Chapter overview

Hox genes orchestrate the segmental patterning of the anterior-posterior (A-P) axis of all bilateral animals (Pearson et al. 2005). In order to activate distinct developmental programs according to axial position the *Hox* genes are expressed in characteristic sub-domains along the head-to-tail axis. The regionalisation of the central nervous system (CNS) along the A-P axis in vertebrates and invertebrates relies centrally on the regulated expression of *Hox* genes (Krumlauf et al. 1993; McGinnis & Krumlauf 1992; Tümpel et al. 2009). Thus, the study of the molecular mechanisms underlying *Hox* expression and function is crucial for the understanding of the development of the CNS.

The *Drosophila Hox* gene *Ultrabithorax* (*Ubx*) is regulated via RNA processing during the formation of the embryonic CNS (Kornfeld et al. 1989; Lopez & Hogness 1991; O'Connor et al. 1988; Thomsen et al. 2010). However, the molecular mechanisms underlying this form of RNA regulation and its impacts on expression and function remain poorly understood.

In this chapter we demonstrate that the pan-neural RNA binding protein (RBP) ELAV (*embryonic lethal abnormal vision*) regulates the RNA processing patterns of *Ubx* within the CNS. Additionally, through a combination of biochemical, genetic and imaging methods we show that ELAV binds to discrete regions within *Ubx* pre-mRNAs and its removal leads to a reduction in UBX expression in the CNS. Finally, we show that ELAV also regulates the RNA processing and protein expression patterns of other *Hox* genes (*abdominal-A* and *Abdominal-B*)

3.2 Results

3.2.1 ELAV regulates Ubx RNA processing

The *Hox* gene *Ubx* produces alternative RNA isoforms via alternative splicing (AS) and alternative polyadenylation (APA) (see Figure 3.1B) throughout embryonic development in different tissues (Kornfeld et al. 1989; Lopez & Hogness 1991; O'Connor et al. 1988; Thomsen et al. 2010). In early development, the predominant AS isoform is *Ubx* Ia with shorter 3'UTRs expressed in the epidermis and mesoderm (Artero et al. 1992; Lopez & Hogness 1991; Thomsen et al. 2010). As development proceeds, the embryonic central nervous system (CNS) starts to develop and *Ubx* IVa isoform with longer 3'UTR increase in expression in the CNS (Lopez & Hogness 1991; Thomsen et al. 2010). How is the RNA processing of *Ubx* controlled during development? Why are *Ubx* RNAs with longer 3'UTR exclusively expressed in the CNS?

The *Drosophila* RNA-binding protein ELAV (*embryonic lethal abnormal visual*) is exclusively expressed in post-mitotic neurons and is commonly used as one of the earliest markers of neuronal differentiation (Pascale et al. 2008; Robinow & White 1991). Notably, within differentiating neurons, ELAV controls the splicing patterns and 3'UTR processing of target transcript RNAs (e.g. *neuroglian* (Koushika et al. 1996; Lisbin et al. 2001) and *erect wing* (Soller & K. White 2003)).This raises the interesting possibility that ELAV may also be involved in *Ubx* RNA processing during neuronal development. If ELAV is

necessary for the increase of *Ubx* long 3'UTR expression in the CNS we expect to observe a significant reduction of *Ubx* long 3'UTRs in the absence of ELAV. To test this hypothesis, we used a null mutant for *elav* (*elav*^{5}, (Robinow & K. White 1991; Yao et al. 1993) and analysed the expression of *Ubx* long 3'UTR RNAs by *in situ* hybridisation. In line with our hypothesis, the signal for *Ubx* long 3'UTR in *elav* mutants was significantly reduced compared with the *wild type* (Figure 3.1C and D) indicating that ELAV is necessary for *Ubx* APA in the embryonic CNS. Using an alternative experimental approach – semi-quantitative RT-PCR – Casandra Villava observed the same effect of a reduction of *Ubx* long 3'UTR in *elav* mutants (Figure 3.1E). Interestingly, C. Villava also observed changes in *Ubx* AS patterns in the absence of ELAV: reduction of *Ubx* IVa isoform and increase of *Ubx* Ia (Figure 3.1F).

Ubx short 3'UTR is the prevalent RNA form expressed during gastrulation (germ band extension) (Thomsen et al. 2010). To see if ELAV is sufficient to instruct a change in the patterns of *Ubx* APA we forced the expression of ELAV during gastrulation. In these conditions we expect an increase in the "CNS-like" *Ubx* long 3'UTR. As expected, we observed an increase of *Ubx* long 3'UTR formation (Figures 3.2A and 3.2B) demonstrating that ELAV is sufficient to change the patterns of *Ubx* APA. We then wondered if ectopic expression of ELAV would increase even more the expression of *Ubx* long 3'UTR at later stages of embryogenesis. In this case we did not see any increase of long 3'UTRs (Figures 3.2C and 3.2D). Altogether these experiments show that ELAV is necessary and sufficient to regulate *Ubx* RNA processing during embryogenesis.

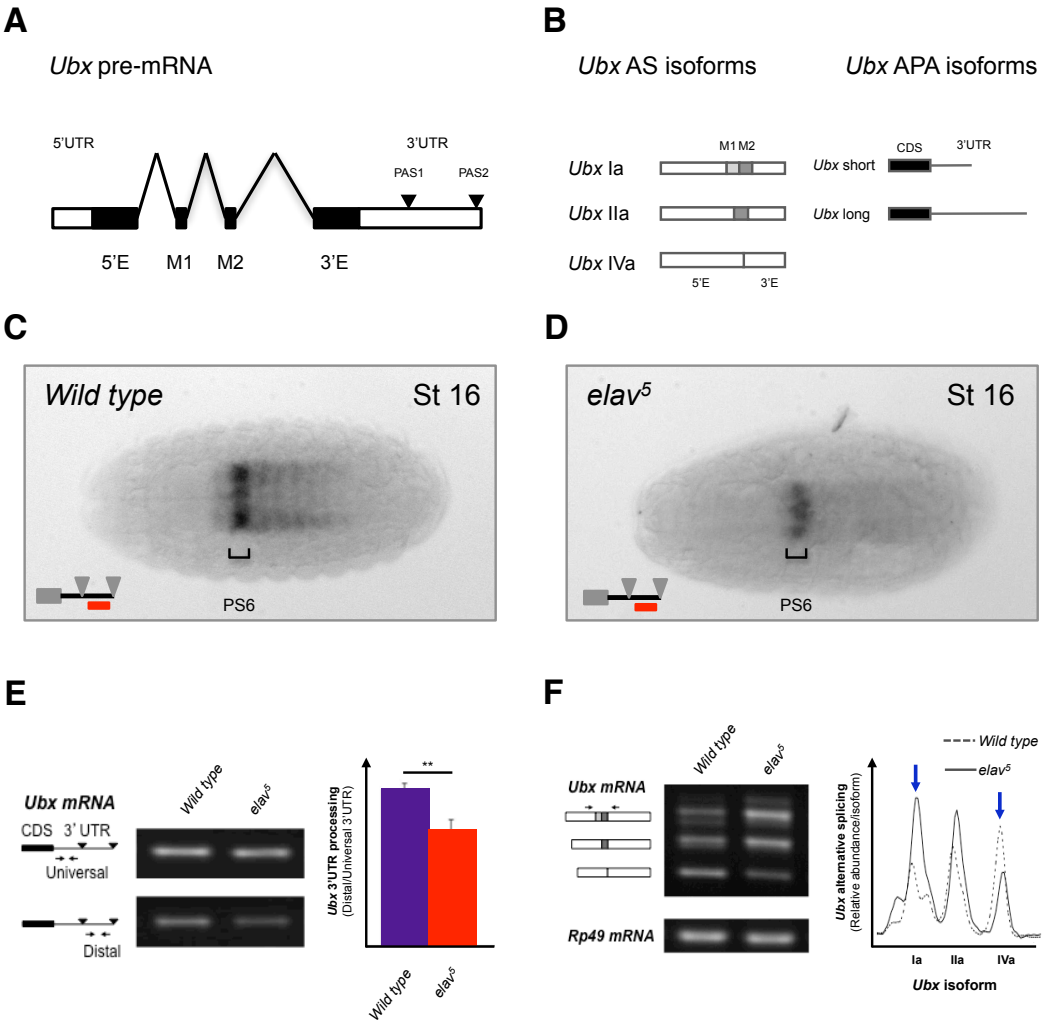

Figure 3.1. ELAV is necessary for *Ubx* RNA processing in the *Drosophila* CNS.

(Legend on the following page)

Figure 3.1. ELAV is necessary for *Ubx* RNA processing in the *Drosophila* CNS. (A-B) Structure of *Ubx* RNA isoforms generated via alternative splicing (AS) and alternative polyadenylation (APA). *Ubx* AS isoforms vary from each other by the inclusion/exclusion of microexons M1 and M2. *Ubx* APA produces mRNAs with variable 3'UTR length: short and long 3'UTR. (**C-D)** Expression of *Ubx* long 3'UTR RNAs in *wild type* and ELAV mutant (*elav*^{5}) embryos on stage 16. Expression of long 3'UTRs was detected by RNA *in situ* hybridisation with *Ubx* distal 3'UTR probes (symbolized by a red line). (D) *elav*^{5} embryos have a reduction in the expression of *Ubx* long 3'UTR forms in the CNS. **(E)** Molecular analysis by semi-quantitative RT-PCR of *Ubx* APA patterns shows a significant decrease in the amount of *Ubx* long 3'UTR in *elav*^{5} in late embryos. A non-parametric Wilcoxon matched-pairs signed rank test was performed to compare treatments; $p < 0.01$ (**). Error bars denote the standard error of the mean (S.E.M.). **(F)** Molecular analysis by semi-quantitative RT-PCR of *Ubx* AS profiles at late embryogenesis shows a significant change in the ratio of AS isoform in *elav*^{5} embryos: isoforms Ia and IVa are over-represented and under-represented, respectively (arrows). *Ubx* pre-mRNA in panel A is not to scale. The data from panels E and F was collected and analysed by Casandra Villava.

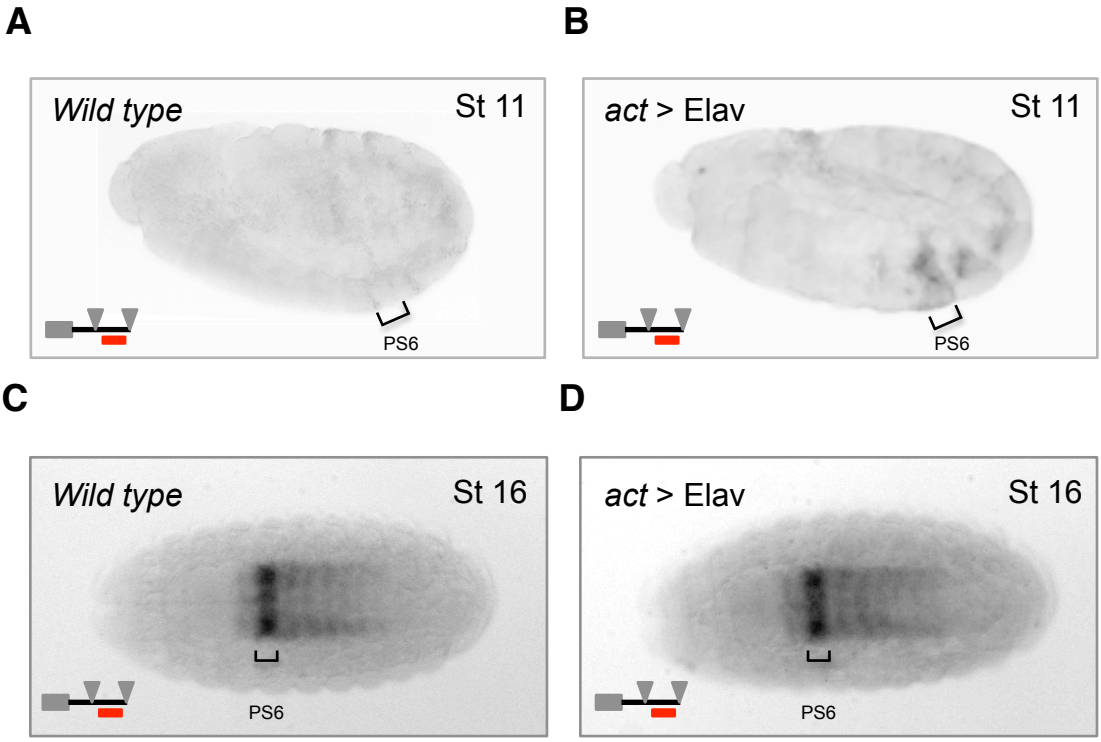

Figure 3.2 ELAV is sufficient to modify the patterns of *Ubx* APA during germ band extension

Expression of *Ubx* long 3'UTR forms in *wild type* and ectopic expressed ELAV embryos at stage 11 **(A-B)** and stage 16 **(C-D).** Ectopic expression of ELAV (*act* > ELAV) at stage 11 (B) reveals a clear increase in the expression of *Ubx* long 3'UTR forms. In contrast, (D) ectopic expression of ELAV during late embryogenesis does not cause any detectable increase in the expression of long 3'UTR Ubx mRNA forms.

3.2.2 ELAV binds to *Ubx* RNAs

ELAV is an RBP shown to affect RNA processing by direct binding to their RNA targets (Lisbin et al. 2001; Soller & K. White 2003). For example, ELAV regulates *neuroglian* (*nrg*) alternative splicing by binding an intronic sequence close to the 3' splice site of the alternative exon (Lisbin et al. 2001). The binding of ELAV to this sequence enhances the exclusion of the alternative exon. Thus we ascertained whether ELAV regulates *Ubx* RNA processing by physical interaction with *Ubx* RNAs. A bioinformatic approach was taken by Pedro Patraquim to scan for putative ELAV Binding Sites (EBS) in the *Ubx* sequence. To this end, P. Patraquim scanned the *Ubx* sequence for elements with high similarity to experimentally validated EBS: *neuroglian* (*nrg*, Nrg-like) (Lisbin et al. 2001), *erect-wing* (*ewg*, ewg-like) (Soller & K. White 2003) and AU-rich elements (X. Wang & Tanaka Hall 2001). Interestingly, sixteen evolutionary conserved putative EBS were found in *Ubx* and four of these are ultraconserved over 60 million years of independent evolution in the *Drosophila* lineage (Figure 3.3). To test if ELAV was binding to the four ultraconserved EBS we used two distinct approaches.

First, C. Villava did a series of *in vitro* RNA binding experiments (protein/RNA UV-crosslinking followed by RNAse treatment and RNA electrophoretic mobility shift assays) to determine if ELAV interacts with any of the four ultraconserved *Ubx* EBS. Indeed, C.Villava demonstrated that ELAV strongly interacts with *Ubx* RNAs in sites EBS3 and EBS8, first and third intron respectively (Rogulja-Ortmann et al. 2014). Even though these experiments were very encouraging in determining *Ubx* EBS, they were *in vitro* experiments

testing the ability of ELAV to bind small *Ubx* RNA fragment outside the normal physiological environment of the cell.

We then tested if ELAV was binding to these two EBS in the developing embryo within the normal physiological context with a series of RNA crosslinking immunoprecipitation experiments (RNA-CLIP) using embryonic nuclear extracts (Figure 3.4). To immunoprecipitate ELAV/pre-mRNA complexes we applied a monoclonal antibody against ELAV and detected immunoprecipitated pre-mRNAs with RT-PCR using primers that amplify the flanking regions of the EBS. As a positive control, we used a previously described ELAV-target, *erect wing* (*ewg*) (Koushika et al. 2000; Soller & K. White 2003). Notably, we observed a significant enrichment of *ewg*, *Ubx* EBS3 and *Ubx* EBS8 pre-mRNAs with anti-ELAV antibody, whereas a negative control antibody (anti-Tubulin) presented a low precipitation of these pre-mRNAs (Figure 3.4), confirming the previous biochemical analysis. Altogether these experiments show that ELAV interacts with the pre-mRNA of *Ubx* in introns 1 and 3 (EBS3 and EBS8, respectively) during development.

3.2.3 ELAV regulates UBX expression

We next sought to understand what were the biological implications of ELAV in the regulation of *Ubx* RNA processing. Since ELAV modulates two aspects of *Ubx* RNA processing (AS and APA, see above), it could impact UBX in two non-exclusive ways. First, changes in the alternative splicing lead to the formation of different UBX protein isoforms that have functional differences

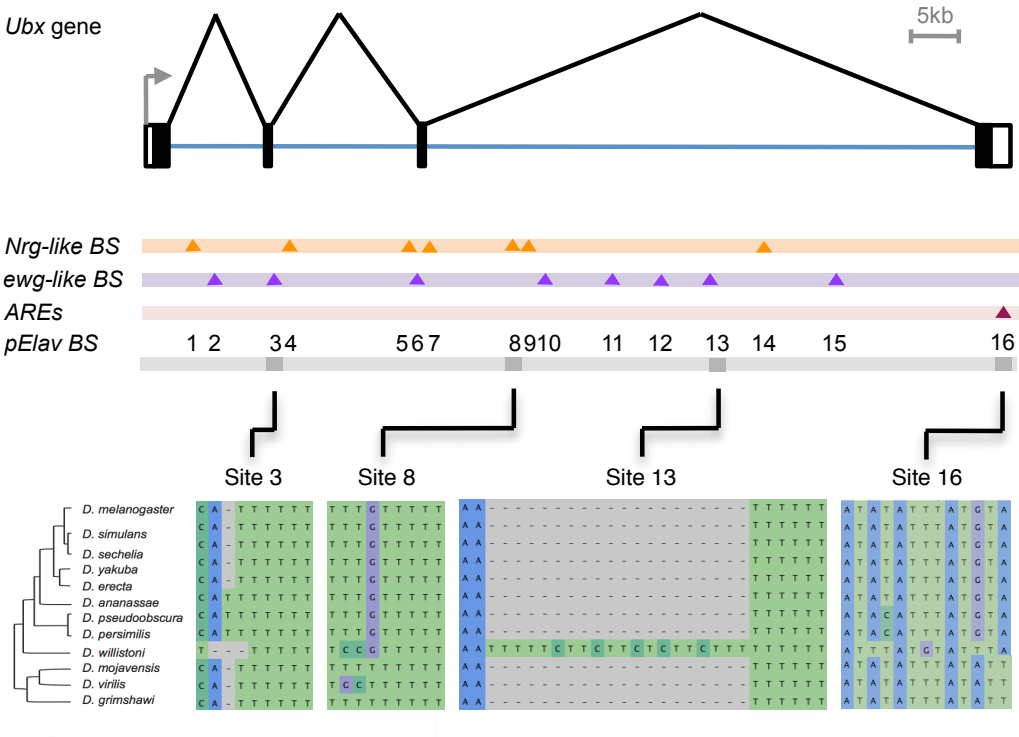

Figure 3.3 Computational prediction of putative ELAV binding-sites on *Ubx* pre-RNAs

The *Ubx* pre-mRNA was scanned for the presence of evolutionary conserved RNA sequence elements matching the sequence of experimentally validated ELAV targets in other genes (*neuroglian*, *Nrg*; *erect wings*, *ewg*) as well as A-U rich elements (ARE). The *Ubx* locus contains at least 16 putative binding sites for ELAV and four of these sites (sites 3, 8, 13 and 16, numbered according to their 5'-3' position) are ultraconserved in drosophilids that diverged over 60 million years ago. The data and analyses shown were obtained and performed by Pedro Patraquim. The figure was taken from Rogulja-Ortmann et *al.* 2014 (unpublished).

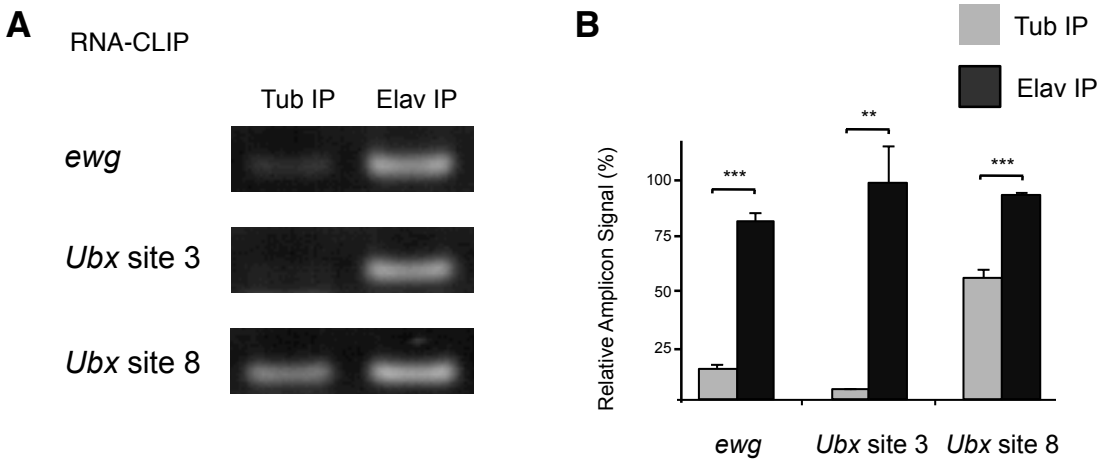

Figure 3.4 ELAV binds to discrete elements within Ubx RNAs.

(A-B) RT-PCR of RNA recovered after RNA cross-linking and immunoprecipitation (RNA-CLIP) of ELAV from embryonic nuclear extracts. (A) RT-PCR amplification of ELAV-immunoprecipitated (ELAV IP) samples shows a significant yield of *ewg, Ubx* site 3 and *Ubx* site 8 RNA products in comparison to an unspecific immunoprecipitation (Tub IP). (B) Quantification of amplicon signal shows that the amount of precipitated *ewg*, *Ubx* site 3 and *Ubx* site 8 RNA is significantly higher in the ELAV IP (n=4). A non-parametric Wilcoxon matched-pairs signed rank test was performed to compare treatments; $p < 0.01$ (**), $p < 0.001$ (***). Error bars denote the S.E.M. Taken together, these results support the model that ELAV binds to ultraconserved sequences EBS3 and EBS8 within *Ubx* RNAs in the normal physiological context.

(Mann & Hogness 1990; de Navas et al. 2011; Reed et al. 2010). Second, variation in the length of the *Ubx* 3'UTR can lead to differential regulation of the transcripts via mRNA stability and degradation, translation efficiency and targets of trans-acting factors like RBP and miRNA (Alonso 2012; Di Giammartino et al. 2011; Lutz 2008). Indeed, previous work in our lab had shown that the different *Ubx* 3'UTRs bear substantially different sets of miRNA target sites and that reporter constructs linked to the 3'UTRs show differential expression patterns: *Ubx* short 3'UTRs have less miRNA target sites and are higher expressed than *Ubx* Long 3'UTRs (Thomsen et al. 2010). Since in the absence of *elav* there is a decrease in *Ubx* Long 3'UTR in the CNS (see Figure 3.1), we expect an increase of UBX protein in the CNS of *elav* mutants embryos.

Therefore, we analysed the protein expression pattern of UBX in the CNS. To this end, we did a series of antibody stainings for UBX in dissected VNCs at embryonic stage 16. Surprisingly, we observed a significant depletion of UBX protein in *elav* mutants in comparison with the wild type (Figures 3.5A and 3.5B). The reduction in protein expression was uniform along the anterior-posterior (A-P) axis and not restricted to a particular region of the CNS (Figure 3.5C). In addition, using a complementary technique - western blot in whole embryos - C. Villava observed the same trend of a reduction in UBX protein amount in *elav* mutants (Rogulja-Ortmann et al. 2014, unpublished).

The effects on UBX protein upon *elav* removal could be explained at multiple levels: *Ubx* transcription/*Ubx* mRNA production, mRNA stability and/or translation efficiency (Colombrita et al. 2013; Simone & Keene 2013). The latter possibility - translation inefficiency - seemed unlikely since ELAV has nuclear localization in neuronal cells (Robinow & K. White 1991; Berger et al. 2007; Yao

et al. 1993; Colombrita et al. 2013) and ELAV affects aspects of *Ubx* RNA processing (see above) that occur co-transcriptionally (Di Giammartino et al. 2011; Proudfoot 2011). To see if ELAV impacted on the transcriptional activity of *Ubx,* we used the *Ubx* transcriptional reporter 35UZ (Irvine et al. 1991) in the absence of ELAV. This reporter is composed of 35 kb of *Ubx* upstream regulatory sequences that drive a *Ubx*-like expression during embryogenesis linked to a *lacZ* reporter (Irvine et al. 1991). We did not observe significant differences in *Ubx* transcription activity in *elav* mutants (Figure 3.6) pointing to ELAV effects on UBX protein expression should be occurring after transcription initiation. Then, we explored the possibility of ELAV affecting the transcription cycle of *Ubx.* For this we developed a series of *Ubx* nascent transcripts fluorescent *in situ* hybridizations (FISH for intronic regions of *Ubx*) to analyse the expression of unprocessed RNA transcripts (Figure 3.7). Unexpectedly, we observed a substantial increase of *Ubx* nascent transcripts in >70% of *elav* mutants (Figures 3.7A and 3.7B). Furthermore, we applied an image segmentation and quantification approach to the *Ubx* nascent transcripts signals, and we observed a higher number of transcriptional foci (Figure 3.7C and D, left panel) and signal intensity level per focus (Figure 3.7D, right panel) in *elav* mutants. These experiments suggest that *Ubx* pre-mRNAs are retained at the site of transcription since an increase of unprocessed RNAs with no transcriptional initiation differences are followed by a drastic reduction of protein in the absence of ELAV. If this hypothesis were to be correct, we would expect a decrease in *Ubx* mRNA in *elav* mutants. Indeed, C.Villava observed that *elav* mutants had reduced levels of *Ubx* mRNA (Rogulja-Ortmann et al. 2014).

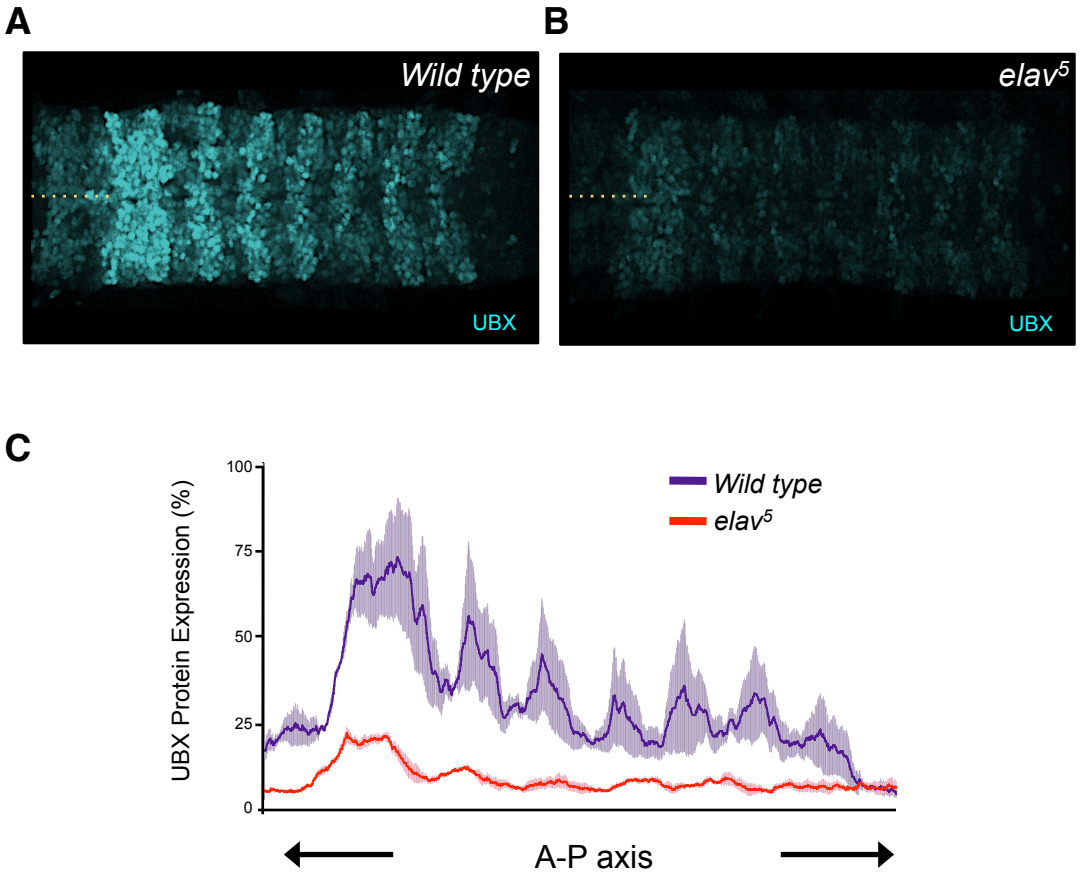

Figure 3.5 ELAV removal leads to reduced expression of UBX protein within the *Drosophila* CNS

(A-B) UBX protein expression of dissected embryonic VNC in *wild type* and *elav* mutant (*elav*^{5}) embryos at stage 16. (B) *elav*^{5} embryos express significantly lower levels of UBX protein in their VNC. **(C)** Profile quantification of UBX protein expression along the A-P axis in *wild type* (purple) and *elav*^{5} (red) embryos. The two thick lines represent the average intensity of *UBX* protein expression in ten embryos of each genotype; and their shadows represent ± S.E.M. Dashed lines mark the midline. Anterior is to the left.

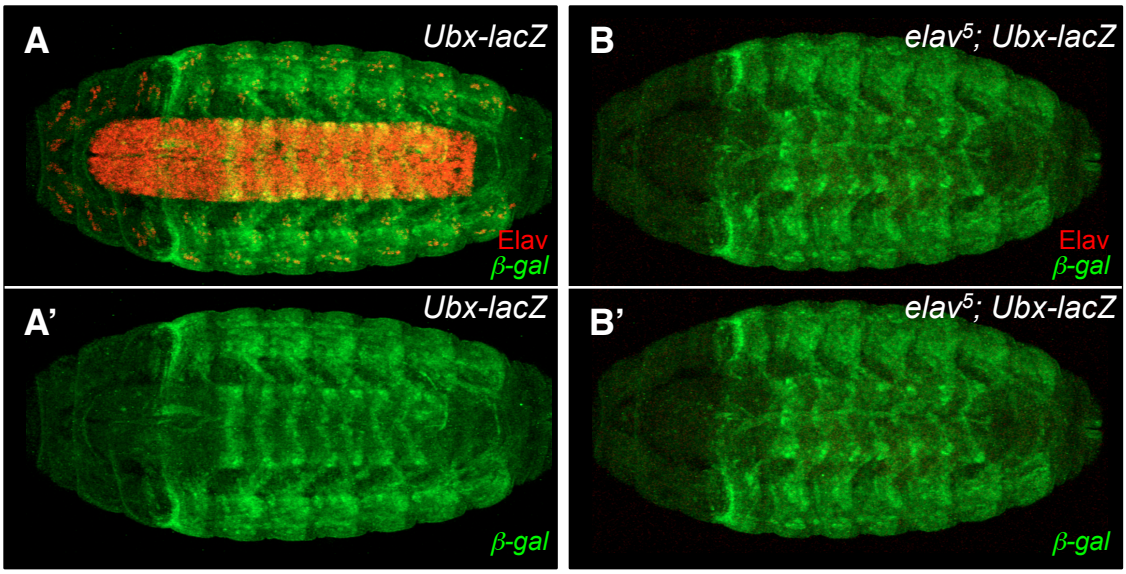

Figure 3.6 ELAV does not affect *Ubx* transcriptional activity

(A-B') Analysis of *Ubx* transcription in stage 16 *elav* mutants (*elav*^{5}) and wild-type embryos, using the *35UZ Ubx-lacZ* promoter fusion construct. (A) *35UZ Ubx-lacZ* expression at stage 16 as detected by *β*-galactosidade immunolabeling (green). (B) *elav*^{5} embryos show no apparent difference to wild-type in *Ubx-lacZ* expression. This result indicates that ELAV does not impact on the transcriptional activity of *Ubx.* Anterior is left.

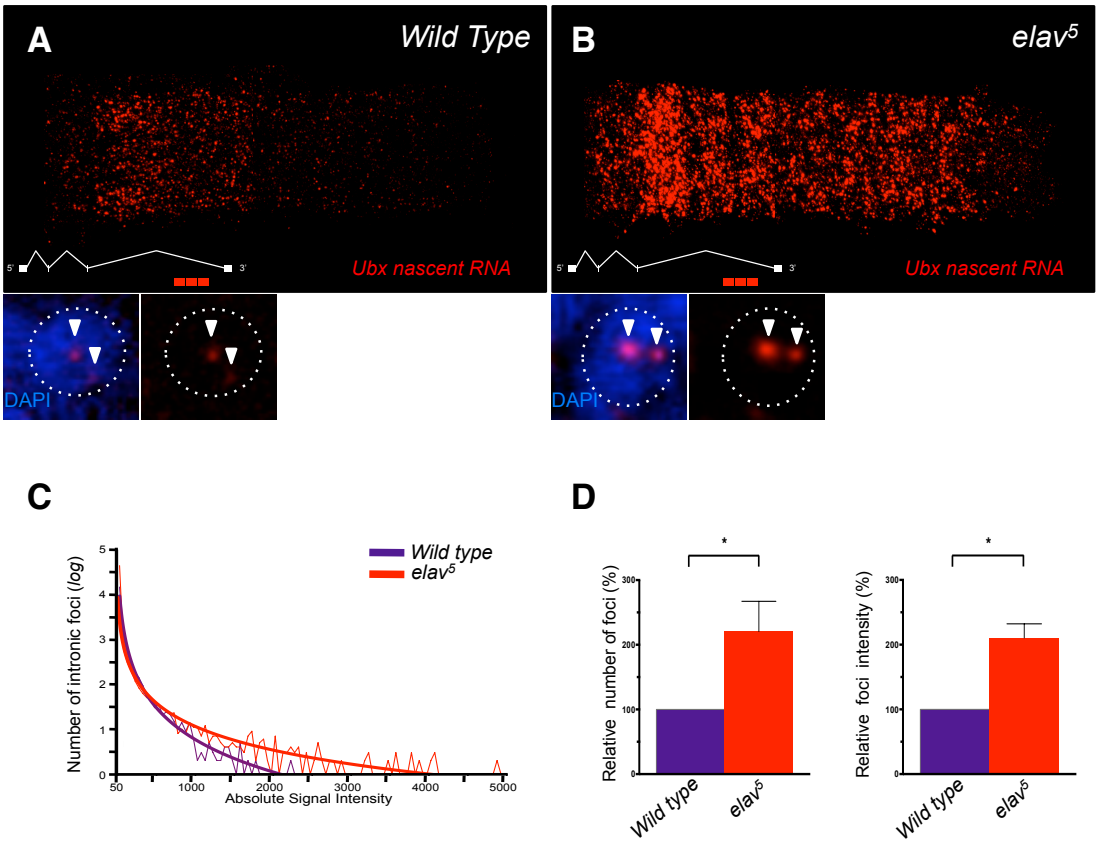

Figure 3.7 ELAV affects *Ubx* nascent RNA expression

(Legend on the following page)

Figure 3.7 ELAV affects *Ubx* nascent RNA expression

(A-B) *Ubx* nascent RNAs as detected by FISH using probes complementary to the *Ubx* third intron. Bottom panels illustrate the two foci of *Ubx* transcription (white arrowheads) per nucleus (DAPI; blue). (A) Wild type expression of *Ubx* nascent RNA transcripts. (B) $elav^5$ embryos display a marked increase in *Ubx* nascent transcript signal. (C) Quantification of *Ubx* nascent transcript signal in the embryonic CNS of both wild type and $elav^5$. The thin lines display the signal intensity measurements for each genotype, whereas the thick lines show their respective best fit curves. The intensity of *Ubx* nascent RNA signal is noticeably distinct between genotypes. (D) Plotting both the relative number of foci displaying *Ubx* nascent RNA signal and their relative intensity further confirms that $elav^5$ mutants exhibit higher expression of *Ubx* nascent RNAs (n=7 per genotype). A non-parametric Wilcoxon matched-pairs signed rank test was performed to compare treatments; $p < 0.05$ (*). Error bars denote the S.E.M.

Altogether, we show that the absence of ELAV causes abnormal *Ubx* RNA processing and RNA retention at the site of transcription leading to a reduction in *Ubx* mRNA and protein.

3.2.4 UBX expression in glia

In general *Hox* proteins are restricted to neurons and absent in glial cells (Miguel-Aliaga et al. 2004). Since ELAV is expressed exclusively in neurons at late embryogenesis (Berger et al. 2007; Robinow & K. White 1991) and affects UBX protein expression (Figure 3.5), we hypothesise that the lack of UBX protein expression in glia could be due to the absence of ELAV. This hypothesis is based on the assumption that *Ubx* is transcribed in glial cells. We tested this assumption by analysing the expression of *Ubx* nascent transcripts (intronic FISH, see above) in glial cells labelled by Repo (Reverse polarity; Halter et al. (1995). We observed that the majority of glia does not show signal for *Ubx* pre-*mRNAs* (Figures 3.8A, 3.8C and 3.8E). Only 30% of glia display *Ubx* transcription in the third thoracic segment (T3) and in first abdominal segment decreases to 16% (data not shown). In spite of this, we still tested the hypothesis of lack of UBX protein in those glia that transcribe *Ubx* by ectopically expressing ELAV in glia using the *repo*-Gal4 driver. Interestingly, forced expression of ELAV in glia that transcribe *Ubx* led to a small increase in the levels of UBX protein (Figures 3.8B, 3.8D and 3.8F), namely: dorsal glia (e.g. posterior longitudinal glia, P-LG), medial glia (e.g. lateral cell body glia, L-CBG) and ventral glia (e.g. medial ventral subperineurial glia, MV-SPG). This result

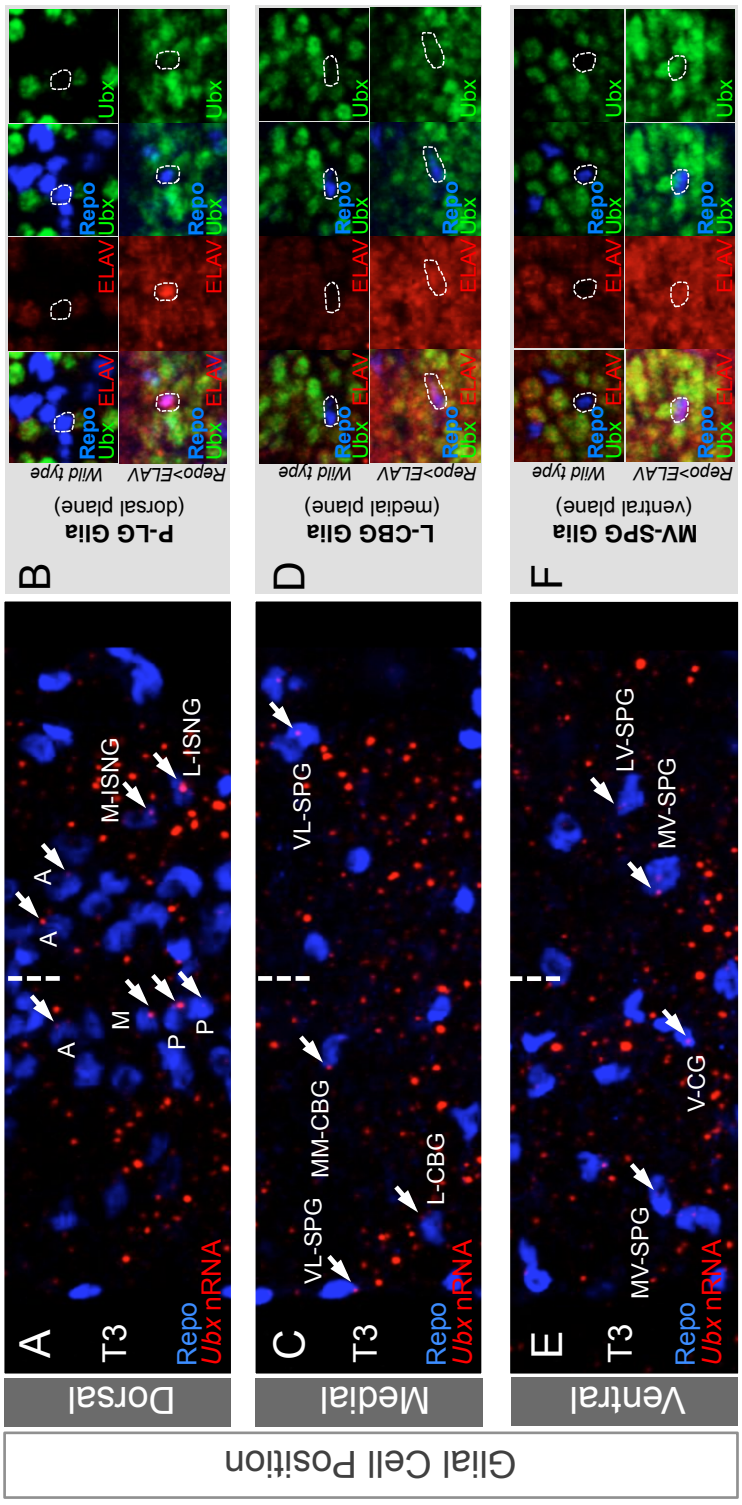

Figure 3.8 Forced expression of ELAV leads to *Ubx* protein expression in glial cells

(Legend on the following page)

Figure 3.8 Forced expression of ELAV leads to *Ubx* protein expression in glial cells

(**A**, **C**, **E**) *Ubx* nascent RNA expression (RNA, red) in glial cells (Repo, blue) across Dorsal (A), Medial (B) and Ventral (C) sections of the T3 segment. Approximately a third of all glial cell nuclei display *Ubx* nascent RNA expression (white arrows). **(B, D, F)** Ectopic expression of ELAV (red) in glial cells (Repo, blue), using the *repo-Gal4* driver, leads to low but detectable expression of *Ubx* protein (green) in the subpopulation of glial cells in which *Ubx* nascent RNAs had been detected. These results suggest that for those glial cells displaying *Ubx* transcription, ELAV is sufficient to stabilise *Ubx* protein expression. Dashed lines mark the midline in A, C and E. Anterior is up. Glial cell nomenclature according to Beckervordersandforth et *al*. 2008.

reinforces the idea that ELAV could “fine-tune” the levels of *Ubx* expression within the nervous system.

3.2.5 ELAV regulation of other *Hox* genes

Previous work in our lab showed that three other *Hox* genes – *Antennapedia* (*Antp*), *abdominal-A* (*abd-A*) and *Abdominal-B* (*Abd-B*) – undergo similar and synchronous RNA processing events to those in *Ubx* and had proposed that a common signal/molecule could be coordinating these events (Thomsen et al. 2010). Therefore, we tested if ELAV was regulating the RNA processing of these other *Hox* genes with semi-quantitative RT-PCR. Strikingly, we observed a significant high reduction of *abd-A* long 3’UTR in *elav* mutants (Figures 3.9A and 3.9E) when compared to *wild type*s and a small reduction of *Abd-B* long 3’UTR in $elav^5$ (Figures 3.9B and 3.9E). Conversely, we observed no detectable difference of *Antp* long 3’UTR in $elav^5$ (Figures 3.9C and 3.9E). Bearing in mind that ELAV affects *Ubx* RNA processing and protein level we wondered if ELAV could also affect the protein level of these other *Hox* genes. Interestingly, we found a significant reduction of ABD-A and ABD-B protein expression in *elav* mutants (Figures 3.10A-F) but not in ANTP (Figures 3.10.F-I). These experiments show that ELAV is necessary for the regulation of alternative polyadenylation and protein expression of *Hox* genes from the Bithorax complex (*Ubx, abd-A* and *Abd-B).*

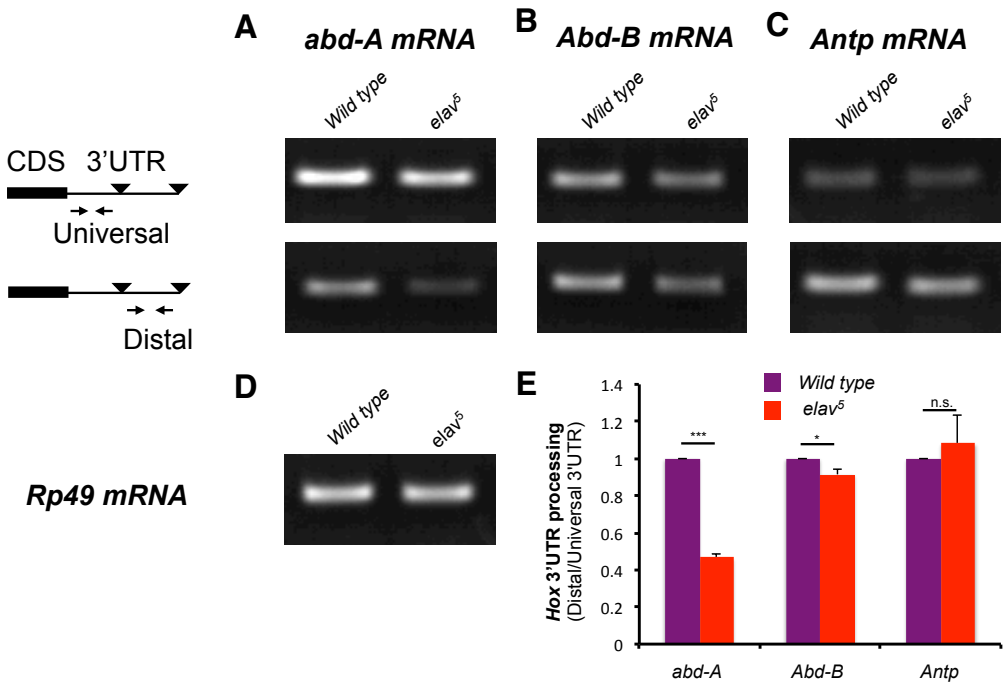

Figure 3.9 The effects of ELAV removal on the RNA processing of other Hox genes

(**A-C**) Molecular analysis of *abd-A*, *Abd-B* and *Antp* RNA processing by semi-quantitative RT-PCR, using universal and distal 3'UTR amplicons in late wild type and *elav*^{5} embryos. (A) Absence of ELAV leads to a marked reduction in *abd-A* distal 3'UTR amplicon signal when compared to wild type levels. (B) *Abd-B* shows a subtle reduction of distal 3'UTR amplicon signal in *elav*^{5} mutants. In contrast (C) *Antp* shows no observable difference in distal 3'UTR signal between wild type and *elav*^{5} embryos. (D) Amplicon signal intensity was normalised using *Rp49* signal. (E) Quantification of normalised Distal to Proximal signal-ratios in *abd-A*, *Abd-B* and *Antp* mRNAs (n=4) further confirms the effect of ELAV on *abd-A* and *Abd-B,* but not *Antp*, RNA processing. A non-parametric Wilcoxon matched-pairs signed rank test was performed to compare treatments; $p > 0.05$ (n.s.); $p < 0.05$ (*); $p < 0.001$ (***). Error bars denote S.E.M.

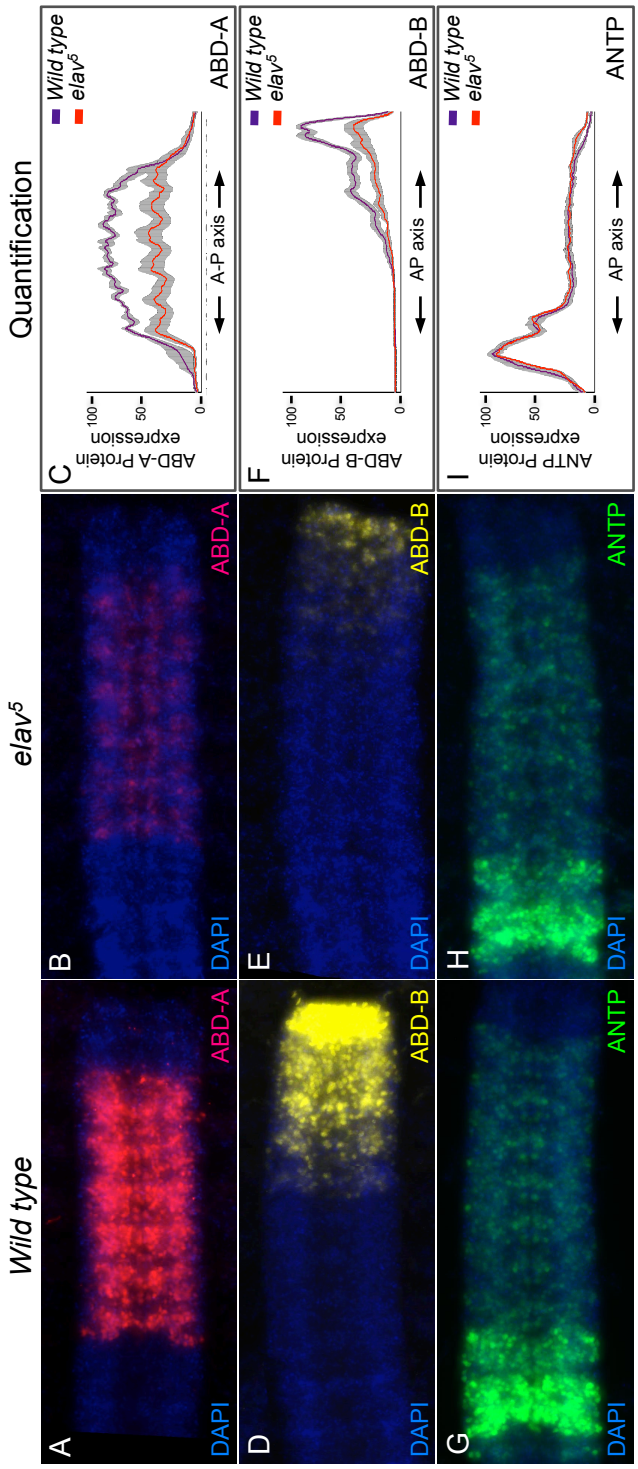

Figure 3.10 The effects of ELAV on the protein expression levels of other Hox genes

(Legend on the following page)

Figure 3.10 The effects of ELAV on the protein expression levels of other *Hox* genes

(A-B) ABD-A protein (red) expression levels are markedly lower in dissected *elav*^{5} nerve cords when compared to wild type. (C) Profile quantification of ABD-A protein expression along the A-P axis in *wild type* (purple) and *elav*^{5} (red) nerve cords shows the same pattern of ABD-A protein depletion in *elav*^{5}. **(D-E)** ABD-B protein (yellow) expression levels are similarly lower in dissected *elav*^{5} nerve cords when compared to wild type. (F) Profile quantification of ABD-B protein expression along the A-P axis in *wild type* and *elav*^{5} nerve cords further confirms the observation of lower ABD-B protein levels in *elav*^{5}. **(G-H)** ANTP protein (green) expression levels are indistinguishable between *elav*^{5} and wild type nerve cords. (F) Profile quantification of ANTP protein expression along the A-P axis shows no difference between *wild type* and *elav*^{5}. (C, F, I) The two thick lines represent the average intensity of protein expression in ten embryos of each genotype; grey shadows represent the S.E.M. Anterior is to the left.

3.3 Discussion

The work presented in this chapter shows that the pan-neural RBP ELAV regulates RNA processing and expression of *Hox* genes from the Bithorax complex (BX-C) within the embryonic CNS of *Drosophila melanogaster*. The absence of ELAV causes inefficient processing of *Ubx* A.S. and A.P.A. via direct interactions with intronic regions of *Ubx* pre-mRNAs (Figures 3.1-3.3) and an accumulation of unprocessed *Ubx* RNA transcripts in the nucleus (Figure 3.7). We suggest that the increase in unprocessed *Ubx* RNA transcripts is represented by a higher number of cells with *Ubx* pre-mRNA transcripts (number of transcriptional foci, Figure 3.7D, left panel) and each cell has a higher number of *Ubx* pre-mRNA transcripts (signal intensity per foci, Figure 3.7D, right panel). Thus, we propose that ELAV affects *Ubx* RNA processing and RNA accumulation at the site of transcription with a consequential impairment on the release of *Ubx* mRNAs and lower production of protein. This model is consistent with previous studies that relate inefficient RNA processing with transcript release (Custodio et al. 1999; J. C. Schwartz et al. 2012).

We also advance a new regulatory mechanism of *Hox* protein expression through the action of ELAV on *Hox* RNA processing (Figures 3.5 and 3.10). This mechanism of ELAV “fine-tuning” the levels of *Hox* expression could be relevant in cellular decision making within the nervous system. Indeed, modulation of ELAV in glia that transcribe *Ubx* was sufficient for the production of UBX protein (Figures 3.8B, 3.8D and 3.8F) while in wild type conditions is totally absent. Furthermore, Ana Rogulja-Ortmann explored the biological consequences of ELAV-regulated *Ubx* expression in specific cellular programs

under *Ubx* control (Rogulja-Ortmann et al. 2014, unpublished). It was shown previously that variations in UBX expression lead to re-specification of apoptotic patterns of the GW neuron from the lineage NB7-3 (Rogulja-Ortmann et al. 2008): decrease in UBX causes significant reduction in the GW apoptotic levels. Thus, A. Rogulja-Ortmann examined to what extent the apoptotic patterns in GW neurons were affected in *elav* mutants. Interestingly, A. Rogulja-Ortmann observed the same *Ubx* effects in *elav* mutants, that is, a significant reduction in the apoptotic levels of GW along the A-P (Rogulja-Ortmann et al. 2014, unpublished). Notably, when UBX expression was restored in GW neurons there was a rescue to the normal levels of apoptosis. Moreover, the different AS isoforms had variable rescue capacities: isoform *Ubx* IVa had a higher percentage of rescue than the isoform *Ubx* Ia. These experiments reinforce the idea that the different *Ubx* AS isoforms have variable functions during development.

In principle, the effects of ELAV on BX-C proteins could be due to a widespread pleiotropic effect on protein synthesis in neuronal tissues and neurodegeneration. Two observations made this possibility very unlikely. First, the levels of expression of *Antp* are not affected by the absence of *elav* (Figures 3.10G-I). And secondly, there is a reduction in the apoptosis of GW neurons upon *elav* removal. Therefore, we demonstrate that the effects of ELAV on BX-C genes are specific and not a general effect on neuronal gene expression and/or tissue degeneration.

ELAV regulates *Hox* genes of the BX-C (*Ubx, abd-A* and *Abd-B*) but not from the ANT-C (*Antp*) (Figure 3.10). We could not find any clear explanation for this observation. Pedro Patraquim analysed the sequences of the four *Hox*

genes and all of them had conserved putative Elav binding sites. At the gene structure, all four have alternative isoforms for splicing and polyadenylation (FlyBase release 5.53 September 2013 and Pedro Patraquim personal communication). The four *Hox* genes were shown to undergo APA during embryogenesis; however *Antp* long 3'UTR expression was not restricted to later stages of embryogenesis in contrast to the BX-C genes (Thomsen et al. 2010). This observation may suggest that other factors could be regulating *Antp* RNA processing. An additional possibility is a differential action of ELAV on each *Hox* complex due to their genomic location. One way of testing this possibility would be to examine to what extent the RNA processing of the remaining *Hox* from the ANT-C (*labial*, *proboscipedia*, *Deformed* and *Sex combs reduced*) is affected by ELAV. An alternative approach would be to analyse the *Hox* RNA processing in *Drosophila* species that have a different genomic arrangement of the *Hox* complexes (e.g. *Drosophila virilis* and *Drosophila buzzati*; Negre et al. (2003) and Negre et al. (2005)

In summary, our findings show the relevance of the RBP ELAV in modulating the expression of BX-C genes during the establishment of cellular decisions within the embryonic CNS of *Drosophila melanogaster*.

Chapter 4

The role of miRNA-dependent *Hox* gene regulation in *Drosophila* larval behaviour

N.B. The next two chapters are part of a collaboration with Dr. Jimena Berni and Dr. Matthias Landgraf of the Department of Zoology in the University of Cambridge.

I conducted all the experiments shown.

4.1 Chapter overview

In the previous chapter we show that ELAV regulates *Ubx* RNA processing during CNS development. Notably, *Ubx* RNAs with longer 3'UTRs are selectively up-regulated within the embryonic CNS after germ band retraction (Thomsen et al. 2010): the point at which post-mitotic *Hox* inputs on neural circuitry begin to develop (Rogulja-Ortmann & Technau 2008). Additionally, these longer *Ubx* 3'UTRs possesses a suite of unique target sequences for miRNAs (Thomsen et al. 2010); raising the intriguing hypothesis that miRNAs might regulate UBX expression during *Drosophila* CNS development which ultimately controls specific patterns of neuronal specification.

Indeed, recent studies showed that UBX protein expression is regulated post-transcriptionally by the miRNAs *miR-iab4/iab8* in the CNS (Bender 2008; Thomsen et al. 2010). However, the biological importance of *Ubx-miR-iab4/iab8* interactions during CNS development remains largely unknown.

In this chapter we investigate the biological role of *Ubx* post-transcriptional regulation by miRNAs *miR-iab4/iab8* during the development of the CNS. Through the combination of genetic and behaviour methods we show that UBX regulation by *miR-iab4/iab8* coordinates the control of a specific larval behaviour: self-righting behaviour. This study provides novel insights on the role of *Hox*-miRNA interactions in the control of behaviour.

4.2 Results

UBX protein expression is regulated by miRNAs *miR-iab4/iab8* during the formation of the embryonic *Drosophila* CNS (Bender 2008; Thomsen et al. 2010). Genetic removal of *miR-iab4/iab8* leads to a striking increase of UBX protein expression in the CNS. In spite of this, *miR-iab4/iab8* mutants do not have any evident homeotic transformation or anatomical abnormalities in their bodies (Bender 2008), raising doubts in the biological relevance of *Ubx* regulation by *miR-iab4/iab8.* Alternatively, *Ubx-miR-iab4/iab8* interactions could exert their functions specifically within the CNS; so that morphological defects would not be manifested at the level of the whole animal but rather in neuronal cells. In support of this alternative, *miR-iab4/iab8* mutant flies are sterile due to behavioural problems affecting nerves and/or muscles involved in posterior abdominal movements (Bender 2008).

Therefore, to investigate the biological significance of UBX regulation by *miR-iab4/iab8* during CNS development, we analysed larval behaviour of *miR-iab4/iab8* mutants. Bearing in mind that different behaviours can be controlled by distinct underlying neuronal circuits (e.g. neuronal circuits of the brain are not required for larval locomotion (Berni et al. 2012)) or genetic programs (e.g. the gene *scribbler* is involved in larval turning frequency (Suster et al. 2004)) we probed a range of different behaviours.

4.2.1 *miR-iab4/iab8* are not required for peristaltic locomotion

Drosophila larvae move over substrates by peristaltic crawling (Berni et al. 2012). Peristaltic crawls consist of coordinated and rhythmic waves of muscle contraction along the body (Crisp et al. 2008; Heckscher et al. 2012). In forward crawls, a wave of contraction is initiated in the most posterior segments (A8/9) and propagates anteriorly until A1 (Figures 4.1A and 4.1B) (Dixit et al. 2008; Crisp et al. 2008). In backward crawls, the wave of contraction is reversed from A1 to A8/9. Usually backward waves are triggered by sensory input from the head (Berni et al. 2012).

miR-iab4/iab8 are expressed in the abdominal CNS from A2 to A9 (Tyler 2008). Based on this, *miR-iab4/iab8* could be involved in the movement of those segments. Should these miRNAs exert any effects in the contraction of abdominal segments A2 to A9 these are likely to be involved in the initiation and/or propagation of forward waves, and/or in the propagation of backward waves but not on their initiation.

To test whether *miR-iab4/iab8* are required for peristaltic locomotion we analysed the frequency of full-body peristaltic contractions in *miR-iab4/iab8* mutants (Δ*miR-iab4/iab8*). To do this, we assayed the number of forward and backward waves of freshly hatched larvae (less than 30 min after hatching) in a dish coated with a thin layer of agarose (see Chapter 2). We used two *wild type* controls: *Oregon-R* (*OR*) and *white* (w^{1118}). *OR* was used as a general *wild type* strain and w^{1118} as a genetic background control since the mutants for *miR-iab4/iab8* were produced in a $white^{1118}$ background. These two controls showed no behaviour difference between them (see below). Larvae mutant for *miR-*

iab4/iab8 (Δ*miR-iab4/iab8*) made normal full-body peristaltic contractions. We quantified the frequency of forward and backward full-body peristaltic waves made during 2 minutes and found no significant differences between the two *wild type* controls (*OR* and w^{1118}) and Δ*miR-iab4/iab8* larvae (Figure 4.1C; $p > 0.05$ Mann-Whitney *U* test). *Wild type* controls generated an average of 22.59 ± 1.05 (*OR*; mean ± SEM) and 21.48 ± 0.84 (w^{1118}) forward waves per minute and the Δ*miR-iab4/iab8* 24.22 ± 1.09. Backward waves were less frequent than forward waves in the three genotypes: *wild types* made 0.40 ± 0.17 (*OR*) and 0.11 ± 0.08 (w^{1118}), and Δ*miR-iab4/iab8* 0.10 ± 0.07 (Figure 4.1D). We concluded that normal patterns of peristaltic locomotion are unaffected by the absence of *miR-iab4/iab8*.

4.2.2 *miR-iab4/iab8* do not affect turning behaviour

Substrate exploration (exploratory behaviour) of *wild type* larvae consists of two alternating movement programs: crawls and turns (Lahiri et al. 2011). Turns are interspersed with forward crawls to redirect crawling trajectory (Berni et al. 2012). During exploratory behaviour larvae crawl straight in forward peristaltic waves, pause and initiate a turn with an asymmetric contraction of the most anterior segments followed by a unilateral backward contraction until abdominal segment 4 (A4) (Figures 4.2A and 4.2B). This movement repositions the anterior part of the animal and if a forward wave is initiated will redirect the crawling trajectory.

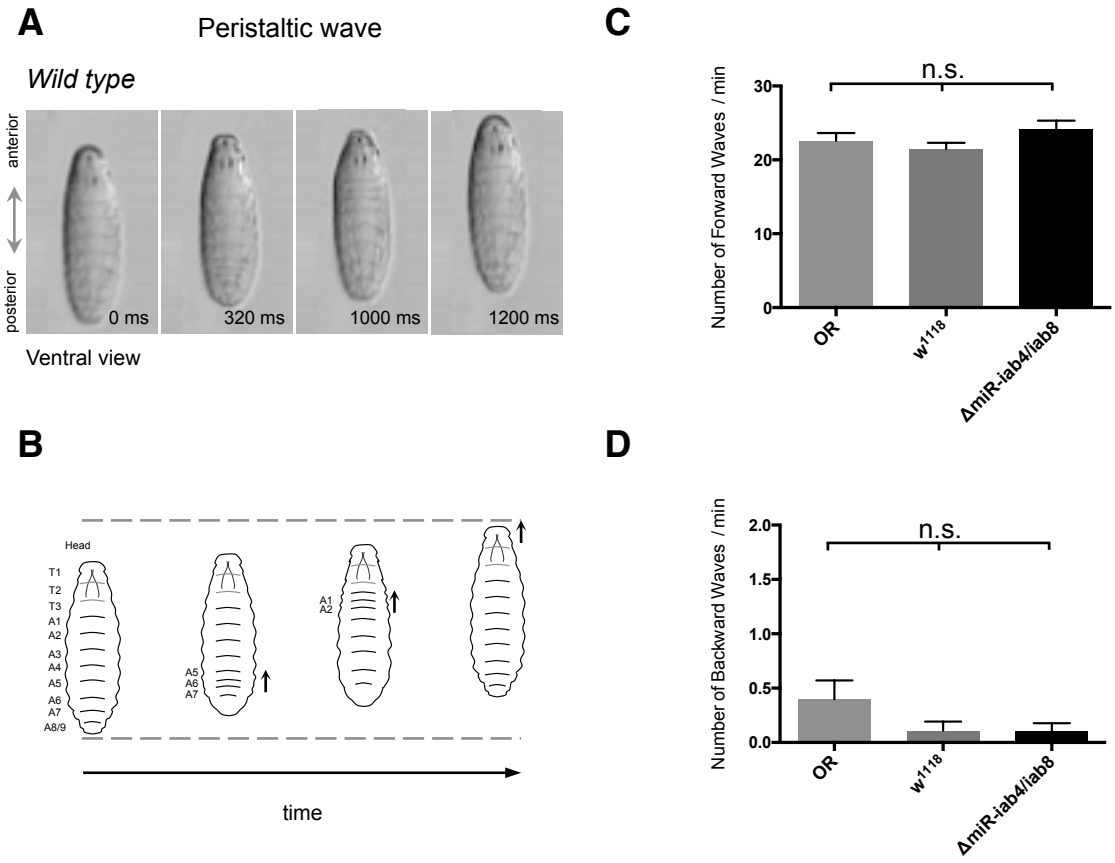

Figure 4.1 Removal of *miR-iab4/iab8* does not affect peristaltic locomotion (A-B)

(Legend on the following page)

Figure 4.1 Removal of *miR-iab4/iab8* does not affect peristaltic locomotion

(A-B) Description of a wild type larval peristaltic wave. (A) Time-lapse of a single peristaltic wave (ventral view). (B) Diagram corresponding to the peristaltic wave shown in (A). Arrows indicate the contracting abdominal segments at each time-point. **(C-D)** Analysis of larval peristalsis upon removal of *miR-iab4/iab8*. (C) The average number of forward peristaltic waves was not significantly different among the two wild type larval genotypes (*OR* and w^{1118}) and the *miR-iab4/iab-8* mutants (Δ*miR-iab4/iab8*). Similarly, (D) the average number of backward waves was not significantly different among the three genotypes. An average of 20 larvae of each genotype was used in all analyses. A non-parametric Mann-Whitney *U* test was performed to compare treatments; $p > 0.05$ (non-significant; n.s). Error bars denote the standard error of the mean (S.E.M.). Altogether, these experiments show that normal patterns of peristaltic locomotion are unaffected in the absence of *miR-iab4/iab8*.

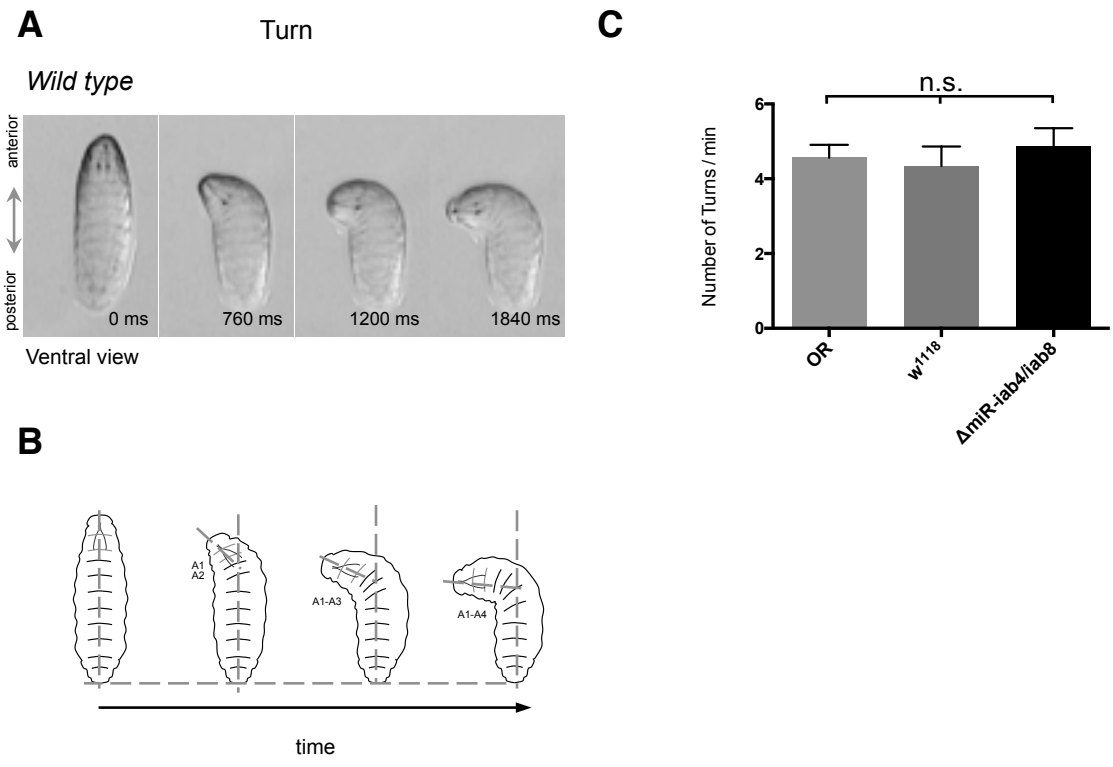

Figure 4.2 Absence of *miR-iab4/iab8* does not alter the number of turns

(A-B) Description of a wild type larval turn. (A) Time-lapse of a single larval turn (ventral view). (B) Diagram corresponding to the turn shown in (A). The numbered abdominal segments correspond to the unilaterally contracting segments at each time-point (from A1 to A4). **(C)** Analysis of larval turning upon removal of *miR-iab4/iab8*. The average number of turns was not significantly different among the two wild type larval genotypes (*OR* and w^{1118}) and the *miR-iab4/iab-8* mutants (Δ*miR-iab4/iab8*). An average of 20 larvae of each genotype was used in all analyses. A non-parametric Mann-Whitney *U* test was performed to compare treatments; $p > 0.05$ (non-significant; n.s). Error bars denote the S.E.M. Altogether, these experiments show that normal patterns of larval turning behaviour are not affected by the removal of *miR-iab4/iab8*.

To investigate if *miR-iab4/iab8* are involved in establishing the circuitry for the turning program, we compared the number of turns between *wild type* controls and Δ*miR-iab4/iab8*. We observed no significant change in the number of turns between both controls (4.56 ± 0.35 and 4.35 ± 0.52 turns per minute in *OR* and w^{1118}, respectively) and the *miR-iab4/iab8* mutants (4.88 ± 0.47) (Figure 4.2C; $p > 0.05$, *U* test). Furthermore, when turning the majority of *miR-iab4/iab8* mutant larvae bent their body until segment A4 as in the controls. Our results therefore show that *miR-iab4/iab8* do not play any detectable role in the exploratory behaviour of newly hatched larvae.

4.2.3 *miR-iab4/iab8* are not involved in touch response

We next probed the mechanosensory response of *miR-iab4/iab8* mutants by tactile stimulation (Figure 4.3) (Kernan et al. 1994; Bodily et al. 2001). We touched Δ*miR-iab4/iab8* larvae in the head with an eyelash and scored their response as follows: no response=0, hesitation=1, withdraws anterior=2, turns=2, single backward wave=3, multiple backward waves =4; for a maximum score of 12 (Figure 4.3A) (Kernan et al. 1994). We found no differences in the touch response essay between the two *wild type* controls and the Δ*miR-iab4/iab8* larvae (Figure 4.3B) The majority of the Δ*miR-iab4/iab8* larvae did a characteristic escape behaviour, *i.e.* one to three backward peristaltic waves, one lateral turn and sequential forward crawling. We conclude that the mechanosensory response is not affected in *miR-iab4/iab8* mutant larvae.

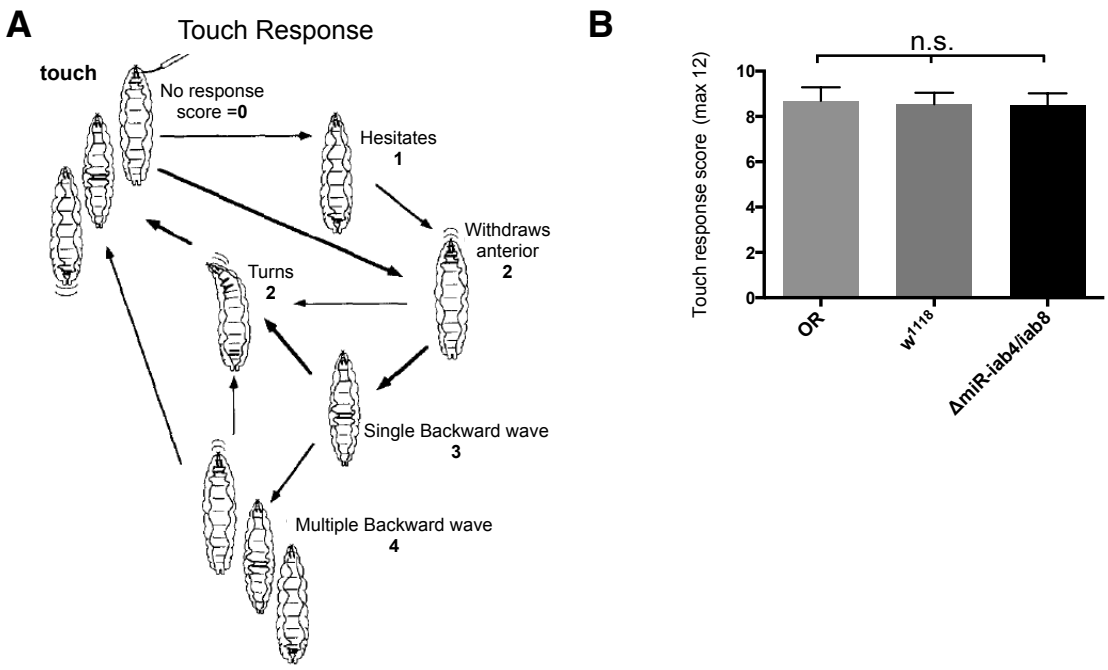

Figure 4.3 *miR-iab4/iab8* are not required for touch response

(A) Diagram representing the stereotypical touch-response behaviour of *Drosophila* larvae (from Kernan et al. 1994). To measure touch responsiveness, we used an eyelash to stimulate the heads of crawling Δ*miR-iab4/iab8*, *OR* and w^{1118} larvae and scored their response as follows: no response=0, hesitation=1, withdraws anterior=2, turns=2, single backward wave=3, multiple backward waves =4; for a maximum score of 12 (after Kernan et al. 1994). **(B)** Quantification of touch response behaviour in Δ*miR-iab4/iab8*, *OR* and w^{1118}. The average score for touch response was not significantly different between *OR*, w^{1118} and Δ*miR-iab4/iab8*. An average of 16 larvae of each genotype was used in all analyses. A non-parametric Mann-Whitney *U* test was performed to compare treatments; $p > 0.05$ (non-significant; n.s). Error bars denote the S.E.M. Altogether, these experiments show that normal patterns of larval touch response behaviour are not affected by the absence of *miR-iab4/iab8*.

4.2.4 *miR-iab4/iab8* disrupt self-righting behaviour

Until this point, we did not detect any abnormal larval behaviour in *miR-iab4/iab8* mutants. This could mean that these miRNAs are not involved in the development of the underlying neuronal circuits of the tested behaviours or that a redundant mechanism compensates for the absence of these miRNAs. To test the former hypothesis we challenged the larvae with a new behaviour, a complex rolling behaviour named self-righting (Crisp et al. 2008). We rolled larvae upside down onto their dorsal side (dorsal down) and measured the time required to self-right (Figure 4.4). *Wild type* larvae placed in an inverted position (ventral up) responded immediately by twisting their heads, grabbing the substrate with the mouth hooks and rolling the body onto their ventral surface (dorsal up) in about 10 seconds (Figures 4.4A and 4.4D; *OR* 9.65 ± 1.78 sec and w^{1118} 11.85 ± 2.37 sec to self-right). This movement requires complex coordinated bilateral motor control with asymmetric muscle contractions. Strikingly, mutant larvae for *miR-iab4/iab8* were significantly slower to self-right themselves, taking at least six times longer to self-right (Figures 4.4B and 4.4D; 63.99 ± 16.75 sec to self-right; $p < 0.001$ *U* test). Detailed analysis of the movement sequence revealed that when Δ*miR-iab4/iab8* larvae were inverted they twisted their heads and grabbed substrate like the *wild types*, but then during the rolling they stopped the movement and would remain in an upside down position (Figure 4.4B). Once upside down, they behaved as if they had engaged in an exploratory routine by performing forward and backward waves alternated by turns while moving the mouth hooks, perhaps in an attempt to "find/localise" the substrate. Then, they would re-initiate the self-righting move-

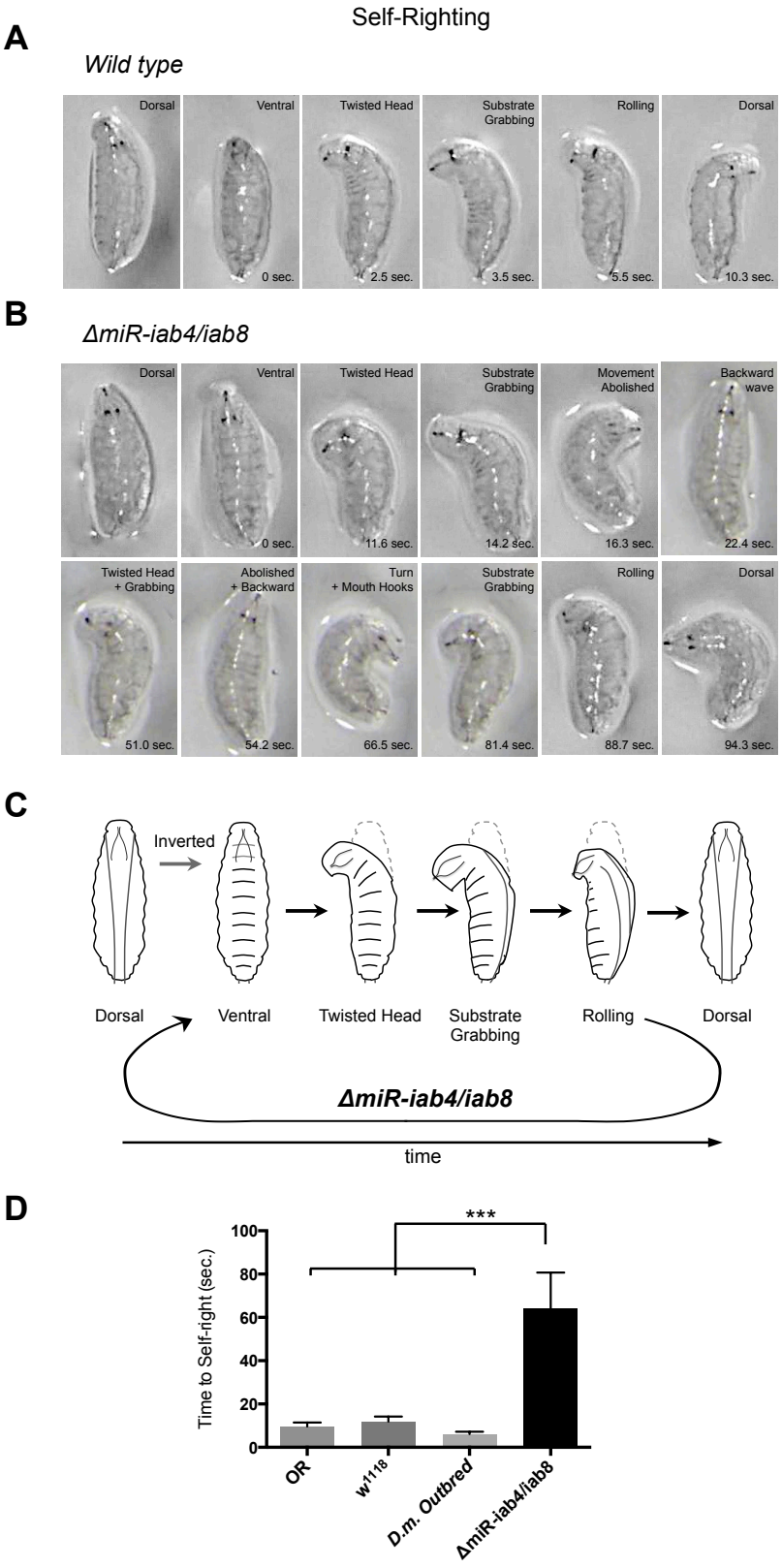

Figure 4.4 *miR-iab4/iab8* disturbs self-righting behaviour

(Legend on the following page)

Figure 4.4 *miR-iab4/iab8* disturbs self-righting behaviour

(A-B) Time-lapse of larval self-righting behaviour. (A) Wild type larvae were placed in an inverted position (ventral up), and proceeded to twist their heads, grabbing the substrate with the mouth hooks and rolling the body onto their ventral surface (dorsal up). In contrast, (B) inverted ∆miR larvae display problems in completely rolling their bodies, often falling back to their initial position and reinitiating the self-righting response. **(C)** Diagram of the self-righting behavioural response. In contrast to wild type larvae, which follow a linear movement sequence, ∆miR larvae fail to roll back to their correct position, looping instead between failed rolling and the reinitiation of the self-righting movement. **(D)** Quantification of the time required for the successful completion of the self-righting behaviour in *OR*, w^{1118}, *Dm.Outbred* and Δ*miR-iab4/iab8* larvae. The average time to self-right was significantly different between the three wild type controls (*OR*, w^{1118}, *Dm.Outbred*) and Δ*miR-iab4/iab8* larvae. An average of 25 larvae of each genotype was used in all analyses. A non-parametric Mann-Whitney *U* test was performed to compare treatments; $p < 0.001$ (***). Error bars denote the standard error of the mean (S.E.M.). Altogether, these experiments show that the absence of *miR-iab4/iab8* significantly impairs the ability of larvae to self-right.

ment. This loop would repeat a few times until the larvae managed to roll their bodies (Figure 4.4C).

To see if these effects were due to the removal of *miR-iab4/iab8* and not the genetic background of the mutant, we used a highly polymorphic outbred *Drosophila melanogaster* population (Martins et al. 2013). Our reasoning was the following: if genetic background and/or genetic variability are relevant for self-righting behaviour, we would expect to observe a wide spectrum on the timing to self-right in a highly polymorphic population. Our concern was based on the studies made by Marla Sokolowski and colleagues where they found natural genetic variation associated with differences in larval foraging behaviour (Osborne et al. 1997; Sokolowski 1980). Interestingly, genetically variable larvae had a very quick response to an inverted position taking approximately 6 seconds to self-right (Figure 4.4D; 6.14 ± 1.06). However they were not significant different from the two inbred *wild type* controls ($p > 0.05$, *U* test).

Altogether these experiments show that miRNAs *miR-iab4/iab8* are necessary for self-righting behaviour, a complex coordinated motor movement.

4.2.5 Self-Righting behaviour is dependent on UBX regulation

In principle, *miR-iab4/iab8* could regulate hundreds of genes involved in self-righting behaviour. Previous studies showed that *miR-iab4/iab8* regulate UBX protein expression by targeting the *Ubx* long 3'UTR during CNS development (see Figure 4.5) (Bender 2008; Ronshaugen et al. 2005; Stark et al. 2008; Tyler et al. 2008; Thomsen et al. 2010). In the ventral nerve cord

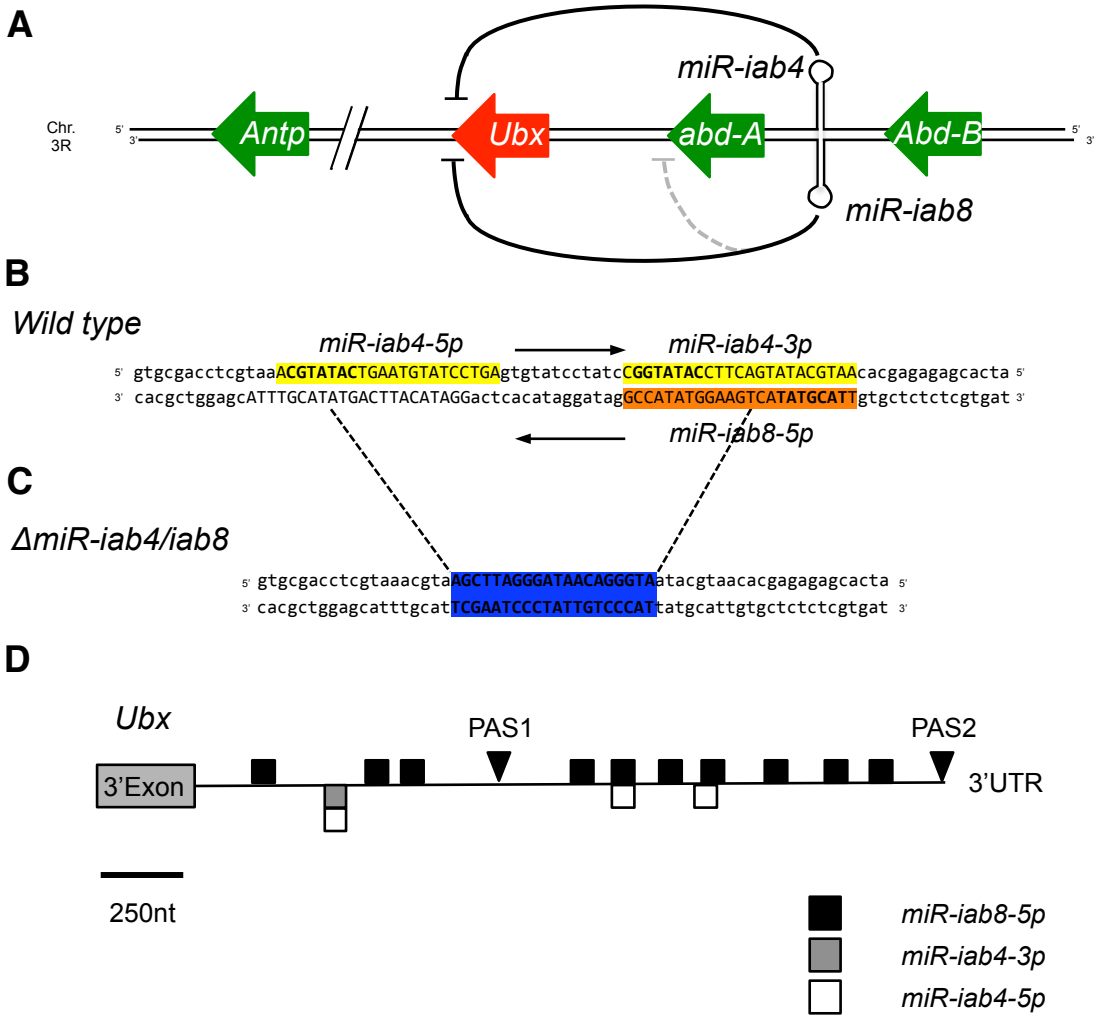

Figure 4.5 The 3'UTR of *Ubx* contains targets for *miR-iab4/iab8*

(Legend on the following page)

Figure 4.5 The 3'UTR of *Ubx* contains targets for *miR-iab4/iab8*

(A) Genomic localisation of *miR-iab4/iab8* within the Bithorax complex (adapted from Tyler et al. 2008). miRNAs *miR-iab4* and *miR-iab8* are produced from complementary strands of a single genomic locus in the Bithorax complex, and are located downstream of the *Hox* gene *Abd-B* and upstream of the *Hox* gene *abd-A*. Additionally, these miRNAs have been shown to target *abd-A* and *Ubx* 3'UTRs *ex-vivo* (luciferase reporter assays on S2 cells; Stark *et al.* 2008) and *in-vivo* (wing and haltere imaginal discs, both heterologous environments; Ronshaugen et al. 2005; Tyler et *al.* 2008). **(B-C)** Nucleotide sequences of the *miR-iab4/iab8* locus in (B) the wild type and (C) mutated versions (Δ*miR-iab4/iab8*). The Δ*miR-iab4/iab8* sequence was previously generated by gene conversion (Bender 2008). **(D)** Location of the predicted target-sites for miRNAs miR-iab4-5p, miR-iab4-3p and miR-iab8-5p within the *Ubx* 3'UTR. These targets were predicted using the PITA online miRNA prediction tool (Kertesz et *al.* 2007). Notice the differential distribution of target-sites for these miRNAs among proximal and distal tracts of the *Ubx* 3'UTR.

(VNC) of *wild type* embryos UBX protein is highly expressed in the posterior part of segment T3 and anterior part of A1 (parasegment 6) and declines towards posterior until A7 (Figures 4.6A and 4.6B) (Akam & Martinez-Arias 1985; R. A. White & Wilcox 1985a). Additionally, in abdominal segments UBX is mainly expressed in the anterior part of each segment. In the absence of *miR-iab4/iab8* there is a drastic increase in UBX protein in the VNC at later stages of embryonic development (Figures 4.6C and 4.6D) (Bender 2008; Thomsen et al. 2010). In Δ*miR-iab4/iab8* late embryos, UBX expression is nearly constant from A2 through A7. Thus, the negative slope towards posterior of UBX expression is abolished. Additionally, UBX is almost completely absent in A8/9 segments in *wild type* embryos but Δ*miR-iab4/iab8* show a small UBX expression in the VNC.

To investigate whether UBX upregulation is responsible for the *miR-iab4/iab8* behaviour phenotype, we overexpressed UBX in its natural domain of expression independently from the *miR-iab4/iab8* regulation. We reasoned that if an artificial increase in UBX protein expression independent from the removal of the miRNAs was sufficient to disrupt self-righting behaviour then *miR-iab4/iab8* control self-righting behaviour through the regulation of UBX protein expression. For this we used two Gal4 lines inserted nearby the *Ubx* promoter – *Ubx*-Gal4^{M1} (*Ubx*.M1) and *Ubx*-Gal4^{M3} (*Ubx*.M3) – that reproduced the endogenous *Ubx* expression (de Navas et al. 2006). The Gal4s are inserted 4 bp apart, have opposite orientations and are *Ubx* null mutant (de Navas et al. 2006). Driving *Ubx* expression with either Gal4 (*Ubx*-Gal4^{M1}/ UAS-*Ubx* Ia or *Ubx*-Gal4^{M3}/ UAS-*Ubx* Ia) it reproduces UBX expression of Δ*miR-iab4/iab8*

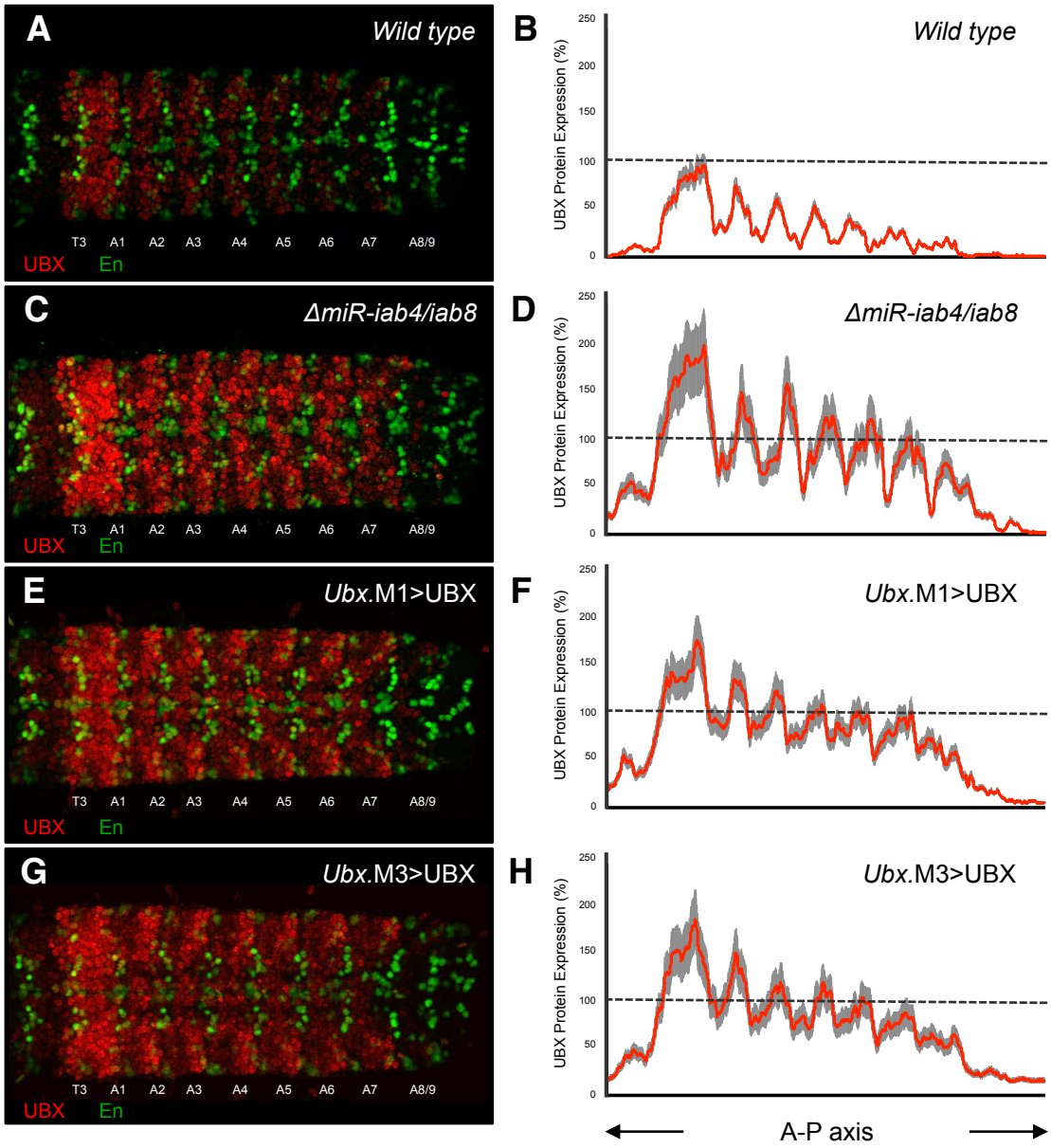

Figure 4.6 Regulation of UBX protein expression by *miR-iab4/iab8* in the CNS

(Legend on the following page)

Figure 4.6 Regulation of UBX protein expression by *miR-iab4/iab8* in the CNS

(A, C, E, G) UBX protein expression (red) of dissected embryonic VNC in (A) *wild* type, (C) ∆miR-*iab4/iab8* (E) *Ubx*.M1>UBX and (G) *Ubx*.M3>UBX embryos at stage 16. Engrailed protein expression (green) was used as a segmental marker. (C) UBX expression levels were significantly higher in the absence of miR-*iab4/iab8*. (E,G) The observed overexpression of UBX was recapitulated using the *Ubx*.M1-*Gal4* and *Ubx*.M3-*Gal4* drivers. **(B, D, F, H)** Profile quantification of UBX protein expression along the A-P axis in dissected VNCs of (B) *wild* type, (D) ∆miR-*iab4/iab8* (F) *Ubx*.M1>UBX and (H) *Ubx*.M3>UBX embryos at stage 16. The thick red line represent the average intensity of UBX protein expression in seven embryos of each genotype; and their grey shadows represent S.E.M. Dashed lines mark the maximum UBX wild type expression. Anterior is to the left.

embryos: high levels of UBX in abdominal segments (no negative modulation towards posterior) and ectopic expression in A8/9 (Figures 4.6E-H)

Given that our previous experiments demonstrate that *miR-iab4/iab8* are necessary for self-righting behaviour but not for exploratory behaviour (Figures 4.1, 4.2 and 4.3), we tested to what extent was this due to *Ubx* misregulation. In line with our hypothesis, overexpression of *Ubx* (*Ubx*.M1>UBX and *Ubx*.M3>UBX) affected significantly self-righting behaviour (Figure 4.7C) but not exploratory behaviour (Figures 4.7A and 4.7B). An increase of UBX protein expression independent from the absence of *miR-iab4/iab8* phenocopied the effects on self-righting observed in the Δ*miR-iab4/iab8* larvae, *i.e.* an increase in the time required for the larvae to self-right (Figure 4.7C). Notably, the magnitude of the self-righting effects (time to self-right) was similar between Δ*miR-iab4/iab8* (63.99 ± 16.75 sec) and the two UBX overexpression lines (*Ubx*.M1>UBX took 63.98 ± 13.74 sec and *Ubx*.M3>UBX 58.84 ± 18.94 sec to self right)($p > 0.05$, *U* test).

We conclude that the regulation of UBX by microRNAs *miR-iab4/iab8* is necessary for the correct coordination of self-righting behaviour.

4.3 Discussion

The experiments described in this chapter show that microRNAs from the BX-C, *miR-iab4/iab8*, affect a specific larva behaviour by regulating the expression of UBX. We did a series of different behaviour essays on newly hatched larvae mutant for *miR-iab4/iab8* and only one behaviour was affected:

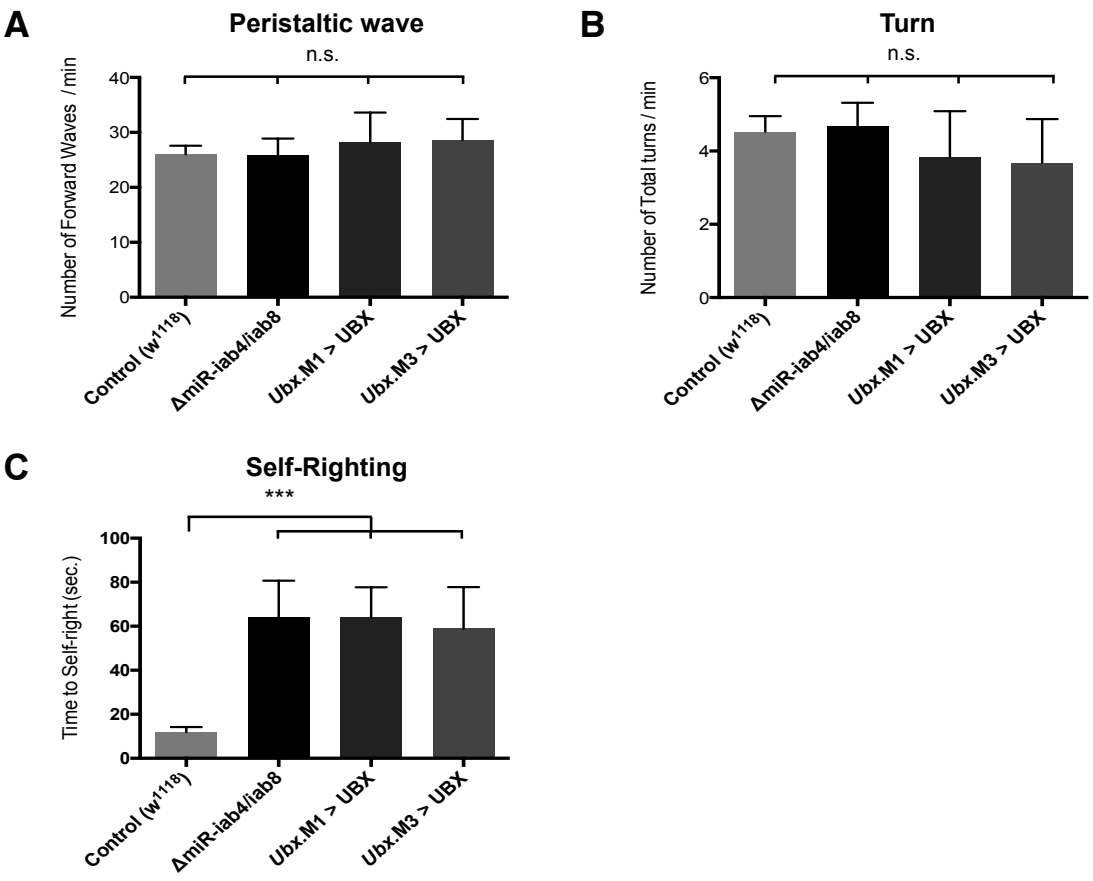

Figure 4.7 Ectopic expression of UBX phenocopies the Δ*miR-iab4/iab8* behaviour phenotype

(Legend on the following page)

Figure 4.7 Ectopic expression of UBX phenocopies the Δ*miR-iab4/iab8* behaviour phenotype

(A-C) Quantification of larval behaviour in *Ubx*.M1>UBX and *Ubx*.M3>UBX artificial overexpression lines. (A) The average number of forward peristaltic waves per minute was not significantly different among w^{1118}, *ΔmiR-iab4/iab8*, *Ubx*.M1>UBX and *Ubx*.M3>UBX. Similarly, (B) larval turning behaviour was indistinguishable between the four genotypes. (C) Quantification of the time required for the successful completion of the self-righting behaviour in w^{1118}, *ΔmiR-iab4/iab8*, *Ubx*.M1>UBX and *Ubx*.M3>UBX larvae. The average time to self-right was significantly different between the two UBX overexpression lines *Ubx*.M1>UBX and *Ubx*.M3>UBX and the wild type (w^{1118}), displaying the same delay in self-righting as the Δ*miR-iab4/iab8* larvae. An average of 20 larvae of each genotype was used in all analyses. A non-parametric Mann-Whitney *U* test was performed to compare treatments; $p > 0.05$ (non-significant; n.s.); $p < 0.001$ (***). Error bars denote the S.E.M. Altogether, these experiments show that the overexpression of UBX is sufficient to phenocopy the abnormal self-righting behaviour of *miR-iab4/iab8* larvae.

self-righting behaviour. These experiments show that *miR-iab4/iab8* affect self-righting behaviour in a specific manner, and that this is not due to a general locomotory defect. To our knowledge, this study reports the first specific locomotory behaviour controlled by a single miRNA system.

Drosophila larvae when placed on a inverted position contract their muscles asymmetrically and carry out a “twist-and-roll” movement to self-right their bodies (Figure 4.4A (Bodily et al. 2001; Crisp et al. 2008). In contrast, when Δ*miR-iab4/iab8* larvae are inverted they move their heads and mouth hooks constantly, probably trying to grab the substrate, and then initiate a twist-and-roll movement. At this point, the larvae stop the rolling movement, return to an inverted position, start doing peristaltic waves alternated with turns like in an exploratory routine and then re-initiate the self-righting movement. This loop of initiation – pause – re-initiation of self-righting movement repeats a few times until the larvae completely roll their bodies (see above). These observations suggest that *miR-iab4/iab8* do not impair the perception of an inverted position, but rather the ability of larvae to roll their bodies in a *wild type* manner.

In theory, *miR-iab4/iab8* could regulate the expression of hundreds of target genes that ultimately control self-righting behaviour. Previous studies showed that *miR-iab4/iab8* negatively regulate UBX protein expression in the VNC (Bender 2008; Thomsen et al. 2010). Thus, we asked to what extent are the self-righting defects observed in the Δ*miR-iab4/iab8* due to an increase in UBX protein expression in the VNC?

Crucially, we find that artificial overexpression of *Ubx* independent from *miR-iab4/iab8* regulation recapitulates the defects in self-righting behaviour without affecting the other behaviours (Figure 4.7C). This demonstrates that an

increase in UBX protein expression in the VNC is sufficient to affect self-righting behaviour, suggesting that *miR-iab4/iab8* influence self-righting behaviour in a *Ubx* dependent manner. To further corroborate this, it would be desirable to reduce UBX protein expression in *miR-iab4/iab8* mutants and test whether the normal self-righting behaviour is restored. In other words, reduce the levels of UBX in a Δ*miR-iab4/iab8* genetic background and assay the time required for the larvae to self-right. Indeed, we attempted to carry out this experiment by having larvae heterozygote for *Ubx* (*Ubx* ^{1}/*Ubx* $^{+}$) in a Δ*miR-iab4/iab8* background. To achieve this, we tried to recombine a *Ubx* ^{1} allele (*Ubx* null allele (Bender et al. 1983)) with a Δ*miR-iab4/iab8*; however we were not able to get recombinants due to the small genetic distance between the two loci (~0.2 centimorgan). We are currently exploring an alternative way of reducing UBX protein in a Δ*miR-iab4/iab8* background by using *Ubx*^{RNAi}.

In our overexpression experiments to phenocopy the defects of Δ*miR-iab4/iab8*, we overexpressed the splicing isoform UBX Ia (see Chapter 1 and 3; (Kornfeld et al. 1989; O'Connor et al. 1988)). Bearing in mind that the different UBX alternative splicing isoforms have distinct functions (Mann & Hogness 1990; de Navas et al. 2011; Reed et al. 2010), it would be interesting to see to what extent the different UBX isoforms have different capacities to phenocopy the Δ*miR-iab4/iab8* self-righting behaviour phenotype? This could give new insights on the function of UBX alternative splicing isoforms in CNS development.

miR-iab4/iab8 are important regulators of UBX protein expression in the VNC: genetic removal of *miR-iab4/iab8* leads to a significant increase in UBX protein expression from T3 to A7 (Figures 4.6C and 4.6D). The increase in UBX

expression in T3 and A1 is contrary to our expectation since *miR-iab4* and *miR-iab8* are expressed in A2-A7 and A8/9 (Thomsen et al. 2010; Tyler et al. 2008). So far we do not have an explanation for this observation but we have several non-exclusive possibilities that we are currently testing. miRNA *in situ* hybridisation in *Drosophila* detects the primary miRNA transcripts and not the mature transcripts. This implies that mature *miR-iab4/iab8* transcripts would not be detected in T3/A1 segments if their transcription is low and/or if mature miRNAs are secreted from posterior cells. Although the latter possibility seems unlikely, a recent example in human cell culture showed that communication of immune cells via secretion of miRNAs modulates gene expression in recipient cells (Mittelbrunn et al. 2011). Expressing a sensor construct in this region could test for the presence of mature *miR-iab4/iab8* transcripts in T3/A1. For example, we could compare the expression profile of a transgenic mCherry fluorescent protein coupled to the long *Ubx* 3'UTR versus that of a mutated long *Ubx* 3'UTR without the *miR-iab4/iab8* target sites (long *Ubx* Δseed 3'UTR). If mature *miR-iab4/iab8* transcripts are present in T3/A1, we would expect a decrease in expression of mCherry-long.*Ubx*.3'UTR in comparison with mCherry-long.*Ubx*.Δseed.3'UTR. Another possibility is that an increase in UBX protein expression in A2-A7 could lead to an increase in UBX in T3/A1 mediated via cell-cell communication. This could be examined by overexpressing *Ubx* in A2-A7 (e.g. *abd*-A-Gal4 X UAS-*Ubx*) and testing whether an increase in UBX protein in T3/A1 is detected. Finally, absence of *miR-iab4/iab8* and/or UBX upregulation could interfere with *Ubx* transcription. Indeed, a *Ubx* enhancer element was identified to positively autoregulate *Ubx* expression in the CNS (Christen & Bienz 1992). This cis-element is linked to a *lacZ* reporter and its

expression varies according to UBX levels in the CNS. Thus, we could test whether the expression of this cis-element linked to *lacZ* changes in the absence of *miR-iab4/iab8*. Additionally, we could test this hypothesis by monitoring if *Ubx* transcription is affected in *miR-iab4/iab8* mutants or in *abd*-A-Gal4 X UAS-UBX with the *Ubx* transcriptional reporter 35UZ (Irvine et al. 1991) and with *Ubx* intronic *in situs* that detect nascent *Ubx* RNAs (see Chapter 3 and 5).

In summary, our experiments show that *Ubx* regulation by *miR-iab4/iab8* is relevant for self-righting behaviour. To our knowledge this is the first example of the relevance of *Hox* regulation by miRNAs in the control of a locomotory behaviour. In the next chapter we will investigate how *Ubx* regulation by *miR-iab4/iab8* is affecting self-righting behaviour.

Chapter 5

Exploring the cellular basis of *Hox*-dependent larval behaviour in *Drosophila*

N.B. This chapter is part of a collaboration with Dr. Jimena Berni and Dr. Matthias Landgraf of the Department of Zoology in the University of Cambridge. I conducted all the experiments shown here.

5.1 Chapter overview

In the preceding Chapter we investigated the biological consequences of UBX regulation by *miR-iab4/iab8* during CNS development by testing a series of different larval behaviours. Analysis of these behaviours showed that the absence of *miR-iab4/iab8* disrupts a specific larval behaviour: self-righting. Furthermore, we show that regulation of UBX protein is involved in the coordination of this behaviour. We thus propose that UBX regulation by *miR-iab4/iab8* controls the coordination of a larval self-righting behaviour.

In this Chapter we explore the cellular basis of self-righting behaviour in the context of miRNA-dependent UBX regulation. Using an array of genetic, imaging and behaviour methods we show that: (i) *miR-iab4/iab8* mutants do not have major anatomical anomalies; (ii) increase in the expression level of UBX protein in cholinergic interneurons impairs self-righting behaviour; and (iii) UBX expression is regulated by *miR-iab4/iab8* in cholinergic interneurons. We suggest that UBX regulation by *miR-iab4/iab8* in cholinergic interneurons controls self-righting behaviour. This study sheds light on the cellular interactions of *Hox*-miRNAs in the control of behaviour.

5.2 Results

The normal coordination of self-righting behaviour is dependent on the regulation of UBX by miRNAs *miR-iab4/iab8.* Disruption of the *wild type* expression levels of UBX protein either by the absence of *miR-iab4/iab8* or by artificial overexpression leads to an abnormal larval self-righting behaviour. Here we investigate how misregulation of UBX by *miR-iab4/iab8* disrupts self-righting behaviour. We conceived two non-exclusive possibilities. First, changes in UBX expression could cause morphological/anatomical defects that impair the coordination of self-righting behaviour. Indeed, UBX gain of function was shown to affect the morphology of the wing (Bender et al. 1983; R. A. White & Akam 1985), the haltere (Crickmore et al. 2009) and larval cuticle (Gonzalez-Reyes & Morata 1990). Second, increase in UBX protein expression could modify the function of the underlying cell network that controls this behaviour. We hypothesise that this change in function can be an alteration in the specialisation and/or the physiology of the cells. In line with this, recent studies showed that *Hox* expression modulates neuropeptide specialisation in the CNS in the end of *Drosophila* embryogenesis (Miguel-Aliaga et al. 2008; Suska et al. 2011).

We started by analysing the morphology of *miR-iab4/iab8* mutants through a series of immunohistochemical experiments that detect different neuronal elements of the system (see below).

5.2.1 – Components of the system

To investigate the effects of *miR-iab4/iab8* mutants on CNS development, we analysed the integrity of the main components of the system that could be affected. From a simplified perspective, when a larva is rolled upside down with a brush the first challenge is to perceive that it is actually in an inverted position. This perception could be given by the sensory system in the body wall either by the touch of the brush when the animals are being rolled or by a different position of the body in respect to the substrate. Alternatively, the message could come from the head region where the animal is incapable of grabbing the substrate with the mouth hooks. In either case, this peripheral information is transmitted to the nerve cord where it is going to be processed. Once in the VNC, interneurons receive peripheral information and transmit it to other interneurons or directly to motoneurons. The process of information flow within the VNC may be extremely complex with hundreds of interneurons communicating with each other (either excitatory or inhibitory connections) and eventually communicating to motoneurons. In other words, the stream of information between interneurons acts as a computational step to decipher the sensory message into an output, motoneuron stimulation. In many of these interactions, glia cells are an important component as they can: recycle neurotransmitters from the synapse (Eaat1, Excitatory amino acid transporter 1 (Besson et al. 1999; Soustelle et al. 2002)); give nutritional support to neurons (Hoyle et al. 1986); and regulate the formation of the network (Hidalgo et al. 1995; Hidalgo & Booth 2000). Then, motorneurons transmit the information to

the muscles which will contract and produce a motor movement. Changes in the motor movement can then feedback on the sensory system so that the flow of information starts again.

5.2.2 - Effects in the anatomy of neuronal axons and muscles

We analysed the morphology of the different “units” of the system, namely: sensory neurons, commissures and longitudinal tracks (as a proxy for interneurons), glia cells, motoneuron projections and muscles. For this we did a series of antibody stainings in flat preparations of *wild type* and Δ*miR-iab4/iab8* late embryos. Although we would have wished to look at the anatomical structure of the system in first instar larvae, we were not able to do flat preparations (flat preps) in newly hatched larvae (indeed, we attempted these dissections many times but without success). As an alternative approach we made flat preps of late embryos (late stage 16) and analysed their morphology. The anatomy of a late embryo is similar to newly hatched larvae. We first analysed motorneuron projections in the muscles and sensory neurons by using anti-HRP (horseradish peroxidase) antibody to visualise neuronal membranes through the recognition of neuronal glycoproteins (Snow et al. 1987) and anti-*Tm1* (*Tropomyosin 1*) antibody to stain the muscles. We detected no obvious abnormalities in sensory neurons (Figure 5.1B, arrowheads) or motoneuron projections of Δ*miR-iab4/iab8* embryos (Figure 5.1B). Embryos without *miR-iab4/iab8* display all three principal motoneuron nerve trunks - intersegmental nerve (ISN), segmental nerve (SN) and transverse nerve (TN) - projecting to

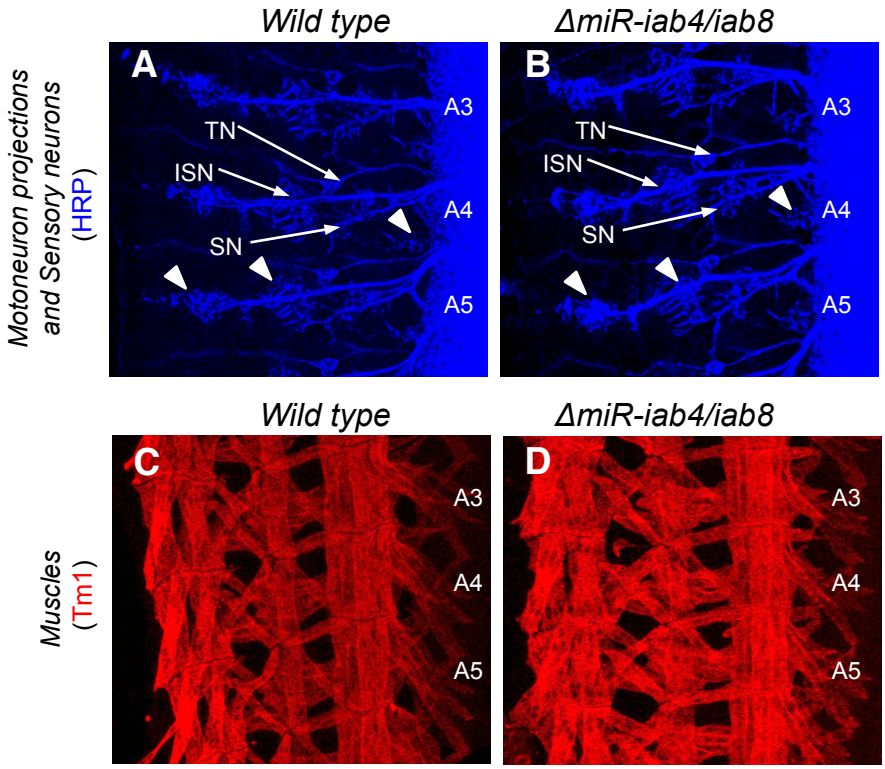

Figure 5.1 Absence of miR-iab4/iab8 does not disrupt the abdominal morphology of motoneuron projections, sensory neurons and muscles

(A-B) Motoneuron projections and sensory neurons (HRP, blue) in abdominal segments A3, A4 and A5 of wild type (A) and Δ*miR-iab4/iab8* (B) late stage 16 embryos. Arrows denote the three main motoneuron nerve trunks [intersegmental nerve (ISN), segmental nerve (SN) and transverse nerve (TN)], while arrowheads indicate the position of sensory neurons. (B) Motoneuron projections and sensory neurons show no obvious defects in the *miR-iab4/iab8* mutant. **(C-D)** Muscle patterns (Tropomyosin 1, red) in abdominal segments A3, A4 and A5 of wild type (C) and Δ*miR-iab4/iab8* (D) late stage 16 embryos. (D) Abdominal muscles show no obvious abnormalities in the *miR-iab4/iab8* mutant when compared to wild type. Anterior is up.

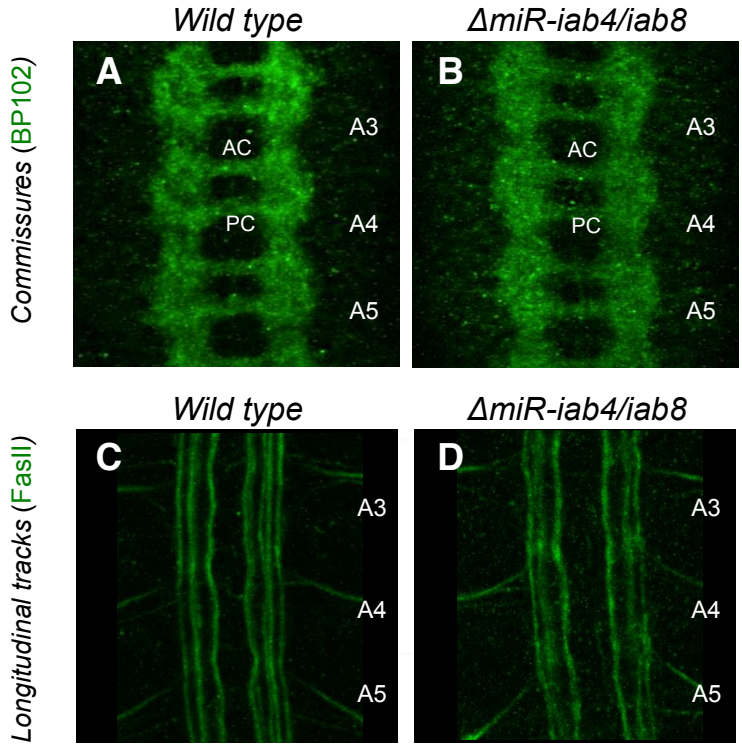

Figure 5.2 Removal of *miR-iab4/iab8* does not affect the morphology of neuronal commissures and longitudinal tracks

(A-B) VNC commissures (BP102, green) in abdominal segments A3, A4 and A5 of wild type (A) and Δ*miR-iab4/iab8* (B) late stage 16 embryos. (B) The Δ*miR-iab4/iab8* pattern and thickness of anterior commissures (AC) and posterior commissures (PC) were similar to that observed in the wild type. **(C-D)** VNC longitudinal tracks (FasII, green) in abdominal segments A3, A4 and A5 of wild type (C) and Δ*miR-iab4/iab8* (D) late stage 16 embryos. (D) The three longitudinal axonal tracks were normally patterned in Δ*miR-iab4/iab8* embryos, thus resembling the wild type VNCs. Anterior is up.

their target muscles: SN and TN innervating external muscles and ISN innervating internal muscles (Landgraf & Thor 2006). Moreover, the muscles were correctly patterned in the mutants with no defects within or between segments (Figure 5.1D).

We then analysed whether axon guidance in the VNC was being affected by examining commissures and longitudinal connectives visualised by BP102 staining (Seeger et al. 1993). The pattern and thickness of anterior commissures (AC), posterior commissures (PC) and longitudinal connectives were similar to *wild type* (Figures 5.2A and 5.2B). Furthermore, the three longitudinal axonal tracks labeled with FasII (Vactor et al. 1993) seemed to form normally in Δ*miR-iab4/iab8* late embryos (Figures 5.2C and 5.2D).

Altogether, these experiments show no major morphological abnormalities in the pattern of neuronal axons and muscles in late Δ*miR-iab4/iab8* embryos.

5.2.3 – miRNA effects in glial cells

We next examined if glia cells were affected by the absence of *miR-iab4/iab8*. To test this, we labelled glial cells with anti-Repo antibody (*Reverse polarity* (Halter et al. 1995)) in both genotypes and analysed their position and number. The positioning of glial cells was invariant along the A-P axis in *miR-iab4/iab8* mutants (Figures 5.3A and 5.3B). On the other hand, when counting the number of *Repo* positive cells we observed a small but significant reduction in the number of glia cells in the abdomen of Δ*miR-iab4/iab8* embryos (Figure

5.3C). In contrast, the number of glia in thorax was similar between *wild types* and Δ*miR-iab4/iab8* (data not shown). Then, we asked whether the reduction in abdomen glia was spread to all the abdominal segments or restricted to some. For this, we used ENGRAILED (α-En) as a segmental marker and counted the Repo positive cells per segment. Interestingly, the reduction in glia was not equal in all the abdominal segments but confined to A2 and A6 (Figure 5.3D).

Bearing in mind that *miR-iab4/iab8* regulate UBX protein expression in the abdominal CNS (see Chapter 4; (Bender 2008; Thomsen et al. 2010)) and that these miRNAs control self-righting behaviour in an UBX-dependent manner (Chapter 4), we wonder to what extent the reduction in glia is dependent on UBX upregulation. For this, we overexpressed UBX protein with *Ubx.*M1 (*Ubx*-Gal4^{M1}/ UAS-*Ubx*, see Chapter 4) and counted the number of Repo positive cells. Contrary to our expectation, overexpression of UBX did not reduce the number of glia cells in any abdominal segment (Figures 5.3F and 5.3G). We conclude that the reduction in glial cell number in the absence of *miR-iab4/iab8* is independent from UBX upregulation.

We then asked whether *miR-iab4/iab8* are regulating UBX expression in glia cells. Since UBX protein expression is absent in glia cells (Miguel-Aliaga & Thor 2004) but it is transcribed in a small proportion of them (see Figure 3.8A,C and E of Chapter 3), it is plausible that *miR-iab4/iab8* are repressing UBX protein formation in glia. To test this, we analysed the protein expression of UBX in glia cells in the absence of *miR-iab4/iab8.* Opposite to our expectation, we did not observe an upregulation of UBX in glia cells in Δ*miR-iab4/iab8* embryos (Figure 5.4). These experiments indicate that *miR-iab4/iab8-Ubx* interactions are likely to occur in neurons, suggesting that other mechanisms re-

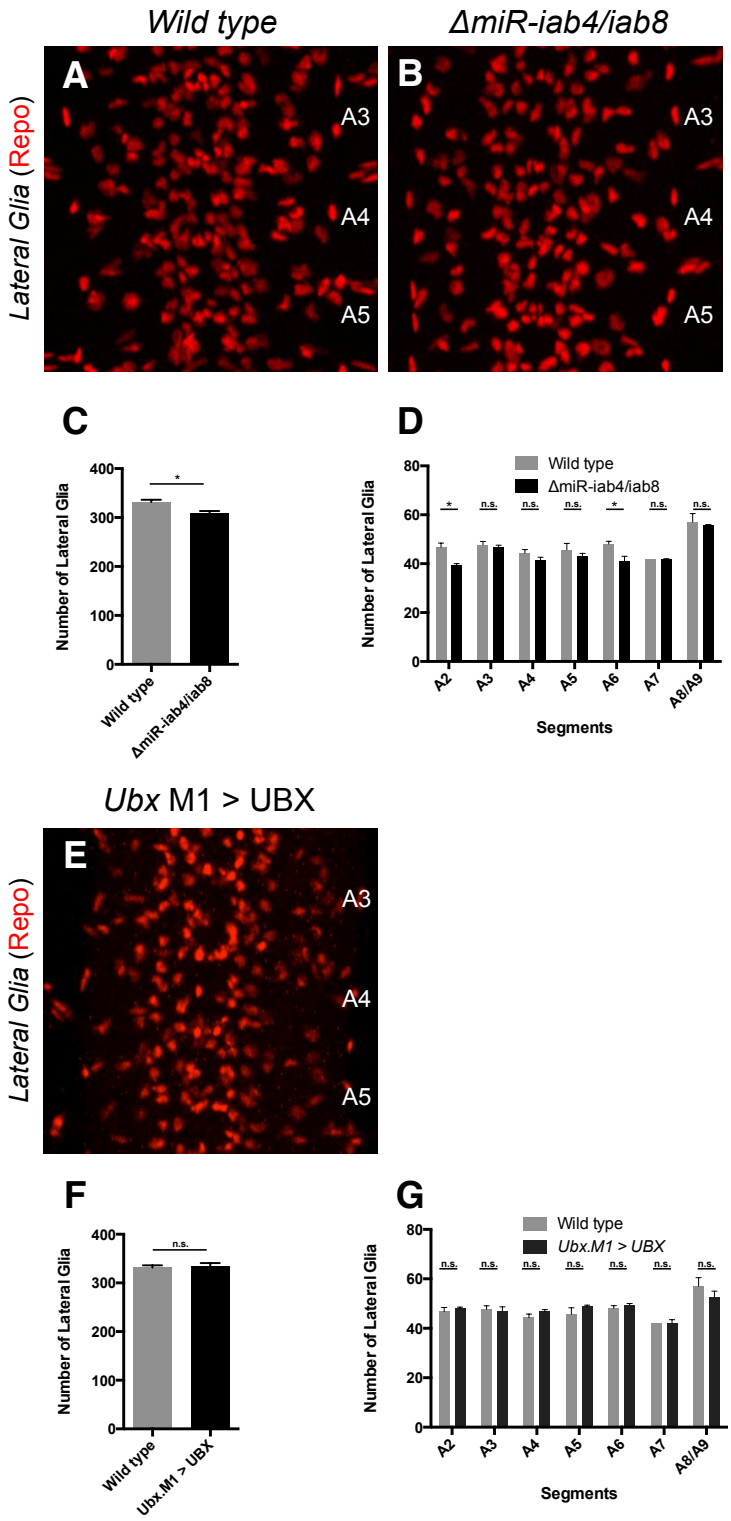

Figure 5.3 Effects of *miR-iab4/iab8* removal on glia cell number

(Legend on the following page)

Figure 5.3 Effects of *miR-iab4/iab8* removal on glia cell number

(A-B) Pattern of glial cells in the VNC visualised with anti-Repo antibody (red) in abdominal segments A3, A4 and A5 of wild type (A) and Δ*miR-iab4/iab8* (B) late stage 16 embryos. (B) The glial positioning in Δ*miR-iab4/iab8 embryos* was comparable to the wild type pattern. **(C-D)** Quantification of total glial cell-numbers in the abdomen (C) and segment-specific (A2-A9) glial cell count. (C) The average number of abdominal glia was a slightly but significantly decreased in Δ*miR-iab4/iab8* embryos when compared to the wild type. (D) This decrease in glial cell count was confined to the abdominal segments A2 and A6 of Δ*miR-iab4/iab8* embryos. **(E)** The pattern of glial cells was not affected upon overexpression of UBX using the *Ubx.M1-Gal4* driver. **(F-G)** Quantification of glial cell numbers upon overexpression of UBX in abdominal segments. (F) Embryos where UBX was overexpressed (*Ubx*.M1>UBX) did not show significantly different abdominal glial cell numbers when compared to the wild type. (G) In line with this observation, individual abdominal segments showed no significant differences in glial count in relation to wild type. An average of 4 VNCs per genotype was used in all analyses. A non-parametric Mann-Whitney *U* test was performed to compare treatments; $p > 0.05$ (non-significant; n.s.); $p < 0.05$ (*). Error bars denote the S.E.M. Taken together, these results suggest that the abdominal reduction in glial cell number in the absence of *miR-iab4/iab8* is independent from the concomitant UBX upregulation.

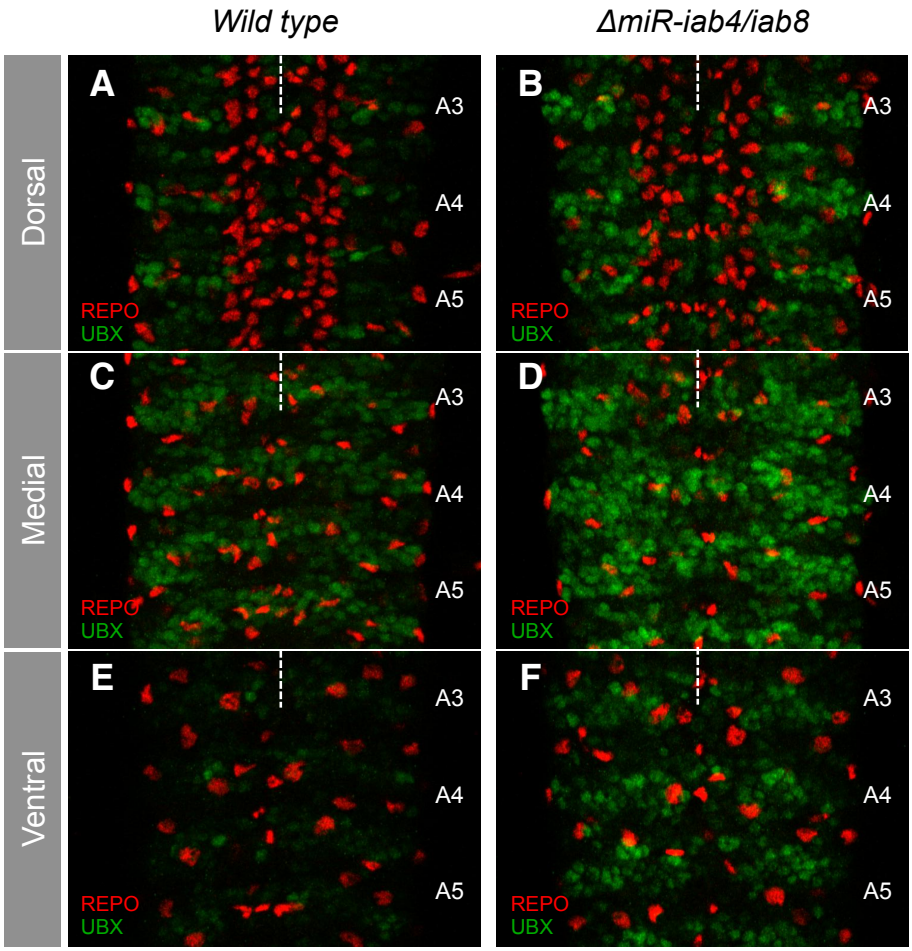

Figure 5.4 UBX protein is not expressed in glia in the absence of *miR-iab4/iab8*

(A, C, E) Wild type glial cell patterning (Repo, red) and UBX expression (green) across Dorsal (A), Medial (C) and Ventral (E) coronal sections of the abdominal segments A3, A4 and A5 in the VNC. As reported before (Miguel-Aliaga and Thor 2004), we did not detect UBX protein in glial cells in any coronal plane. **(B, D, F)** Glial cell patterning and UBX protein expression in abdominal segments A3, A4 and A5 of Δ*miR-iab4/iab8* VNCs. As observed previously for the wild type, there is no UBX expression in glial cells upon the removal of *miR-iab4/iab8*. Altogether, these results suggest that the exclusion of UBX expression in glial cells is not due to *miR-iab4/iab8* repression. Thin dashed line marks the midline. Anterior is up.

gulate the formation of UBX protein in glia cells (see Chapter 3).

5.2.4 Overexpression of UBX in cholinergic interneurons is sufficient to phenocopy abnormal self-righting behaviour

Until this point, our experiments did not show any major morphological defects in *miR-iab4/iab8* mutants. This indicates that the abnormal self-righting behaviour of these mutants might not be a consequence of an anatomical problem, but rather a change in the function of the underlying neuronal network of self-righting behaviour. In order to probe how the functionality of the circuit is affected, we first needed to identify which neurons mediate this behaviour. Having in mind that an increase in UBX protein expression is sufficient to trigger an irregular self-righting response (Chapter 4), we reasoned that if we were to overexpress UBX in different groups of neuronal cells we might identify the group of cells that are affected by the removal of the miRNAs and mediate abnormal behaviour. The expectation here is to identify a group of cells where overexpression of UBX is sufficient to produce an anomalous behaviour and subsequently investigate if *miR-iab4/iab8* are regulating UBX expression in these cells.

A previous study had shown that manipulation of neural activity in class IV multidendritic sensory neurons (ddaC, dorsal dendritic arborisation C) was necessary and sufficient for rolling behaviour in larvae (Hwang et al. 2007). Therefore, we wondered if an increase in UBX protein expression could affect the function of ddaC sensory neurons and induce an anomalous self-righting response. To test this idea, we overexpressed UBX in ddaC sensory neurons

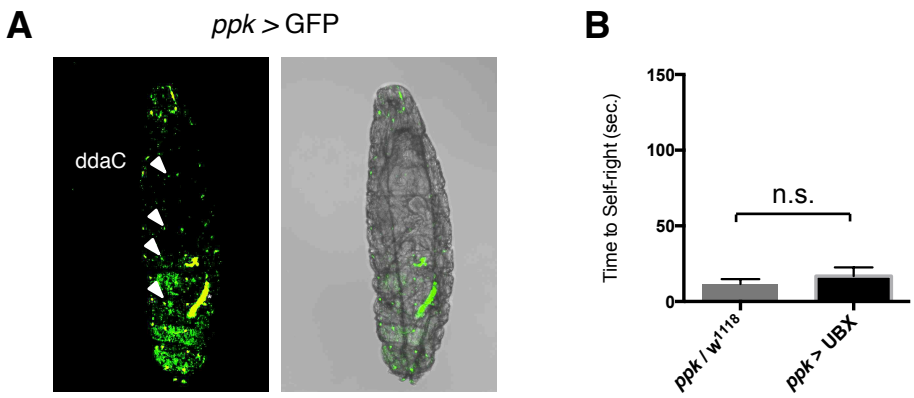

Figure 5.5 Ectopic expression of UBX protein in ddaC sensory neurons does not alter self-righting behaviour

(A) The dorsal dendritic arborisation C (ddaC) sensory neurons. The anatomical localisation the ddaC sensory neurons (white arrowheads) in first instar larva as highlighted by the expression of GFP in the *pickpocket* domain (*ppk-Gal4,* Ainsley et al. 2003). **(B)** Quantification of self-righting time upon overexpression of UBX in ddaC sensory neurons. UBX protein was overexpressed in ddaC sensory neurons (*ppk* > UBX), and the larval time to self-right was assayed. When compared to wild type (ppk / w^{1118}), the overexpression of UBX in ddaC cells yielded no difference in self-righting behaviour. An average of 15 larvae of each genotype was used in all analyses. A non-parametric Mann-Whitney *U* test was performed to compare treatments; $p > 0.05$ (non-significant). Error bars denote the S.E.M. These results led us to conclude that the overexpression of UBX protein in ddaC sensory cells does not disrupt larval self-righting behaviour.

and recorded the time required for first instar larvae to self-right. We made use of the driver line *pickpocket1.9*-Gal4 (*ppk*-Gal4, Figure 5.5A) to express UBX in ddaC sensory neurons (Ainsley et al. 2003; Hwang et al. 2007). Our experiments did not show a significant difference between controls (*ppk*-Gal4/+) and experimental larvae (*ppk* > UBX) in the time required to self-right (Figure 5.5B; $p>0.05$, *U* test). These experiments show that an increase in UBX protein expression in ddaC neurons is not sufficient to affect self-righting behaviour, suggesting that these neurons are not involved in the abnormal behaviour of miRNA mutants.

We then asked if the operation of sensory neurons was disturbed by an elevation in UBX protein and consequential impact the timing of self-righting response. Thus, we assessed whether ectopic expression of UBX in all sensory neurons was sufficient to affect the behaviour. For this, we used *PO163*-Gal4 (Figure 5.6A)(Hummel et al. 2000) to drive expression of UBX in all peripheral neurons (*PO163* > UBX). As before, overexpression of UBX in all sensory neurons did not disturb significantly the time to self-right (Figure 5.6B; $p>0.05$, *U* test). These experiments show that overexpression of UBX in peripheral sensory neurons is not sufficient to affect self-righting behaviour, suggesting that neurons from the VNC are likely those coordinating this behaviour.

We then asked whether regulation of UBX in interneurons was relevant for the synchronisation of self-righting behaviour. We started by analysing cholinergic interneurons for two reasons. First, cholinergic interneurons are the only known excitatory input to motoneurons in *Drosophila* (Baines & Bate 1998; Tripodi et al. 2008). These interneurons express the products of the *Choline Acetyltransferase* gene (*Cha*) which encodes an enzyme essential for the bio-

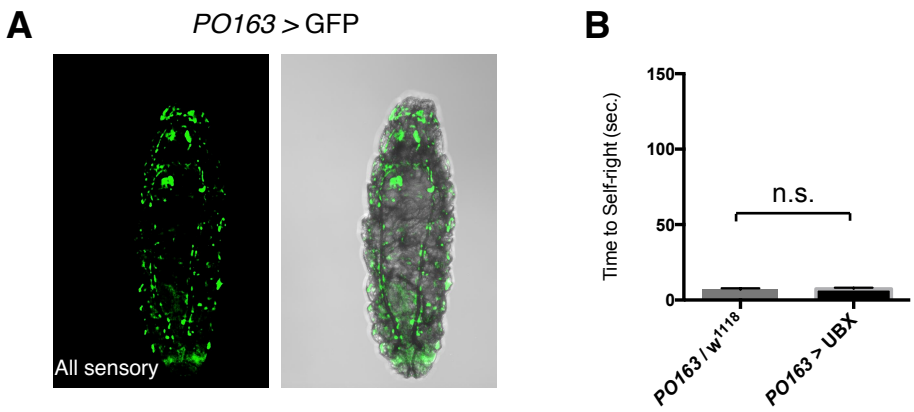

Figure 5.6 Misexpression expression of UBX protein in all sensory neurons does not affect self-righting behaviour

(A) The pattern of all sensory neurons of first instar larve was visualized using GFP expression driven by *PO163-Gal4* (Hummel et al. 2000). **(B)** Quantification of self-righting time upon overexpression of UBX in all sensory neurons. UBX protein was overexpressed in all sensory neurons (*PO163* > UBX), and the larval time to self-right was assayed. When compared to wild type (PO163 / w^{1118}), the overexpression of UBX in sensory neurons yielded no difference in self-righting behaviour. An average of 25 larvae of each genotype was used in all analyses. A non-parametric Mann-Whitney *U* test was performed to compare treatments; $p > 0.05$ (non-significant). Error bars denote the S.E.M. These results led us to conclude that the overexpression of UBX protein in all the sensory neurons does not affect larval self-righting behaviour.

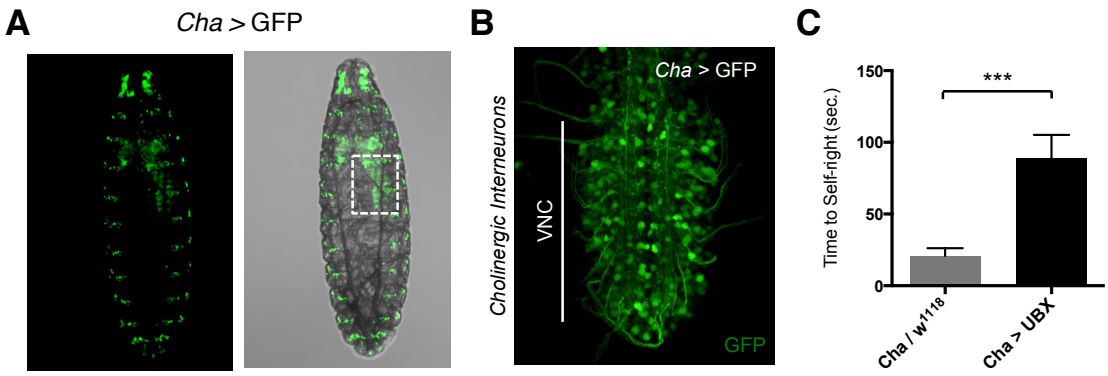

Figure 5.7 Overexpression of UBX protein in cholinergic interneurons disrupts self-righting behaviour

(A) Cholinergic neuronal pattern in first instar larvae. *cha7.4-Gal4* (*Cha-Gal4*) was used to drive GFP expression in all cholinergic neurons (*Cha-positive,* Salvaterra & Kitamoto 2001). **(B)** Detail showing the pattern of cholinergic interneurons in the VNC. **(C)** Quantification of self-righting time upon overexpression of UBX in all cholinergic neurons. UBX protein was overexpressed in all cholinergic neurons (*Cha* > UBX), and the larval time to self-right was assayed. When compared to wild type (*Cha* / w^{1118}), the overexpression of UBX in cholinergic neurons resulted in larvae showing a significantly longer time to complete self-righting behaviour. An average of 25 larvae of each genotype was used in all analyses. A non-parametric Mann-Whitney *U* test was performed to compare treatments; $p < 0.001$ (***). Error bars denote the S.E.M. These show that high levels of UBX protein in *Cha* neurons phenocopy the abnormal self-righting behaviour of Δ*miR-iab4/iab8* larvae.

synthesises of the neurotransmitter Acetylcholine (ACh) (Hall & Kankel 1976; Greenspan 1980). Second, cholinergic interneurons were shown to be involved in the coordination of several behaviours: turning (Suster et al. 2004), peristalsis (Berni et al. 2012), touch response (Zhou et al. 2012) and general locomotion problems (Iyengar et al. 2011). Based on this, we tested if overexpression of UBX in cholinergic interneurons was sufficient to produce an abnormal self-righting behaviour. To do this, we used the driver *cha7.4*-Gal4 (Figures 5.8A and 5.8B) (Salvaterra & Kitamoto 2001) to express UBX in all *Cha* neurons (*Cha* > UBX). Remarkably, larvae overexpressing UBX in *Cha* neurons took significant more time to self-right than control larvae (Figure 5.7C, $p < 0.001$, *U* test), whereas exploratory behaviours (peristalsis and turns) were not affected (data not shown). These observations show that high levels of UBX protein in *Cha* neurons phenocopies the abnormal self-righting behaviour of Δ*miR-iab4/iab8* larvae. Even though the entire population of *Cha* neurons includes all cholinergic interneurons and sensory neurons (Figure 5.7A) (Yasuyama & Salvaterra 1999; Salvaterra & Kitamoto 2001), our previous experiments excluded a sensory contribution (Figures 5.5C and 5.7C). Therefore, we conclude that the behaviour defects observed in *Cha* > UBX larvae were due to an increase of *UBX* protein in cholinergic interneurons.

5.2.5 Regulation of UBX expression in cholinergic interneurons by *miR-iab4/iab8*

Our findings show that an artificial increase of UBX protein in cholinergic interneurons is sufficient to induce a significant delay in the time to self-righting,

emulating the abnormal self-righting behaviour in Δ*miR-iab4/iab8* larvae (see Chapter 4). This observation brought us to propose the hypothesis that deregulation of UBX in cholinergic interneurons due to the absence of *miR-iab4/iab8* leads to defects in self-righting behaviour. For this idea to be true though, a number of pre-requisites must be met. In *wild type* larvae, both microRNAs *miR-iab4/iab8* and *Ubx* RNAs must be expressed in cholinergic interneurons; however, formation of UBX protein should be precluded. To test these pre-requisites, we did a series of fluorescent RNA *in situ* hybridisations (FISH) to detect primary transcripts of *miR-iab4* (*pri-miR*-iab4) and *Ubx* nascent RNA transcripts in cholinergic interneurons. In line with our reasoning, we detected in *wild type* larvae expression of *miR-iab4* (*pri-miR*-iab4) and *Ubx* nascent RNA transcripts in cholinergic interneurons (Figure 5.8A and Figure 5.8B, respectively). Furthermore, in *wild type* larvae UBX protein expression in cholinergic interneurons was mostly present in T3-A1 segments and in a few interneurons close to the midline from A2 to A4 (Figure 5.8C – cells in yellow/orange).

To test the hypothesis that UBX protein expression is regulated by *miR-iab4/iab8* in cholinergic interneurons, we analysed UBX protein expression in *Cha* interneurons in the absence of *miR-iab4/iab8.* In contrast to *wild types*, in *miR-iab4/iab8* mutant larvae many cholinergic interneurons expressed UBX protein in segments A2 to A6 (Figure 5.8D – cells in yellow/orange). This region is precisely where the expression of *miR-iab4* is highest (Figure 5.8A). As an example of *miR-iab4* regulation on UBX expression in cholinergic interneurons, we chose two lateral *Cha* interneurons localised on the same dorsal-ventral axis

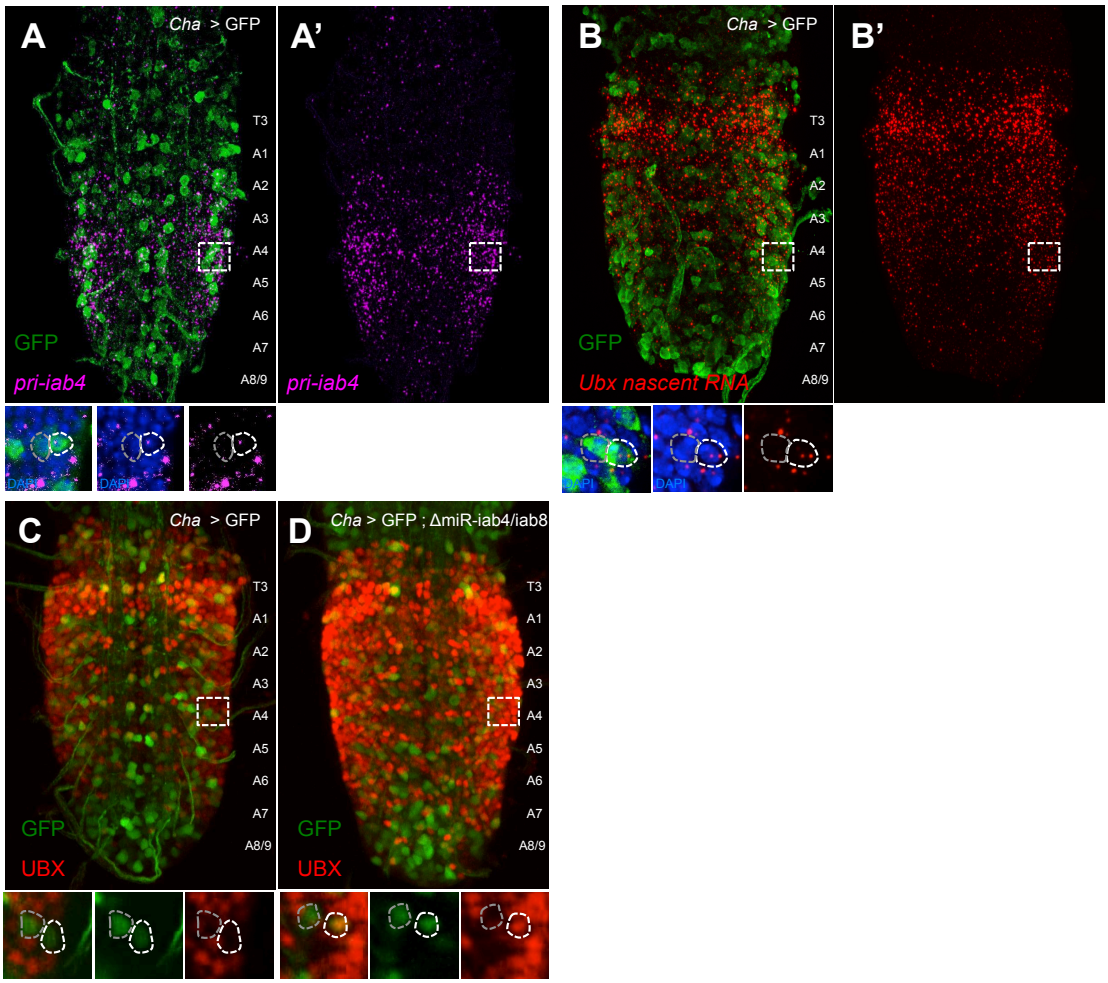

Figure 5.8 Regulation of UBX protein expression in cholinergic interneurons by *miR-iab4/iab8*

(Legend on the following page)

Figure 5.8 Regulation of UBX protein expression in cholinergic interneurons by *miR-iab4/iab8*

(A) Wild type expression of *pri-miR-iab4* (RNA-FISH, magenta) in the VNC of first-instar larvae. Cholinergic interneurons (GFP, green) were visualized using the *Cha-Gal4* driver. The *pri-miR-iab4* is highly expressed in cholinergic interneurons in segments A3 to A5. We isolated two lateral *Cha* interneurons localised on the same dorsal-ventral axis as the neuropile (dashed rectangles and subpanels) and observed the co-expression of *pri-miR-iab4* and GFP, suggesting that this miRNA is expressed in cholinergic interneurons. **(B)** Wild type expression of *Ubx* nascent RNA (RNA-FISH, red) in the VNC of first instar larvae. *Ubx* nascent RNAs were mostly detected in segments T3 to A5. We observed *Ubx* nascent RNA expression in the distal-most of the two lateral *Cha* interneurons previously identified, indicating that *Ubx* is transcribed in cholinergic interneurons that also express *pri-miR-iab4*. (**C)** UBX protein expression (red) in wild-type VNCs. UBX expression was mostly present in T3-A1 segments and in a few interneurons close to the midline from A2 to A4 (co-localization indicated in orange). UBX protein seems to be excluded from the two lateral cholinergic interneurons previously isolated. **(D)** In the miR-iab4/iab8 mutant, UBX expression noticeably expanded posteriorly, with many cholinergic interneurons expressing UBX protein in segments A2 to A6. The lateral Cha interneuron where *Ubx* nascent RNA and *pri-miR-iab4* expression (but not UBX protein) was previously detected in the wild type condition, now exhibited UBX protein expression in the miR-iab4/iab8 mutant (Bottom right panel). We conclude that *Ubx* is transcribed in abdominal cholinergic interneurons but the formation of UBX protein is inhibited by *miR-iab4/iab8* in these cells.

as the neuropile (dashed rectangles and subpanels of Figure 5.8A-D). We selected these two lateral *Cha* because they were identifiable by position in different individuals. In the *Cha* interneuron on the right (dashed white circle) we observed expression of *miR-iab4* (Figure 5.8A, small panels on the bottom, magenta) and signal for *Ubx* nascent RNAs (two transcription foci in red, Figure 5.8B, small panels on the bottom) but we could not detect UBX protein expression (Figure 5.8C, small panels on the bottom,). Nevertheless, upon removal of *miR-iab4/iab8* we saw expression of UBX protein in the cholinergic interneuron on the right (Figure 5.8D, small panels on the bottom). We conclude that *Ubx* is transcribed in abdominal cholinergic interneurons but the formation of UBX protein is inhibited by *miR-iab4/iab8* in these cells.

5.3 Discussion

In the previous Chapter we showed that *Ubx* regulation by *miR-iab4/iab8* is relevant for self-righting behaviour. In this Chapter we investigated the molecular and cellular basis of this behaviour change. We find that UBX expression is regulated in cholinergic interneurons by *miR-iab4/iab8* and that increase in UBX protein expression in cholinergic interneurons is sufficient to recapitulate the self-righting behaviour abnormalities seen in *miR-iab4/iab8* mutants.

We reasoned two non-exclusive possibilities for how misregulation of UBX by *miR-iab4/iab8* leads to abnormalities in self-righting behaviour: morphological problems in structures that are required for movement

coordination and functional changes in the underlying cell network that controls this behaviour. To probe the morphological hypothesis we analysed the anatomy of sensory neurons, VNC and muscles in the absence of *miR-iab4/iab8*. We found no evidence of major developmental abnormalities in *miR-iab4/iab8* mutants (except in glia cells, see below). Nevertheless, we cannot rule out that subtle and/or specific developmental defects were not revealed in our experiments, such as: axonal pathfinding abnormalities in small subsets of neurons, defects in dendritic arbours, lineage alteration, etc.

We next explored on which group of neuronal cells their functionality is impaired by the removal of *miR-iab4/iab8* and ultimately disrupts self-righting behaviour. Since ectopic UBX expression is sufficient to disrupt this behaviour, we reasoned that we could identify those cells if artificial expression of UBX in these cells causes abnormal self-righting behaviour. We demonstrate that overexpression of *Ubx* in cholinergic interneurons was sufficient to phenocopy the abnormal self-righting behaviour (Figure 5.7C). Additionally, we show that *Ubx* expression is regulated by *miR-iab4/iab8* in cholinergic interneurons (Figure 5.8). These observations suggest that UBX regulation by *miR-iab4/iab8* in cholinergic interneurons is important for self-righting behaviour. To further support this hypothesis, it would be possible to carry out a rescue experiment where UBX protein expression is reduced in cholinergic interneurons in *miR-iab4/iab8* mutants. We would expect a reduction in the time required for the larvae to self-right if UBX regulation by *miR-iab4/iab8* in cholinergic interneurons is necessary for the normal coordination of self-righting behaviour. We are currently doing this experiment by expressing *Ubx*-RNAi in cholinergic

interneurons in a Δ*miR-iab4/iab8* genetic background (*Cha*-Gal4; UAS-*Ubx*-RNAi, Δ*miR-iab4/iab8*).

Another important yet open question is in which specific cholinergic interneurons is UBX regulated by *miR-iab4/iab8*. And of these, which ones have a role in self-righting behaviour? To address this question, we will map cholinergic interneurons with different CNS markers (antibodies and Gal4 lines). Additionally, we will overexpress *Ubx* in subsets of cholinergic interneurons with the recently developed neuronal driver lines by laboratories in Janelia Farms (Jenett et al. 2012; Manning et al. 2012).

How does an increase in UBX protein expression in cholinergic interneurons affect self-righting behaviour? We speculate different nonexclusive possibilities to explore this question. First, the axonal pathfinding of specific neurons could be affected and as a consequence the assembly of a neural networks would change, *i.e.* the connection between neurons. Second, the communication/information between neurons may be affected in a way that the "message" from pre-synaptic neurons and/or the "interpretation" in post-synaptic neurons would differ from *wild type*. A change in the "message" might be biologically encoded in a difference of neurotransmitter and/or neuropeptide release (type and/or amount). Disruption in the "interpretation" of the message could come from a change in the receptors and/or their sensitivity of the post-synaptic neuron. Third, communication between neurons could also be impaired by the connectivity between the pre- and post-synaptic parts, that is, dendritic arbour growth. Fourth, the identity and/or physiology of specific neurons could be changed in a way that these neurons would not function as in a *wild-type* condition (e.g. neural activity). Interestingly, two studies showed that

neural activity of cholinergic neurons regulates the growth and electrical properties of motoneurons (Baines et al. 2001; Tripodi et al. 2008). Finally, a *Hox* code could act on cholinergic interneurons along the A-P axis, so that each *Hox* gene would be expressed in cholinergic interneurons according to the segmental position.

In order to expand our observations in the cholinergic interneurons, we will test if overexpression of *Ubx* in other groups of neurons phenocopies the abnormal self-righting behaviour of *miR-iab4/iab8* mutants, namely: GABAergic neurons (major inhibitory neurotransmitter in *Drosophila* and other insects (Enell et al. 2007; Hosie et al. 1997); *Gad1*-Gal4 (Ng et al. 2002)) and Glutamatergic neurons (motorneurons and a subset of visual and olfactory neurons (L. Y. Jan & Y. N. Jan 1976; Raghu & Borst 2011; Liu & Wilson 2013); *VGlut*^{OK371}-Gal4 (Mahr & Aberle 2006)

We observed that in the absence of *miR-iab4/iab8* there is a small reduction in glia cells in segments A2 and A6 (Figure 5.4D). However, ectopic expression of UBX does not reduce the number of glia cells in any segment (Figure 5.4G), suggesting that the decrease in glia cells in *miR-iab4/iab8* is independent of UBX misregulation. Since the abnormal self-righting behaviour is dependent on the increase in UBX protein expression, we propose that glia reduction in Δ*miR-iab4/iab8* may not be involved in the abnormal self-righting behaviour. To confirm this hypothesis we would have to kill the glia that are absent in the Δ*miR-iab4/iab8* and see if this affects self-righting behaviour. How does the absence of *miR-iab4/iab8* leads to a decrease in glia cells in these two segments, and what is the cellular mechanism? Glia apoptosis, lack of

proliferation or lineage differentiation are questions to be resolved in a future study.

In summary, our findings suggest that UBX regulation by *miR-iab4/iab8* in cholinergic interneurons controls self-righting behaviour.

Chapter 6

General Discussion

6.1 General Discussion

The work presented in this thesis provides novel insights on the regulation of *Hox* RNA processing and expression, and in the biological role of *Hox* regulation by miRNAs within the development of the *Drosophila* central nervous system.

Hox genes encode a family of transcriptional factors involved in the segmental patterning of the anterior-posterior axis of bilateral animals (McGinnis & Krumlauf 1992) . To achieve their functions, segmented patterns of *Hox* genes are expressed in characteristic sub domains along the head-to-tail axis. Mutations affecting *Hox* gene expression lead to the development of gross body abnormalities underlying the biological relevance of *Hox* function during normal development.

Experiments in *Drosophila* revealed a wide spectrum of molecular mechanisms involved in the regulation of *Hox* expression and function during development. Transcriptional initiation is set by the activity of segmentation genes (gap, pair-rule and segment-polarity genes), transcription maintenance through epigenetic regulators (*Polycomb* and *trithorax group* genes), the regulation of RNA processing via alternative splicing (AS) and alternative polyadenylation (APA), and miRNA regulation (see Chapter1; (Alonso 2012; Alonso & Wilkins 2005; Maeda & Karch 2009; Mallo & Alonso 2013).

In this thesis we focused on the study of *Hox* post-transcriptional regulation during neuronal development. The work was centred on the following questions: (i) what are the molecular factors that control *Hox* RNA processing during development? (ii) what is the relevance of this process for *Hox*

expression and function? (iii) what is the biological role of *Hox* post-transcriptional regulation by miRNAs? To address these questions we used the *Drosophila melanogaster Hox* gene *Ultrabithorax* (*Ubx*) as a paradigm for *Hox* regulation and function.

6.2 Regulation of *Hox* RNA processing and expression via RNA binding proteins

The combination of *Ubx* alternative splicing (AS) and alternative polyadenylation (APA) generates a family of mRNA transcripts with distinct exons and 3'UTR lengths (O'Connor et al. 1988; Kornfeld et al. 1989). AS gives rise to six *Ubx* mRNA (and protein) isoforms that share the 5' and 3' exons but differ in two small internal microexons and a "b element" located at the end of the common 5' exon. APA in turn produces *Ubx* transcripts with two 3'UTR lengths (short and long *Ubx* 3'UTRs). Interestingly, there is an association between the splicing isoforms and the length of their 3'UTRs. Furthermore, the two RNA processing events are developmentally controlled in space and time during embryogenesis (O'Connor et al. 1988; Lopez & Hogness 1991; Kornfeld et al. 1989; Thomsen et al. 2010). After gastrulation, the predominant AS isoform is *Ubx* Ia with shorter 3'UTRs expressed in the epidermis and mesoderm (Artero et al. 1992; Lopez & Hogness 1991; Thomsen et al. 2010). As development proceeds, the CNS starts to develop and *Ubx* IVa isoform with longer 3'UTR increase in expression in this tissue (Lopez & Hogness 1991; Thomsen et al. 2010). How is the RNA processing of *Ubx* controlled during

development? Why are *Ubx* RNAs with longer 3'UTR exclusively expressed in the CNS?

Our work shows that the pan-neural RNA binding protein (RBP) ELAV regulates *Ubx* RNA processing (AS and APA) within the *Drosophila* embryonic CNS (Chapter 3). The absence of ELAV modifies the normal *Ubx* RNA processing patterns in the CNS from AS isoforms without the microexons (*Ubx* IVa) with longer 3'UTRs to isoforms with the microexons (*Ubx* Ia) with shorter 3'UTRs. This suggests that ELAV enhances the exclusion of the microexons and the use of the first polyadenylation site. A previous study suggested that *Ubx* AS isoforms are generated in a stepwise manner by a mechanism of resplicing (also known as recursive splicing) (Hatton et al. 1998). First, the splicing of the first intron generates a consensus 5' splice site between the 5'exon and microexon 1 (M1) that is used as a transcript substrate for sequential events. On the second step, either the second intron is spliced out (substrate for *Ubx* Ia) or M1 and second intron are spliced out (substrate for *Ubx* IIa and IVa). On the final step either the third intron is spliced out – generating *Ubx* IIa isoform – or M2 and third intron are spliced out – generating *Ubx* IVa isoform. We showed that ELAV binds to the *Ubx* pre-mRNA in intron 1 close to M1 (37nt from M1, EBS3) and in intron 3 (around 8400nt from M3, EBS8). Thus, we propose that the binding of ELAV on EBS3 enhances the use of the M1 3' splice site and consequently the amount of transcript substrate for further splicing steps; and the binding to EBS8 silences the use of the M2 5' splice site generating the isoform *Ubx* IVa. This hypothesis could be tested by mutating the ELAV binding sites (EBS) one at the time and observing how the different *Ubx* splicing steps are affected. Alternatively, it would be possible to

use a *Ubx* splicing reporter – *Ubx* mini gene (Hatton et al. 1998) – and test to what extent the different EBS are controlling *Ubx* AS. This dual role of ELAV in the enhancing or silencing of exon inclusion dependent on the binding position (3' and 5' splice sites) was shown recently for other mammalian RBPs such as: Nova, hnRNP, Fox, PTB and TIA (König et al. 2010; Licatalosi et al. 2008; Ule et al. 2006; Z. Wang et al. 2010; Xue et al. 2009; Zhang et al. 2008). However, in those cases the pattern was reversed; silencing exon inclusion by binding close to the 3' splice site and enhancing exon exclusion by binding downstream of the exon.

We also show that ELAV regulates the expression of UBX protein in the CNS. We propose a molecular model where abnormal *Ubx* RNA processing leads to a retention and accumulation of *Ubx* RNAs at the site of transcription in the absence of ELAV. As a consequence, there is a reduction in the amount of *Ubx* mRNA to be translated. This model is in line with previous studies on other systems indicating that inefficient RNA processing prevents RNA release from the DNA (Custodio et al. 1999; Custodio et al. 2007; J. C. Schwartz et al. 2012). We speculate that cells must have a molecular surveillance mechanism that prevents unsuccessful RNA processing reactions to be exported to the cytoplasm and translated, avoiding potential deleterious proteins to be formed.

Given that *Ubx* RNA processing events are conserved in *Drosophila* species that diverged over 60 million years ago (Bomze & Lopez 1994; Patraquim et al. 2011) and that ELAV also regulates the RNA processing and protein expression of other *Hox* genes (*abd-A* and *Abd-A*), we propose that ELAV-dependent *Hox* RNA processing can regulate the expression levels of Hox proteins in the CNS. Furthermore, a recent study shows that ELAV

regulates APA of several other *D. melanogaster* RNAs (Hilgers et al. 2012) suggesting the generality of ELAV in modulating gene expression during the formation of the nervous system.

6.3 Control of behaviour via miRNAs

Ubx produces RNAs with distinct 3'UTR lengths during the formation of the embryonic CNS. Notably, longer 3'UTRs possess a suite of unique target sequences for miRNAs and are selectively up-regulated within the CNS shortly after germ band retraction (Thomsen et al. 2010): the point at which post-mitotic *Hox* inputs on neural circuitry begin to develop (Rogulja-Ortmann & Technau 2008). Moreover, *Ubx* is regulated post-transcriptionally by the *miR-iab4/iab8* microRNAs during the formation of the CNS (Bender 2008; Thomsen et al. 2010). These findings raise the intriguing hypothesis that miRNA-regulation of *Ubx* might be dictating the fine-grain expression and function of UBX during *Drosophila* CNS development.

Our work shows that UBX regulation by *miR-iab4/iab8* is relevant for a specific larval locomotory behaviour, self-righting behaviour (Chapter 4). We tested a series of different larval behaviours – peristaltic crawls, turning, touch response and self-righting – but only self-righting behaviour was affected by the de-regulation of UBX in the absence of *miR-iab4/iab8*. Previous studies have shown the involvement of miRNAs in a variety of behaviours, such as sensory olfaction in the worm *C.elegans* (Chang et al. 2004; Johnston & Hobert 2003) and in *Drosophila* (Cayirlioglu et al. 2008), and pace maker (circadian rhythms)

function in *Drosophila* (Kadener et al. 2009). In motor coordination behaviour, we only found one study in mice that shows that miRNAs in the midbrain impair locomotory activity (Kim et al. 2008). However, in that study the locomotory activity of mice was affected by the function depletion of all miRNAs through a mutation in *Dicer*. Thus, to our knowledge, we report the first specific motor coordinated behaviour controlled by a single miRNA system.

Given that the unavailability of *miR-iab4/iab8* leads to a significant increase in UBX expression in thousands of neuronal cells, why is only a specific behaviour affected? We speculate that different behaviours might have distinct underlying neuronal networks, so that the increase in UBX expression only affects a specific network while the other networks are not sensitive to this increase in expression. In favour of this are our overexpression experiments of UBX throughout the abdominal segments (*Ubx*.M1>UBX and *Ubx*.M3>UBX) that only disrupt self-righting behaviour.

We conceived two non-exclusive hypotheses of how regulation of UBX protein by *miR-iab4/iab8* could impair self-righting behaviour (Chapter 5). First, since UBX is a transcription factor involved in segmental morphology, de-regulation of UBX could result in anatomical abnormalities which could in turn affect self-righting behaviour. Secondly, overexpression of UBX protein could modify the specification and/or physiology of certain neurons changing the way in which specific neural networks operate. Our results do not support the first hypothesis since we did not detect any major anatomical defects in mutants for *miR-iab4/iab8*. However, we cannot exclude the possibility of subtle morphological anomalies in the axonal pathfinding of small subsets of neurons and/or in dentritic arbours. In contrast, several observations do support the

second hypothesis. First, UBX protein expression is regulated in the CNS by *miR-iab4/iab8* only after germ band retraction (from stage 13/14 until larval stages) (Thomsen et al. 2010), the moment at which *Hox* activity controls neuronal differentiation (Rogulja-Ortmann et al. 2008; Rogulja-Ortmann & Technau 2008). Second, the maturation of self-righting behaviour in the embryo only occurs just before larval hatching (Crisp et al. 2008). Third, ectopic expression of UBX in cholinergic interneurons in the end of embryogenesis was sufficient to disturb self-righting behaviour (Chapter 5). Fourth, by late stage 17 neuropeptide specification is controlled in neurons and this varies along the A-P axis (Miguel-Aliaga et al. 2008; Park et al. 2008; Santos et al. 2007). Neuropeptides act as co-transmitters that modulate neural activity in insects, crustaceans, molluscs and vertebrates (Baker & Truman 2002; Baraban & Tallent 2004; Blitz & Nusbaum 1999; Nässel & Homberg 2006; Nusbaum et al. 2001). Finally, neuropeptide specification was shown to be regulated by *Hox* genes (Miguel-Aliaga et al. 2008; Suska et al. 2011). Taking into consideration the previous points and also that UBX protein expression is regulated by *miR-iab4/iab8* in cholinergic interneurons, we speculate that the miRNA-*Ubx* interactions in cholinergic interneurons could be shaping the neuropeptide specification of these neurons along the A-P axis with consequential relevance for the establishment of the underlying neuronal network that control self-righting behaviour.

Recent studies show that *Ubx* APA is conserved in *Drosophila* species that diverged over 60 million years ago (Patraquim et al. 2011) and that the seed sequences of *miR-iab4/iab8* are ultraconserved in these same species (Ruby et al. 2007). However, the *miR-iab4/iab8* targeting on *Ubx* transcripts

evolved quite dynamically in different *Drosophila* species (Patraquim et al. 2011). These observations suggest that the *miR-iab4/iab8–Ubx* interactions might have changed during the course of *Drosophila* evolution. Thus, we propose that our findings in *Drosophila melanogaster* might be relevant for the evolution of self-righting behaviour in different *Drosophila* species.

Furthermore, at the ecological level, several species of parasitoid wasps attack *Drosophila* larvae to complete their life cycle, which affects the survival of these larvae (Fleury et al. 2009). These wasps require *Drosophila* larvae as host for their progeny to develop. For example, the wasp *Leptopilina boulardi* pierces the larval cuticle of *D.melanogaster* with a sharp ovipositor and lays their eggs within the larva (Carton et al. 1987). A recent study showed that *D.melanogaster* larvae escape attacks of these wasps by vigorously rolling their bodies (Hwang et al. 2007). Since *miR-iab4/iab8* mutants have major problems in rolling their bodies into a correct position (self-righting behaviour), we conjecture that *miR-iab4/iab8-Ubx* interaction could have ecological implications in the survival of *Drosophila* larvae species.

6.4 Concluding remarks

In conclusion, this thesis explores different aspects of *Hox* regulation and function via RNA processing and miRNA interaction during the development of the central nervous system of *Drosophila melanogaster*. We present a novel regulatory framework of *Hox* regulation that can dictate cellular decisions in the development of neuronal tissue along the A-P axis. We also show the biological

relevance of *Hox*-miRNA interactions in the coordination of larval movement. Our findings advance the current understanding of the molecular mechanisms underlying *Hox* post-transcriptional regulation, and identify one of the biological roles played by these regulatory steps during neuronal development.

References

Ainsley, J. A., Pettus, J. M., Bosenko, D., and Gerstein, C. E., Zinkevich, N., Anderson, M.G., Adams, C.M., Welsh, M.J. & Johnson, W.A., 2003. Enhanced Locomotion Caused by Loss of the *Drosophila* DEG/ENaC Protein Pickpocket1. *Current biology*, (13), pp. 1557-1563

Akam, M., 1989. Hox and HOM: homologous gene clusters in insects and vertebrates. *Cell*, 57(3), pp.347–349.

Akam, M., 1987. The molecular basis for metameric pattern in the *Drosophila* embryo. *Development*, (101), pp.1-22

Akam, M.E., 1983. The location of Ultrabithorax transcripts in *Drosophila* tissue sections. *EMBO J*, 2(11), pp.2075–2084.

Akam, M.E. & Martinez-Arias, A., 1985. The distribution of Ultrabithorax transcripts in *Drosophila* embryos. *EMBO J*, 4(7), pp.1689–1700.

Alexander, T., Nolte, C., & Krumlauf, R. (2009). Hox genes and segmentation of the hindbrain and axial skeleton. *Annual Review of Cell and Developmental Biology*, *25*(1), pp.431-456.

Alonso, C.R., 2012. A complex “mRNA degradation code” controls gene expression during animal development. *Trends in Genetics*, 28(2), pp.78–88.

Alonso, C.R. & Wilkins, A.S., 2005. The molecular elements that underlie developmental evolution. *Nat Rev Genet*, 6(9), pp.709–715.

Aravin, A. A., Lagos-Quintana, M., Yalcin, A., Zavolan, M., Marks, D., Snyder, B., Gaasterland, T., Meyer, J., & Tuschl, T., 2003. The Small RNA Profile during *Drosophila melanogaster* Development. *Developmental Cell*, 5(2), pp.337–350.

Artero, R.D., Akam, M. & Pérez-Alonso, M., 1992. Oligonucleotide probes detect splicing variants *in situ* in *Drosophila* embryos. *Nucleic Acids Research*, 20(21), pp.5687–5690.

Averof, M. & Akam, M., 1995. Hox genes and the diversification of insect and crustacean body plans. *Nature*, 376(6539), pp.420–423.

Averof, M. & Patel, N.H., 1997. Crustacean appendage evolution associated with changes in Hox gene expression. *Nature*, 388(6643), pp.682–686.

Baines, R.A. & Bate, M., 1998. Electrophysiological development of central neurons in the *Drosophila* Embryo. *The Journal of Neuroscience*, 18(12), pp.4673–4683.

Baines, R. A., Uhler, J. P., Thompson, A., Sweeney, S. T., & Bate, M, 2001.

Altered electrical properties in *Drosophila* neurons developing without synaptic transmission. *The Journal of Neuroscience*, 21(5), pp.1523–1531.

Baker, J.D. & Truman, J.W., 2002. Mutations in the *Drosophila* glycoprotein hormone receptor, rickets, eliminate neuropeptide-induced tanning and selectively block a stereotyped behavioral program. *Journal of Experimental Biology*, 205(17), pp.2555–2565.

Baraban, S.C. & Tallent, M.K., 2004. Interneuron diversity series: Interneuronal neuropeptides – endogenous regulators of neuronal excitability. *Trends in Neurosciences*, 27(3), pp.135–142.

Bartel, D.P., 2009. MicroRNAs: target recognition and regulatory functions. *Cell*, 136(2), pp.215–233.

Bartel, D.P. & Chen, C.-Z., 2004. Micromanagers of gene expression: the potentially widespread influence of metazoan microRNAs. *Nat Rev Genet*, 5(5), pp.396–400.

Bateson, W., 1894. *Materials for the Study of Variation, Treated with Especial Regard to Discontinuity in the Origin of Species*, New York: Macmillan.

Baumgardt, M., Karlsson, D., Terriente, J., Díaz-Benjumea, F. J., & Thor, S., 2009. Neuronal subtype specification within a lineage by opposing temporal feed-forward loops. *Cell*, 139(5), pp.969–982.

Beachy, P.A., Helfand, S.L. & Hogness, D.S., 1985. Segmental distribution of bithorax complex proteins during *Drosophila* development. *Nature*, 313(6003), pp.545–551.

Beckervordersandforth, R. M., Rickert, C., Altenhein, B., & Technau, G. M., 2008. Subtypes of glial cells in the *Drosophila* embryonic ventral nerve cord as related to lineage and gene expression. *Mechanisms of Development*, (125), pp.542–557.

Bello, B.C., Hirth, F. & Gould, A.P., 2003. A pulse of the *Drosophila* Hox protein Abdominal-A schedules the end of neural proliferation via neuroblast apoptosis. *Neuron*, 37(2), pp.209–219.

Bender, W., 2008. MicroRNAs in the *Drosophila* bithorax complex. *Genes Dev*, 22(1), pp.14–19.

Bender, W. & Hudson, A., 2000. P element homing to the *Drosophila* bithorax complex. *Development*, 127(18), pp.3981–3992.

Bender, W., Akam, M., Karch, F., Beachy, P. A., Peifer, M., Spierer, P., Lewis, E. B., & Hogness, D. S., 1983. Molecular genetics of the bithorax complex in *Drosophila melanogaster*. *Science*, 221(4605), pp.23–29.

Berger, C., Renner, S., Luer, K., & Technau, G. M., 2007. The commonly used marker ELAV is transiently expressed in neuroblasts and glial cells in the *Drosophila* embryonic CNS. *Developmental Dynamics*, 236(12), pp.3562–

3568.

Berger, C., Pallavi, S.K., Prasad, M., Shashidhara, L.S. & Technau, G.M., 2005a. A critical role for Cyclin E in cell fate determination in the central nervous system of *Drosophila* melanogaster. *Nat Cell Biol*, 7(1), pp.56–62.

Berger, C., Pallavi, S.K., Prasad, M., Shashidhara, L.S. & Technau, G.M., 2005b. Cyclin E acts under the control of Hox-genes as a cell fate determinant in the developing central nervous system. *Cell Cycle*, 4(3), pp.422–425.

Berni, J., Pulver, S. R., Griffith, L. C., & Bate, M., 2012. Autonomous circuitry for substrate exploration in freely moving *Drosophila* larvae. *Current Biology,* 22(20), pp.1861-1870

Besson, M.T.R.S., Soustelle, L. & Birman, S., 1999. Identification and structural characterization of two genes encoding glutamate transporter homologues differently expressed in the nervous system of *Drosophila melanogaster*. *FEBS Letters*, 443(2), pp.97–104.

Blitz, D.M. & Nusbaum, M.P., 1999. Distinct functions for cotransmitters mediating motor pattern selection. *The Journal of Neuroscience*, 19(16), pp.6774–6783.

Bodily, K.D., Morrison, C.M. & Renden, R.B., 2001. A novel member of the Ig superfamily, turtle, is a CNS-specific protein required for coordinated motor control. *J Neurosci*, 21(9), pp.3113–3125.

Bomze, H.M. & Lopez, A.J., 1994. Evolutionary conservation of the structure and expression of alternatively spliced Ultrabithorax isoforms from *Drosophila*. *Genetics*, 136(3), pp.965–977.

Boncinelli, E., 1997. Homeobox genes and disease. *Curr Opin Genet Dev*, 7(3), pp.331–337.

Bossing, T., Udolph, G., Doe, C. Q., & Technau, G. M., 1996. The Embryonic central nervous system lineages of *Drosophila melanogaster*: I. Neuroblast lineages derived from the ventral half of the neuroectoderm. *Developmental Biology*, 179(1), pp.41–64.

Branson, K., Robie, A. A., Bender, J., Perona, P., & Dickinson, M. H., 2009. High-throughput ethomics in large groups of *Drosophila*. *Nat Meth*, 6(6), pp.451–457.

Bridges, C.B. & Morgan, T.H., 1923. *The Third-Chromosome Group of Mutant Characters of Drosophila melanogaster*, Carnegie Institution of Washington.

Broadus, J., Skeath, J. B., Spana, E. P., Bossing, T., Technau, G., & Doe, C. Q., 1995. New neuroblast markers and the origin of the aCC/pCC neurons in the *Drosophila* central nervous system. *Mechanisms of Development*, 53(3), pp.393–402.

Brody, T. & Odenwald, W.F., 2000. Programmed transformations in neuroblast gene expression during *Drosophila* CNS lineage development. *Developmental Biology*, 226(1), pp.34–44.

Burke, A. C., Nelson, C. E., Morgan, B. A., & Tabin, C, 1995. Hox genes and the evolution of vertebrate axial morphology. *Development*, 121(2), pp.333–346.

Cabrera, C.V., Botas, J. & Garcia-Bellido, A., 1985. Distribution of Ultrabithorax proteins in mutants of *Drosophila* bithorax complex and its transregulatory genes. *Nature*, 318(6046), pp.569–571.

Campos-Ortega, J., 1995. Genetic mechanisms of early neurogenesis in *Drosophila melanogaster*. *Molecular Neurobiology*, 10(2-3), pp.75–89.

Campos-Ortega, J.A. & Hartenstein, V, 1985. *The embryonic development of Drosophila melanogaster*. Springer-Verlag, ed., Berlin.

Carroll, S.B., 1995. Homeotic genes and the evolution of arthropods and chordates. *Nature*, 376(6540), pp.479–485.

Carton, Y. et al., 1987. Egg-laying strategy under natural conditions of *Leptopilina boulardi*, a hymenopteran parasitoid of *Drosophila spp*. *Entomologia Experimentalis et Applicata*, 43(2), pp.193–201.

Castle, J. C., Zhang, C., Shah, J. K., Kulkarni, A. V., Kalsotra, A., Cooper, T. A., & Johnson, J. M, 2008. Expression of 24426 human alternative splicing events and predicted cis regulation in 48 tissues and cell lines. *Nature Genetics*, 40(12), pp.1416–1425.

Cayirlioglu, P., Kadow, I. G., Zhan, X., Okamura, K., Suh, G. S. B., Gunning, D., Lai, E. C., & Zipursky, S. L., 2008. Hybrid neurons in a microRNA mutant are putative evolutionary intermediates in insect CO2 sensory systems. *Science*, 319(5867), pp.1256–1260.

Cenci, C. & Gould, A.P., 2005. *Drosophila* Grainyhead specifies late programmes of neural proliferation by regulating the mitotic activity and Hox-dependent apoptosis of neuroblasts. *Development*, 132(17), pp.3835–3845.

Chan, C.S., Rastelli, L. & Pirrotta, V., 1994. A Polycomb response element in the Ubx gene that determines an epigenetically inherited state of repression. *EMBO J*, 13(11), pp.2553–2564.

Chang, S., Johnston, R. J., Frøkjaer-Jensen, C., Lockery, S., & Hobert, O., 2004. MicroRNAs act sequentially and asymmetrically to control chemosensory laterality in the nematode. *Nature*, 430(7001), pp.785–789.

Christen, B. & Bienz, M., 1992. A cis-element mediating Ultrabithorax autoregulation in the central nervous system. *Mechanisms of Development*, 39(1-2), pp.73–80.

Clark, A. G., Eisen, M. B., Smith, D. R., Bergman, C. M., Oliver, B., Markow, T. A., Kaufman, T. C., Kellis, M., Gelbart, W., Iyer, V. N., *et al*., 2007. Evolution of genes and genomes on the *Drosophila* phylogeny. *Nature*, 450(7167), pp.203–218.

Colombrita, C., Silani, V. & Ratti, A., 2013. ELAV proteins along evolution: Back to the nucleus? *Molecular and cellular neurosciences*, 56, pp.447–455.

Crickmore, M.A., Ranade, V. & Mann, R.S., 2009. Regulation of *Ubx* expression by epigenetic enhancer silencing in response to Ubx Levels and Genetic Variation. *PLoS Genet*, 5(9), p.e1000633.

Crisp, S., Evers, J. F., Fiala, A., & Bate, M., 2008. The development of motor coordination in *Drosophila* embryos. *Development*, 135(22), pp.3707–3717.

Crisp, S.J., Evers, J.F. & Bate, M., 2011. Endogenous patterns of activity are required for the maturation of a motor network. *The Journal of Neuroscience*, 31(29), pp.10445–10450.

Custodio, N., Carmo-Fonseca, M., Geraghty, F., Periera, H. S., Grosveld, F., & Antoniou, M., 1999. Inefficient processing impairs release of RNA from the site of transcription. *EMBO J*, 18(10), pp.2855–2866.

Custodio, N., Vivo, M., Antoniou, M., & Carmo-Fonseca, M., 2007. Splicing- and cleavage-independent requirement of RNA polymerase II CTD for mRNA release from the transcription site. *Journal of Cell Biology*, 179(2), pp.199–207.

Dasen, J. S., & Jessell, T. M. (2009). Hox Networks and the Origins of Motor Neuron Diversity. *Current Topics in Developmental Biology*,. 88, pp.169–200).

Dasen, J. S., Liu, J.-P., & Jessell, T. M. (2003). Motor neuron columnar fate imposed by sequential phases of Hox-c activity. *Nature*, *425*(6961), pp.926–933.

Dasen, J. S., Tice, B. C., Brenner-Morton, S., & Jessell, T. M. (2005). A Hox regulatory network establishes motor neuron pool identity and target-muscle connectivity. *Cell*, *123*(3), pp.477–491.

de Navas, L., Foronda, D., Suzanne, M., & Sánchez-Herrero, E., 2006. A simple and efficient method to identify replacements of P-lacZ by P-Gal4 lines allows obtaining Gal4 insertions in the bithorax complex of *Drosophila*. *Mechanisms of Development*, 123(11), pp.860–867.

de Navas, L. F., Reed, H., Akam, M., Barrio, R., Alonso, C. R., & Sánchez-Herrero, E.., 2011. Integration of RNA processing and expression level control modulates the function of the *Drosophila* Hox gene Ultrabithorax during adult development. *Development*, 138(1), pp.107–116.

Del Bene, F. & Wittbrodt, J., 2005. Cell cycle control by homeobox genes in development and disease. *Seminars in Cell & Developmental Biology*,

16(3), pp.449–460.

Desplan, C., Theis, J. & O'Farrell, P.H., 1985. The *Drosophila* developmental gene, engrailed, encodes a sequence-specific DNA binding activity. *Nature*, 318(6047), pp.630–635.

Desplan, C., Theis, J. & O'Farrell, P.H., 1988. The sequence specificity of homeodomain-DNA interaction. *Cell*, 54(7), pp.1081–1090.

Di Giammartino, D.C., Nishida, K. & Manley, J.L., 2011. Mechanisms and consequences of alternative polyadenylation. *Molecular cell*, 43(6), pp.853–866.

Dixit, R., Vijayraghavan, K. & Bate, M., 2008. Hox genes and the regulation of movement in *Drosophila*. *Developmental Neurobiol*, 68(3), pp.309–316.

Doe, C.Q., 1992. Molecular markers for identified neuroblasts and ganglion mother cells in the *Drosophila* central nervous system. *Development*, 116(4), pp.855–863.

Duboule, D. & Dollé, P., 1989. The structural and functional organization of the murine HOX gene family resembles that of *Drosophila* homeotic genes. *EMBO J*, 8(5), pp.1497–1505.

Duboule, D. & Morata, G., 1994. Colinearity and functional hierarchy among genes of the homeotic complexes. *Trends in Genetics*, 10(10), pp.358–364.

Enell, L., Hamasaka, Y., Kolodziejczyk, A., & Nässel, D. R., 2007. gamma-Aminobutyric acid (GABA) signaling components in *Drosophila*: immunocytochemical localization of GABA(B) receptors in relation to the GABA(A) receptor subunit RDL and a vesicular GABA transporter. *Journal of Comparative Neurology*, 505(1), pp.18–31.

Fleury, F., Gibert, P., Ris, N., & Allemand, R., 2009. Ecology and life history evolution of frugivorous *Drosophila* parasitoids. *Advances in parasitology*, 70, pp.3–44.

Garcia-Fernandez, J. & Holland, P.W., 1994. Archetypal organization of the amphioxus Hox gene cluster. *Nature*, 370(6490), pp.563–566.

Gavalas, A., Davenne, M., Lumsden, A., Chambon, P., & Rijli, F. M.,1997. Role of Hoxa-2 in axon pathfinding and rostral hindbrain patterning. *Development* 124, pp.3693–3702.

Gehring, W. J., Qian, Y. Q., Billeter, M., Furukubo-Tokunaga, K., Schier, A. F., Resendez-Perez, D., Affolter, M., Otting, G., & Wüthrich, K., 1994. Homeodomain-DNA recognition. *Cell*, 78(2), pp.211–223.

Gomez-Marin, A., Partoune, N., Stephens, G. J., & Louis, M., 2012. Automated tracking of animal posture and movement during exploration and sensory orientation behaviors. *PloS one*, 7(8), p.e41642.

Gonzalez-Reyes, A. & Morata, G., 1990. The developmental effect of overexpressing a *Ubx* product in *Drosophila* embryos is dependent on its interactions with other homeotic products. *Cell*, 61(3), pp.515–522.

Gould, A. P., Brookman, J. J., Strutt, D. I., & White, R. A., 1990. Targets of homeotic gene control in *Drosophila*. *Nature*, 348(6299), pp.308–312.

Graham, A., Papalopulu, N. & Krumlauf, R., 1989. The murine and *Drosophila* homeobox gene complexes have common features of organization and expression. *Cell*, 57(3), pp.367–378.

Greenspan, R.J., 1980. Mutations of choline acetyltransferase and associated neural defects. *Journal of comparative physiology*, 137, pp.83-92.

Guthrie, S. (2007). Patterning and axon guidance of cranial motor neurons. *Nat Rev Neurosci*, *8*(11), 859–871.

Hafen, E., Levine, M. & Gehring, W.J., 1984. Regulation of Antennapedia transcript distribution by the bithorax complex in *Drosophila*. *Nature*, 307(5948), pp.287–289.

Hall, J.C. & Kankel, D.R., 1976. Genetics of Acetylcholinesterase in *Drosophila melanogaster*. *Genetics*.

Halter, D. A., Urban, J., Rickert, C., Ner, S. S., Ito, K., Travers, A. A., and Technau, G. M., 1995. The homeobox gene repo is required for the differentiation and maintenance of glia function in the embryonic nervous system of *Drosophila melanogaster*. *Development*, 121(2), pp.317–332.

Harding, K., Wedeen, C., McGinnis, W., & Levine, M., 1985. Spatially regulated expression of homeotic genes in *Drosophila*. *Science*, 299, pp.1236-1242

Hartenstein, V. & Campos-Ortega, J.A., 1984. Early neurogenesis in wild-type *Drosophila melanogaster*. *Rouxs Archives of Developmental Biology*, 193(5), pp.308–325.

Hatton, A.R., Subramaniam, V. & Lopez, A.J., 1998. Generation of alternative Ultrabithorax isoforms and stepwise removal of a large intron by resplicing at exon-exon junctions. *Molecular Cell*, 2(6), pp.787–796.

Heckscher, E.S., Lockery, S.R. & Doe, C.Q., 2012. Characterization of *Drosophila* larval crawling at the level of organism, segment, and somatic body wall musculature. *The Journal of Neuroscience*, 32(36), pp.12460–12471.

Hidalgo, A. & Booth, G.E., 2000. Glia dictate pioneer axon trajectories in the *Drosophila* embryonic CNS. *Development*, 127(2), pp.393–402.

Hidalgo, A., Urban, J. & Brand, A.H., 1995. Targeted ablation of glia disrupts axon tract formation in the *Drosophila* CNS. *Development*, 121(11), pp.3703–3712.

Hilgers, V., Perry, M. W., Hendrix, D., Stark, A., Levine, M., & Haley, B., 2011. Neural-specific elongation of 3'UTRs during *Drosophila* development. *Proceedings of the National Academy of Sciences*, 108(38), pp.15864–15869.

Hilgers, V., Lemke, S.B. & Levine, M., 2012. ELAV mediates 3' UTR extension in the *Drosophila* nervous system. *Genes & Development*, 26(20), pp.2259–2264.

Holland, P.W.H. & Hogan, B.L.M., 1986. Phylogenetic distribution of Antennapedia-like homoeo boxes. *Nature*, 321, 251-253

Hosie, A. M., Aronstein, K., Sattelle, D. B., & ffrench-Constant, R. H., 1997. Molecular biology of insect neuronal GABA receptors. *Trends in Neurosciences*, 20(12), pp.578–583.

Hoyle, G., Williams, M. & Phillips, C., 1986. Functional morphology of insect neuronal cell-surface/glial contacts: the trophospongium. *Journal of Comparative Neurology*, 246(1), pp.113–128.

Hughes, C.L. & Kaufman, T.C., 2002. Hox genes and the evolution of the arthropod body plan. *Evolution & Development*, 4(6), pp.459–499.

Hummel, T., Schimmelpfeng, K., & Klämbt, C., 2000. *Drosophila* Futsch/22C10 is a MAP1B-like protein required for dendritic and axonal development. *Neuron*, 26, 357-370

Hwang, R. Y., Zhong, L., Xu, Y., Johnson, T., Zhang, F., Deisseroth, K., & Tracey, W. D., 2007. Nociceptive neurons protect *Drosophila* larvae from parasitoid wasps. *Current Biology*, 17(24), pp.2105–2116.

Ingham, P.W. & Martinez-Arias, A., 1986. The correct activation of Antennapedia and bithorax complex genes requires the fushi tarazu gene. *Nature*, 324(6097), pp.592–597.

Irish, V.F., Martinez-Arias, A. & Akam, M., 1989. Spatial regulation of the Antennapedia and Ultrabithorax homeotic genes during *Drosophila* early development. *EMBO J*, 8(5), pp.1527–1537.

Irvine, K.D., Helfand, S.L. & Hogness, D.S., 1991. The large upstream control region of the *Drosophila* homeotic gene Ultrabithorax. *Development*, 111(2), pp.407–424.

Isshiki, T., Pearson, B., Holbrook, S., & Doe, C. Q., 2001. *Drosophila* neuroblasts sequentially express transcription factors which specify the temporal identity of their neuronal progeny. *Cell*, 106(4), pp.511–521.

Iyengar, B. G., Chou, C. J., Vandamme, K. M., Klose, M. K., Zhao, X., Akhtar-Danesh, N., Campos, A. R., & Atwood, H. L., 2011. Silencing synaptic communication between random interneurons during *Drosophila* larval locomotion. *Genes, Brain & Behavior*, 10(8), pp.883–900.

Jan, L.Y. & Jan, Y.N., 1976. L-glutamate as an excitatory transmitter at the *Drosophila* larval neuromuscular junction. *The Journal of physiology*, 262(1), pp.215–236.

Jenett, A., Rubin, G. M., Ngo, T. T. B., Shepherd, D., Murphy, C., Dionne, H., Pfeiffer, B. D., Cavallaro, A., Hall, D., Jeter, J., *et al.*, 2012. A GAL4-driver line resource for *Drosophila* neurobiology. *Cell Reports*, 2(4), pp.991–1001.

Jiménez, F. & Campos-Ortega, J.A., 1990. Defective neuroblast commitment in mutants of the achaete-scute complex and adjacent genes of *D. melanogaster*. *Neuron*, 5(1), pp.81–89.

Johnston, R.J. & Hobert, O., 2003. A microRNA controlling left/right neuronal asymmetry in *Caenorhabditis elegans*. *Nature*, 426(6968), pp.845–849.

Jung, H., Lacombe, J., Mazzoni, E. O., Liem, K. F., Grinstein, J., Mahony, S., Mukhopadhyay, D., Gifford, D.K., Young,R.A., Anderson, K.V., Wichterle, H., Dasen, J.S., (2010). Global control of motor neuron topography mediated by the repressive actions of a single hox gene. *Neuron*, *67*(5), pp.781–796.

Kadener, S., Menet, J. S., Sugino, K., Horwich, M. D., Weissbein, U., Nawathean, P., Vagin, V. V., Zamore, P. D., Nelson, S. B., & Rosbash, M., 2009. A role for microRNAs in the *Drosophila* circadian clock. *Genes Dev*, 23(18), pp.2179–2191.

Kannan, R., Berger, C., Myneni, S., Technau, G. M., & Shashidhara, L. S., 2010. Abdominal-A mediated repression of Cyclin E expression during cell-fate specification in the *Drosophila* central nervous system. *Mechanisms of Development*, 127(1-2), pp.137–145.

Karch, F., Weiffenbach, B., Peifer, M., Bender, W., Duncan, I., Celniker, S., Crosby, M., & Lewis, E. B., 1985. The abdominal region of the bithorax complex. *Cell*, 43(1), pp.81–96.

Karch, F., Bender, W. & Weiffenbach, B., 1990. abdA expression in *Drosophila* embryos. *Genes & Development*, 4(9), pp.1573–1587.

Karlsson, D., Baumgardt, M. & Thor, S., 2010. Segment-specific neuronal subtype specification by the integration of Anteroposterior and temporal Cues. *PLoS Biol*, 8(5), p.e1000368.

Kaufman, T.C., Lewis, R. & Wakimoto, B., 1980. Cytogenetic analysis of chromosome 3 in *Drosophila melanogaster*: The homoeotic gene complex in polytene chromosome interval 84a-B. *Genetics*, 94(1), pp.115–133.

Kedde, M. et al., 2010. A Pumilio-induced RNA structure switch in p27-3' UTR controls miR-221 and miR-222 accessibility. *Nature Cell Biology*, 12(10), pp.1014-1020.

Kernan, M., Cowan, D., & Zuker, C., 1994. Genetic dissection of mechanosensory transduction: Mechanoreception-defective mutations of

Drosophila. *Neuron*, 12(6), pp.1195–1206.

Keynes, R., & Krumlauf, R. (1994). Hox genes and regionalization of the nervous system. *Annu. Rev. Neurosci*, *17*(1), pp.109–132.

Khila, A., Abouheif, E. & Rowe, L., 2009. Evolution of a novel appendage ground plan in water striders is driven by changes in the Hox gene Ultrabithorax. *PLoS Genet*, 5(7), p.e1000583.

Kim, M., Cui, M. L., Cubas, P., Gillies, A., Lee, K., Chapman, M. A., Abbott, R. J., & Coen, E., 2008. Regulatory genes control a key morphological and ecological trait transferred between species. *Science*, 322(5904), pp.1116–1119.

Kornblihtt, A. R., Schor, I. E., Alló, M., Dujardin, G., Petrillo, E., & Muñoz, M. J., 2013. Alternative splicing: a pivotal step between eukaryotic transcription and translation. *Nat Rev Mol Cell Biol*, 14(3), pp.153–165.

Kornfeld, K., Saint, R. B., Beachy, P. A., Harte, P. J., Peattie, D. A., & Hogness, D. S., 1989. Structure and expression of a family of Ultrabithorax mRNAs generated by alternative splicing and polyadenylation in Drosophila. *Genes Dev*, 3(2), pp.243–258.

Kourakis, M. J., Master, V. A., Lokhorst, D. K., Nardelli-Haefliger, D., Wedeen, C. J., Martindale, M. Q., & Shankland, M., 1997. Conserved anterior boundaries of Hox gene expression in the central nervous system of the leech *Helobdella*. *Developmental Biology*, 190(2), pp.284–300.

Koushika, S.P., Lisbin, M.J. & White, K., 1996. ELAV, a *Drosophila* neuron-specific protein, mediates the generation of an alternatively spliced neural protein isoform. *Current Biology*, 6(12), pp.1634–1641.

Koushika, S.P., Soller, M. & White, K., 2000. The neuron-enriched splicing pattern of *Drosophila* erect wing is dependent on the presence of ELAV protein. *Mol. Cell. Biol.*, 20(5), pp.1836–1845.

König, J., Zarnack, K., Rot, G., Curk, T., Kayikci, M., Zupan, B., Turner, D. J., Luscombe, N. M., & Ule, J., 2010. iCLIP reveals the function of hnRNP particles in splicing at individual nucleotide resolution. *Nat Struct Mol Biol*, 17(7), pp.909–915.

Krumlauf, R., Marshall, H., Studer, M. L., Nonchev, S., Sham, M. H., & Lumsden, A., 1993. Hox homeobox genes and regionalisation of the nervous system. *Journal of neurobiology*, 24(10), pp.1328–1340.

la Mata, de, M., Alonso, C. R., Kadener, S., Fededa, J. P., Blaustein, M., Pelisch, F., Cramer, P., Bentley, D., & Kornblihtt, A. R., 2003. A slow RNA polymerase II affects alternative splicing in vivo. *Molecular cell*, 12(2), pp.525–532.

Lahiri, S., Shen, K., Klein, M., Tang, A., Kane, E., Gershow, M., Garrity, P., & Samuel, A. D. T., 2011. Two alternating motor programs drive navigation in

Drosophila larva. *PloS one*, 6(8), p.e23180.

Landgraf, M. & Thor, S., 2006. Development of *Drosophila* motoneurons: Specification and morphology. *Seminars in Cell & Developmental Biology*, 17(1), pp.3–11.

Landgraf, M., Bossing, T., Technau, G. M., & Bate, M., 1997. The origin, location, and projections of the embryonic abdominal motorneurons of *Drosophila*. *The Journal of Neuroscience*, 17(24), pp.9642–9655.

Lewis, E.B., 1978. A gene complex controlling segmentation in *Drosophila*. *Nature*, 276(5688), pp.565–570.

Lewis, R. A., Kaufman, T. C., Denell, R. E., & Tallerico, P.,1980. Genetic analysis of the Antennapedia gene complex (Ant-C) and adjacent chromosomal regions of *Drosophila melanogaster*. I. Polytene chromosome segments 84b-D. *Genetics*, 95(2), pp.367–381.

Licatalosi, D. D., Mele, A., Fak, J. J., Ule, J., Kayikci, M., Chi, S. W., Clark, T. A., Schweitzer, A. C., Blume, J. E., Wang, X., *et al.*, 2008. HITS-CLIP yields genome-wide insights into brain alternative RNA processing. *Nature*, 456(7221), pp.464–469.

Lisbin, M.J., Qiu, J. & White, K., 2001. The neuron-specific RNA-binding protein ELAV regulates neuroglian alternative splicing in neurons and binds directly to its pre-mRNA. *Genes & Development*, 15(19), pp.2546–2561.

Liu, W.W. & Wilson, R.I., 2013. Glutamate is an inhibitory neurotransmitter in the *Drosophila* olfactory system. *Proceedings of the National Academy of Sciences*, 110(25), pp.10294–10299.

Lopez, A.J. & Hogness, D.S., 1991. Immunochemical dissection of the Ultrabithorax homeoprotein family in *Drosophila melanogaster*. *Proceedings of the National Academy of Sciences*, 88(22), pp.9924–9928.

Lutz, C.S., 2008. Alternative Polyadenylation: A Twist on mRNA 3′ End Formation. *ACS Chemical Biology*, 3(10), pp.609–617.

Maconochie, M., Nonchev, S., Morrison, A., & Krumlauf, R. (1996). Paralogous Hox genes: function and regulation. *Annual Review of Genetics*, *30*(1), pp.529–556.

Maeda, R.K. & Karch, F., 2009. The bithorax complex of *Drosophila* an exceptional Hox cluster. *Current topics in developmental biology*, 88, pp.1–33.

Mahr, A. & Aberle, H., 2006. The expression pattern of the *Drosophila* vesicular glutamate transporter: A marker protein for motoneurons and glutamatergic centers in the brain. *Gene Expression Patterns*, 6(3), pp.299–309.

Mallo, M. & Alonso, C.R., 2013. The regulation of Hox gene expression during animal development. *Development*, 140(19), pp.3951–3963.

Mann, R.S. & Hogness, D.S., 1990. Functional dissection of ultrabithorax proteins in *D. melanogaster. Cell*, 60(4), pp.597–610.

Manning, L., Heckscher, E. S., Purice, M. D., Roberts, J., Bennett, A. L., Kroll, J. R., Pollard, J. L., Strader, M. E., Lupton, J. R., Dyukareva, A. V., *et al*., 2012. A resource for manipulating gene expression and analyzing cis-regulatory modules in the *Drosophila* CNS. *Cell Reports*, 2(4), pp.1002–1013.

Marder, E., Bucher, D., Schulz, D. J., & Taylor, A. L., 2005. Invertebrate central pattern generation moves along. *Current Biology,* 15(17), pp.685–699.

Martins, N. E., Faria, V. G., Teixeira, L., Magalhães, S., & Sucena, É., 2013. Host adaptation is contingent upon the infection route taken by pathogens. *PLoS pathogens*, 9(9), p.e1003601.

Matlin, A.J., Clark, F. & Smith, C.W.J., 2005. Understanding alternative splicing: towards a cellular code. *Nat Rev Mol Cell Biol*, 6(5), pp.386–398.

McGinnis, W. & Krumlauf, R., 1992. Homeobox genes and axial patterning. *Cell*, 68(2), pp.283–302.

McGinnis, W., Garber, R. L., Wirz, J., Kuroiwa, A., & Gehring, W. J., 1984a. A homologous protein-coding sequence in *Drosophila* homeotic genes and its conservation in other metazoans. *Cell*, 37(2), pp.403–408.

McGinnis, W., Hart, C. P., Gehring, W. J., & Ruddle, F. H., 1984b. Molecular cloning and chromosome mapping of a mouse DNA sequence homologous to homeotic genes of *Drosophila*. *Cell*, 38(3), pp.675–680.

McGinnis, W., Levine, M. S., Hafen, E., Kuroiwa, A., & Gehring, W. J., 1984c. A conserved DNA sequence in homoeotic genes of the *Drosophila* Antennapedia and bithorax complexes. *Nature*, 308(5958), pp.428–433.

Miguel-Aliaga, I. & Thor, S., 2004. Segment-specific prevention of pioneer neuron apoptosis by cell-autonomous, postmitotic Hox gene activity. *Development*, 131(24), pp.6093–6105.

Miguel-Aliaga, I., Allan, D.W. & Thor, S., 2004. Independent roles of the dachshund and eyes absent genes in BMP signaling, axon pathfinding and neuronal specification. *Development*, 131(23), pp.5837–5848.

Miguel-Aliaga, I., Thor, S. & Gould, A.P., 2008. Postmitotic specification of Drosophila insulinergic neurons from pioneer neurons. *PLoS Biol*, 6(3), p.e58.

Mittelbrunn, M., Gutiérrez-Vázquez, C., Villarroya-Beltri, C., González, S., Sánchez-Cabo, F., González, M. Á., Bernad, A., & Sánchez-Madrid, F., 2011. Unidirectional transfer of microRNA-loaded exosomes from T cells to antigen-presenting cells. *Nat Commun*, 2, p.282.

Moore, M.J., 2005. From birth to death: the complex lives of eukaryotic mRNAs.

Science, 309(5740), pp.1514–1518.

Morata, G. & Kerridge, S., 1981. Sequential functions of the bithorax complex of *Drosophila*. *Nature*, 290(5809), pp.778–781.

Müller, J. & Bienz, M., 1991. Long range repression conferring boundaries of Ultrabithorax expression in the *Drosophila* embryo. *EMBO J*, 10(11), pp.3147–3155.

Müller, J. & Bienz, M., 1992. Sharp anterior boundary of homeotic gene expression conferred by the fushi tarazu protein. *EMBO J*, 11(10), pp.3653–3661.

Murphy, P., Davidson, D. R., & Hill, R. E.,1989. Segment-specific expression of a homeobox-containing gene in the mouse hindbrain. Nature ,341, pp.156–159.

Nässel, D.R. & Homberg, U., 2006. Neuropeptides in interneurons of the insect brain. *Cell and Tissue Research*, 326(1), pp.1–24.

Negre, B., Ranz, J. M., Casals, F., Cáceres, M., & Ruiz, A., 2003. A new split of the Hox gene complex in *Drosophila*: relocation and evolution of the gene labial. *Mol Biol Evol*, 20(12), pp.2042–2054.

Negre, B., Casillas, S., Suzanne, M., Sánchez-Herrero, E., Akam, M., Nefedov, M., Barbadilla, A., de Jong, P., & Ruiz, A, 2005. Conservation of regulatory sequences and gene expression patterns in the disintegrating *Drosophila* Hox gene complex. *Genome Research*, 15(5), pp.692–700.

Ng, M., Roorda, R. D., Lima, S. Q., Zemelman, B. V., Morcillo, P., & Miesenböck, G., 2002. Transmission of olfactory information between three populations of neurons in the antennal lobe of the fly. *Neuron*, 36(3), pp.463–474.

Novotny, T., Eiselt, R. & Urban, J., 2002. Hunchback is required for the specification of the early sublineage of neuroblast 7-3 in the *Drosophila* central nervous system. *Development*, 129(4), pp.1027–1036.

Nusbaum, M. P., Blitz, D. M., Swensen, A. M., Wood, D., & Marder, E, 2001. The roles of co-transmission in neural network modulation. *Trends in Neurosciences*, 24(3), pp.146–154.

O'Connor, M. B., Binari, R., Perkins, L. A., & Bender, W., 1988. Alternative RNA products from the Ultrabithorax domain of the bithorax complex. *EMBO J*, 7(2), pp.435–445.

Oktaba, K., Gutiérrez, L., Gagneur, J., Girardot, C., Sengupta, A. K., Furlong, E. E. M., & Müller, J., 2008. Dynamic regulation by polycomb group protein complexes controls pattern formation and the cell cycle in *Drosophila*. *Developmental Cell*, 15(6), pp.877–889.

Osborne, K. A., Robichon, A., Burgess, E., Butland, S., Shaw, R. A., Coulthard,

A., Pereira, H. S., Greenspan, R. J., & Sokolowski, M. B., 1997. Natural behavior polymorphism due to a cGMP-dependent protein kinase of *Drosophila*. *Science*, 277(5327), pp.834–836.

Park, D., Veenstra, J. A., Park, J. H., & Taghert, P. H, 2008. Mapping peptidergic cells in *Drosophila*: where DIMM fits in. *PloS one*, 3(3), pp.e1896–e1896.

Pascale, A., Amadio, M. & Quattrone, A., 2008. Defining a neuron: neuronal ELAV proteins. *Cellular and Molecular Life Sciences*, 65(1), pp.128–140.

Patraquim, P., Warnefors, M. & Alonso, C.R., 2011. Evolution of Hox post-transcriptional regulation by alternative polyadenylation and microRNA modulation within twelve Drosophila genomes. *Molecular Biology and Evolution*, 28(9), pp.2453–2460.

Pavlopoulos, A., Kontarakis, Z., Liubicich, D. M., Serano, J. M., Akam, M., Patel, N. H., & Averof, M., 2009. Probing the evolution of appendage specialization by Hox gene misexpression in an emerging model crustacean. *Proceedings of the National Academy of Sciences*, 106(33), pp.13897–13902.

Pearson, J.C., Lemons, D. & McGinnis, W., 2005. Modulating Hox gene functions during animal body patterning. *Nat Rev Genet*, 6(12), pp.893–904.

Pfeiffer, B. D., Jenett, A., Hammonds, A. S., Ngo, T. T. B., Misra, S., Murphy, C., Scully, A., Carlson, J. W., Wan, K. H., Laverty, T. R., *et al.*, 2008. Tools for neuroanatomy and neurogenetics in *Drosophila*. *Proceedings of the National Academy of Sciences*, 105(28), pp.9715–9720.

Pirrotta, V., 1997. Chromatin-silencing mechanisms in *Drosophila* maintain patterns of gene expression. *Trends in Genetics*, 13(8), pp.314–318.

Prokop, A. & Technau, G.M., 1994. Early tagma-specific commitment of *Drosophila* CNS progenitor NB1-1. *Development*, 120(9), pp.2567–2578.

Proudfoot, N.J., 2011. Ending the message: poly(A) signals then and now. *Genes Dev*, 25(17), pp.1770–1782.

Raghu, S.V. & Borst, A., 2011. Candidate glutamatergic neurons in the visual system of *Drosophila*. *PloS one*, 6(5), p.e19472.

Raman, V., Martensen, S. A., Reisman, D., Evron, E., Odenwald, W. F., Jaffee, E., Marks, J., & Sukumar, S., 2000. Compromised HOXA5 function can limit p53 expression in human breast tumours. *Nature*, 405(6789), pp.974–978.

Reed, H. C., Hoare, T., Thomsen, S., Weaver, T. A., White, R. A. H., Akam, M., & Alonso, C. R., 2010. Alternative splicing modulates Ubx protein function in *Drosophila melanogaster*. *Genetics*, p.genetics.109.112086.

Reinitz, J. & Levine, M., 1990. Control of the initiation of homeotic gene expression by the gap genes giant and tailless in *Drosophila*.

Developmental Biology, 140(1), pp.57–72.

Robinow, S. & White, K., 1991. Characterization and spatial distribution of the ELAV protein during *Drosophila melanogaster* development. *Journal of neurobiology*, 22(5), pp.443–461.

Rogulja-Ortmann, A. & Technau, G.M., 2008. Multiple roles for Hox genes in segment-specific shaping of CNS lineages. *Fly (Austin)*, 2(6), pp.316–319.

Rogulja-Ortmann, A., Lüer, K., Seibert, J., Rickert, C., & Technau, G. M., 2007. Programmed cell death in the embryonic central nervous system of *Drosophila melanogaster*. *Development*, 134(1), pp.105–116.

Rogulja-Ortmann, A., Renner, S. & Technau, G.M., 2008. Antagonistic roles for Ultrabithorax and Antennapedia in regulating segment-specific apoptosis of differentiated motoneurons in the *Drosophila* embryonic central nervous system. *Development*, 135(20), pp.3435–3445.

Ronshaugen, M., Biemar, F., Piel, J., Levine, M., & Lai, E. C., 2005. The *Drosophila* microRNA iab-4 causes a dominant homeotic transformation of halteres to wings. *Genes Dev*, 19(24), pp.2947–2952.

Ruby, J. G., Stark, A., Johnston, W. K., Kellis, M., Bartel, D. P., & Lai, E. C., 2007. Evolution, biogenesis, expression, and target predictions of a substantially expanded set of *Drosophila* microRNAs. *Genome Research*, 17(12), pp.1850–1864.

Salvaterra, P.M. & Kitamoto, T., 2001. *Drosophila* cholinergic neurons and processes visualized with Gal4/UAS-GFP. *Gene Expression Patterns*, 1(1), pp.73–82.

Santos, J. G., Vömel, M., Struck, R., Homberg, U., Nässel, D. R., & Wegener, C., 2007. Neuroarchitecture of peptidergic systems in the larval ventral ganglion of *Drosophila melanogaster*. *PloS one*, 2(8), pp.e695–e695.

Schmid, A., Chiba, A. & Doe, C.Q., 1999. Clonal analysis of *Drosophila* embryonic neuroblasts: neural cell types, axon projections and muscle targets. *Development*, 126(21), pp.4653–4689.

Schmidt, H., Rickert, C., Bossing, T., Vef, O., Urban, J., & Technau, G. M., 1997. The Embryonic central nervous system lineages of *Drosophila melanogaster*.II. Neuroblast lineages derived from the dorsal part of the neuroectoderm. *Developmental Biology*, 189(2), pp.186–204.

Schwartz, J. C., Ebmeier, C. C., Podell, E. R., Heimiller, J., Taatjes, D. J.,& Cech, T. R., 2012. FUS binds the CTD of RNA polymerase II and regulates its phosphorylation at Ser2. *Genes Dev*, 26(24), pp.2690–2695.

Schwartz, Y.B. & Pirrotta, V., 2008. Polycomb complexes and epigenetic states. *Current Opinion in Cell Biology*, 20(3), pp.266–273.

Scott, M.P. & Weiner, A.J., 1984. Structural relationships among genes that

control development: sequence homology between the Antennapedia, Ultrabithorax, and fushi tarazu loci of *Drosophila*. *Proceedings of the National Academy of Sciences of the United States of America*, 81(13), pp.4115–4119.

Seeger, M., Tear, G., Ferres-Marco, D., & Goodman, C. S., 1993. Mutations affecting growth cone guidance in drosophila: Genes necessary for guidance toward or away from the midline. *Neuron*, 10, pp.409-426

Simon, J., Chiang, A., Bender, W., Shimell, M. J., & O'Connor, M, 1993. Elements of the *Drosophila* bithorax complex that mediate repression by Polycomb group products. *Developmental Biology*, 158(1), pp.131–144.

Simon, J., Peifer, M., Bender, W., & O'Connor, M, 1990. Regulatory elements of the bithorax complex that control expression along the anterior-posterior axis. *EMBO J*, 9(12), pp.3945–3956.

Simone, L.E. & Keene, J.D., 2013. Mechanisms coordinating ELAV/Hu mRNA regulons. *Curr Opin Genet Dev*, 23(1), pp.35–43.

Skeath, J.B. & Thor, S., 2003. Genetic control of Drosophila nerve cord development. *Current Opinion in Neurobiology*, 13(1), pp.8–15.

Smith, C.W. & Valcárcel, J., 2000. Alternative pre-mRNA splicing: the logic of combinatorial control. *Trends in Biochemical Sciences*, 25(8), pp.381–388.

Snow, P. M., Patel, N. H., Harrelson, A. L., and Goodman, C. S., 1987. Neural-specific carbohydrate moiety shared by many surface glycoproteins in *Drosophila* and grasshopper embryos. *The Journal of Neuroscience*, 7(12), pp.4137–4144.

Sokolowski, M.B., 1980. Foraging strategies of *Drosophila melanogaster*: A chromosomal analysis. *Behavior genetics*, 10(3), pp.291–302.

Soller, M. & White, K., 2003. ELAV inhibits 3′-end processing to promote neural splicing of ewg pre-mRNA. *Genes & Development*, 17(20), pp.2526–2538.

Soustelle, L., Besson, M.-T., Rival, T., & Birman, S., 2002. Terminal glial differentiation involves regulated expression of the excitatory amino acid transporters in the *Drosophila* embryonic CNS. *Developmental Biology*, 248(2), pp.294–306.

Stark, A., Bushati, N., Jan, C. H., Kheradpour, P., Hodges, E., Brennecke, J., Bartel, D. P., Cohen, S. M., & Kellis, M., 2008. A single Hox locus in *Drosophila* produces functional microRNAs from opposite DNA strands. *Genes Dev*, 22(1), pp.8–13.

Stern, D.L., 1998. A role of Ultrabithorax in morphological differences between *Drosophila* species. *Nature*, 396(6710), pp.463–466.

Struhl, G. & White, R.A., 1985. Regulation of the Ultrabithorax gene of *Drosophila* by other bithorax complex genes. *Cell*, 43(2 Pt 1), pp.507–519.

Sun, M., Song, C.-X., Huang, H., Frankenberger, C. A., Sankarasharma, D., Gomes, S., Chen, P., Chen, J., Chada, K. K., He, C., *et al.*, 2013. HMGA2/TET1/HOXA9 signaling pathway regulates breast cancer growth and metastasis. *Proceedings of the National Academy of Sciences of the United States of America*, 110(24), pp.9920–9925.

Suska, A., Miguel-Aliaga, I. & Thor, S., 2011. Segment-specific generation of *Drosophila* Capability neuropeptide neurons by multi-faceted Hox cues. *Developmental Biology*, 353(1), pp.72–80.

Suster, M.L. & Bate, M., 2002. Embryonic assembly of a central pattern generator without sensory input. *Nature*, 416(6877), pp.174–178.

Suster, M. L., Martin, J.-R., Sung, C., & Robinow, S., 2003. Targeted expression of tetanus toxin reveals sets of neurons involved in larval locomotion in *Drosophila*. *Journal of neurobiology*, 55(2), pp.233–246.

Suster, M. L., Karunanithi, S., Atwood, H. L., & Sokolowski, M. B., 2004. Turning behavior in *Drosophila* larvae: a role for the small scribbler transcript. *Genes, Brain & Behavior*, 3(5), pp.273–286.

Technau, G.M., Berger, C. & Urbach, R., 2006. Generation of cell diversity and segmental pattern in the embryonic central nervous system of *Drosophila*. *Developmental Dynamics*, 235(4), pp.861–869.

Thomsen, S., Azzam, G., Kaschula, R., Williams, L. S., & Alonso, C. R, 2010. Developmental RNA processing of 3′UTRs in Hox mRNAs as a context-dependent mechanism modulating visibility to microRNAs. *Development*, 137(17), pp.2951–2960.

Tripodi, M., Evers, J. F., Mauss, A., Bate, M., & Landgraf, M., 2008. Structural Homeostasis: Compensatory Adjustments of Dendritic Arbor Geometry in Response to Variations of Synaptic Input. *PLoS Biol*, 6(10), p.e260.

Tümpel, S., Wiedemann, L.M. & Krumlauf, R., 2009. Hox Genes and Segmentation of the Vertebrate Hindbrain. *Current Topics in Developmental Biology*, 88, pp.103-137

Tyler, D. M., Okamura, K., Chung, W. J., Hagen, J. W., Berezikov, E., Hannon, G. J., & Lai, E. C., 2008. Functionally distinct regulatory RNAs generated by bidirectional transcription and processing of microRNA loci. *Genes Dev*, 22(1), pp.26–36.

Udolph, G., Prokop, A., Bossing, T., & Technau, G. M., 1993. A common precursor for glia and neurons in the embryonic CNS of *Drosophila* gives rise to segment-specific lineage variants. *Development*, 118(3), pp.765–775.

Ule, J., Stefani, G., Mele, A., Ruggiu, M., Wang, X., Taneri, B., Gaasterland, T., Blencowe, B. J., & Darnell, R. B., 2006. An RNA map predicting Nova-dependent splicing regulation. *Nature*, 444(7119), pp.580–586.

Vactor, D. V., Sink, H., Fambrough, D., Tsoo, R., & Goodman, C. S., 1993. Genes that control neuromuscular specificity in *Drosophila*. *Cell*, 73(6), pp.1137–1153.

Wang, X. & Tanaka Hall, T.M., 2001. Structural basis for recognition of AU-rich element RNA by the HuD protein. *Nature structural biology*, 8(2), pp.141–145.

Wang, Z., Kayikci, M., Briese, M., Zarnack, K., Luscombe, N. M., Rot, G., Zupan, B., Curk, T., & Ule, J., 2010. iCLIP predicts the dual splicing effects of TIA-RNA interactions. *Plos Biology*, 8(10), pp.e1000530–e1000530.

White, R.A. & Akam, M.E., 1985. Contrabithorax mutations cause inappropriate expression of Ultrabithorax products in *Drosophila*. *Nature*, 318(6046), pp.567–569.

White, R.A. & Lehmann, R., 1986. A gap gene, hunchback, regulates the spatial expression of Ultrabithorax. *Cell*, 47(2), pp.311–321.

White, R.A. & Wilcox, M., 1985a. Distribution of Ultrabithorax proteins in *Drosophila*. *EMBO J*, 4(8), pp.2035–2043.

White, R.A. & Wilcox, M., 1985b. Regulation of the distribution of Ultrabithorax proteins in *Drosophila*. *Nature*, 318(6046), pp.563–567.

White, R.A.H. & Wilcox, M., 1984. Protein products of the bithorax complex in *Drosophila*. *Cell*, 39(1), pp.163–171.

Winter, J., Jung, S., Keller, S., Gregory, R. I., & Diederichs, S., 2009. Many roads to maturity: microRNA biogenesis pathways and their regulation. *Nat Cell Biol*, 11(3), pp.228–234.

Xue, Y., Zhou, Y., Wu, T., Zhu, T., Ji, X., Kwon, Y.-S., Zhang, C., Yeo, G., Black, D. L., Sun, H., *et al.*, 2009. Genome-wide analysis of PTB-RNA interactions reveals a strategy used by the general splicing repressor to modulate exon inclusion or skipping. *Molecular cell*, 36(6), pp.996–1006.

Yao, K. M., Samson, M. L., Reeves, R., & White, K., 1993. Gene elav of *Drosophila melanogaster*: a prototype for neuronal-specific RNA binding protein gene family that is conserved in flies and humans. *J Neurobiol.*, 24(6), pp.723–739.

Yasuyama, K. & Salvaterra, P.M., 1999. Localization of choline acetyltransferase-expressing neurons in *Drosophila* nervous system - Microscopy Research and Technique , 45, pp.65-79.

Zhang, C., Zhang, Z., Castle, J., Sun, S., Johnson, J., Krainer, A. R., & Zhang, M. Q., 2008. Defining the regulatory network of the tissue-specific splicing factors Fox-1 and Fox-2. *Genes & Development*, 22(18), pp.2550–2563.

Zhang, C.C. & Bienz, M., 1992. Segmental determination in *Drosophila* conferred by hunchback (hb), a repressor of the homeotic gene

Ultrabithorax (Ubx). *Proceedings of the National Academy of Sciences of the United States of America*, 89(16), pp.7511–7515.

Zhou, Y., Cameron, S., Chang, W.-T., & Rao, Y., 2012. Control of directional change after mechanical stimulation in *Drosophila*. *Molecular brain*, 5, p.39.